# RHIZOBIAL INFECTION IN NODULATION

DIAN GUAN

A THESIS

SUBMITTED IN PARTIAL FULFILMENT OF THE REQUIREMENTS FOR THE DEGREE OF PH.D.

SUPERVISED BY

PROFESSOR GILES OLDROYD AND DOCTOR JEREMY MURRAY

CELL AND DEVELOPMENTAL BIOLOGY DEPARTMENT

JOHN INNES CENTRE

UNIVERSITY OF EAST ANGLIA

NORWICH, UNITED KINGDOM

SEP, 2012

# Abstract

Nodulation is a symbiosis between plants and bacteria called rhizobia which leads to the formation of a lateral organ called a nodule where nitrogen fixation occurs. Nodulation can be divided into two developmental programmes, rhizobial infection, and nodule organogenesis, both of which are required for nitrogen fixation. In my PhD studies, I focused on the study of rhizobial infection using the *Medicago truncatula-Sinorhizobium meliloti* model system.

NIN is an important transcription factor in the nodulation signalling pathway that functions both in rhizobial infection and nodule organogenesis. Gene expression profiling of *nin* during rhizobial infection has enabled me to identify its potential downstream targets including several NIN-dependent infection-related genes and, surprisingly, genes involved in mycorrhization that are apparently repressed by NIN. The identification of these genes has provided insight into how NIN functions in rhizobial infection and revealed potential cross-talk between nodulation and mycorrhization pathways.

In the course of this work I discovered two infection mutants. One of the mutants, *cbs1*, was cloned in collaboration with a colleague in the lab. It encodes a Cystathionine Beta-Synthase domain containing protein with a potential role in reactive oxygen species homeostasis.

The other mutant, which I named *knocks but can't enter* (*kce)*, is blocked at an early stage of infection. I used conventional mapping and next-generation sequencing technologies to genetically map *kce* to a known rhizobial infection gene *LIN*. The *kce* mutant developed nodules with central rather than peripheral vascular bundles resembling nodules from the more ancient Frankia-actinorhizal symbiosis. Using *kce* and other infection mutants I demonstrate that this abnormal nodule architecture results from a failure of infection to reach the nodule cortex. Based on this finding, I predict that Nod factor activated signalling in the nodule cortex plays a role in determining nodule structure.

# Table of Contents

# Acknowledgements

I would like first of all express my gratitude to my supervisors Prof. Giles Oldroyd and Dr. Jeremy Murray for offering me the opportunity to carry out my PhD study on such an interesting topic, and for three years patient guidance on the scientific road. This thesis could not have been completed without their support and guidance. I would like to thank Prof. Allan Downie for kindly answering my naïve questions and Prof. Philip Poole for providing me with ideas in my researches. I would also like to thank my advisor Prof. Caroline Dean for her generous help, support and advice in the first rotation year and during my later studies.

I want to thank everybody in the Oldroyd, Downie, Murray and Poole labs for helping familiarize me with life in the lab and for teaching me in every aspect. Especially I want to thank Nicola Stacey for doing all the nodule and root sections for me and showing me the RNA *in situ* hybridization method; Dr. Chengwu Liu for helping my work; Dr. Tatiana Vernie for providing me with constructs; Dr. Andy Breakspear for sharing the root hair RNA isolation method with me; Dr. Anne Edwards for answering all kinds of questions; Dr. Ertao Wang for discussing scientific questions; Dr. Fang Xie for giving guidance in my experiments; Dr. Enrico Gabbato for sharing happiness and pain in the lab life; Dr. Yiliang Ding for helping me at the start of my PhD; Ben Miller for sharing cheers and complaints in the PhD life; Sonali Roy for adding beautiful colours to the boring moments.

In addition, I would like to thank all the people at the institute that helped me along the way. John Innes Centre is a great place to learn science, I have learned different things from different people. Prof. Nick Brewin was very patient with me and helped a lot in the rotation program.

Outside life in the lab, I have had great friends in these four years in Norwich. They were there when I was bored. I had fun and learned a lot from them. They will not bother I don’t mention the names. But one of them, Ruoyu, I spent a great year with him. With him, I didn’t need to worry about a lot of things which of course may have added a lot of pressure on him. I renewed myself during that year and identified a better me. No matter where I am in the future, friends are always friends; the good memories will last forever.

Four years of PhD life in John Innes Centre has not only taught me scientific technique, but has also trained me mentally in the scientific approach. My biggest achievement these past four years has been gaining the confidence to carry out independent research in the future.

# List of Abbreviations

| | |
|---|---|
| A, C, G, T | Adenine, cytosine, guanine, thymine |
| bp | base pairs |
| BSA | Bovine serum albumin |
| DNA | deoxyribonucleic acid |
| GFP | green fluorescent protein |
| Kb | kilobase |
| LTR | long tandem repeat |
| Mb | megabase |
| min | minute |
| mRNA | messenger RNA |
| NB-LRRs | nucleotide-binding leucine-rich repeats |
| OD | optical density |
| PBS | phosphate buffered saline |
| PCR | polymerase Chain Reaction |
| RNA | ribonucleic acid |
| rpm | revolutions per minute |
| SDS | Sodium dodecyl sulfate |
| sec | second |
| Nod factor | Nodulation factor |
| WGD | Whole genome duplication |
| PPA | Prepenetration apparatus |
| LysM | Lysine motif |
| X-gal | 5-bromo-4-chloro-3-indolyl-beta-D-galactopyranosid |
| ABC transporter | ATP-binding cassette transporter |
| AVG | Aminoethoxyvinylglycine |
| EPS | exopolysaccharide |
| ARR | Arabidopsis response regulator |
| AHK | Arabidopsis histidine kinase |
| PIT | Preinfection threads |

| | |
|---|---|
| IAA | Indole-3-acetic acid |
| NLS | Nuclear localisation signal |
| ChIP | Chromatin immunoprecipitation |
| NLP | NIN-like protein |
| CDS | Coding sequence |
| ROS | Reactive oxygen species |
| WT | Wild type |
| BC1F2 | Backcross once the second generation |
| dNTP | Deoxyribonucleotide triphosphate |
| bHLH | basic helix-loop-helix |
| EF | Elongation factor |
| QPCR | Quantitative PCR |
| PVB | Peripheral vascular bundle |
| CVB | Central vascular bundle |
| GUS | Beta-glucuronidases |
| X-Gluc | 5-bromo-4-chloro-3-indolyl-beta-glucuronic acid |
| BNM | Buffered nodulation medium |
| DWA | Distilled water agar |
| MFP | Modified Fahraeus medium |
| dpi | Days post inoculation |

# CHAPTER I General Introduction

## 1 The rhizobial and arbuscular mycorrhiza symbioses

Symbiosis describes when beneficial relationships form after species associate with each other and represents a widespread phenomenon in the biological world. We can classify symbioses into two main kinds, endosymbiosis and ectosymbiosis. Endosymbiosis refers to examples where the symbiont lives in the tissue of the host while in an ectosymbiosis the symbiont lives on the body surface of the host.

In the plant, there are two endosymbioses that are widely studied, one is the legume rhizobia association called nodulation and the other is the plant-arbuscular mycorrhiza symbiosis.

### 1.1 Legume-rhizobia symbiosis

The legumes-rhizobia symbiosis evolved approximately 58 million years (Myr) ago associated with a whole genome duplication (WGD) event (Young et al., 2011). Dry air contains 78.09% nitrogen that can't be normally used by plants. This beneficial interaction allows legumes to obtain fixed nitrogen produced by the rhizobia's nitrogenase enzyme which converts $N_2$ to ammonia and in exchange the rhizobia get dicarboxylates. Since nitrogen availability is often a limiting factor in crop production, biological nitrogen fixation is very important in agriculture. In the legume-rhizobia interaction, legume roots form nodules where the nitrogen fixation takes place. Nodulation begins with a signal exchange between the host plant and symbiont. Legume roots continuously secret flavonoids that switch on rhizobia Nodulation (Nod) factor production genes (Nod genes) (Kosuta et al., 2008). The Nod factors secreted by rhizobia act as signalling molecules, and play an essential role in nodulation. Nod factors consist of a chitin backbone with an *N*-linked fatty acid moiety attached to the non-reducing terminal sugar (Kosuta et al., 2008) and the structure varies across rhizobia species. *Sinorhizobium meliloti* Nod factors carry a 6-O-sulphate moiety on the reducing terminus, the non-reducing terminus is N-acylated with a C16:2 acyl chain and an O-acetylated with a glucosamine (Kosuta et al., 2008). The type of Nod factor decorations determine host specificities which is determined by their compatibility with Nod factor receptors. For instance, it has been shown that transformation of *Lotus japonicus* Nod factor receptors NFR1 and NFR5 into

*Medicago truncatula* facilitate the *L. japonicus* symbiont *Mesorhizobium loti* to enter *M. truncatula* (Radutoiu et al., 2007). The rhizobial production of NFs can trigger a series of morphological changes on the plant. In the epidermis: root hair deformation, root hair curling and infection thread initiation; in the cortex: cortical cell divisions leading to nodule formation (Jones et al., 2007; Kosuta et al., 2008). Nod factors alone are able to induce root hair deformations, calcium spiking early nodulation 11 (ENOD11) gene induction and cortical cells leading to nodule primordium formation. These processes have lower stringency on Nod factor structure than is required for rhizobial infection (Ardourel et al., 1994). Rhizobia colonize the infection threads to invade the nodule where they are taken up into nodule cells enclosed by plant plasma membrane where they differentiate into bacteroids and fix nitrogen (Kosuta et al., 2008; Oldroyd et al., 2011). This organelle-like structure is called a symbiosome.

## 1.2 Mycorrhizal symbiosis

Mycorrhizal fungi form a symbiosis with 95% of plant families. Mycorrhiza facilitate plants to absorb organic phosphate ions in the soil that plants themselves would otherwise not have access to. And in return up to 20% of the plant fixed carbon is transferred to the mycorrhiza (Parniske, 2008). The most widely studied mycorrhiza is arbuscular mycorrhiza. Fossil evidences suggest that this symbiosis evolved 400-460 MYA (Remy et al., 1994). The mycorrhizal interaction starts with plant roots secreting strigolactones, which can stimulate hyphal branching in the mycorrhiza , and in some species, spore germination (Parniske, 2008). The branching mycorrhiza fungi reach the plant root surface where it forms a specialised penetration apparatus, called the hyphopodium, in preparation for penetrating the root cell. Right after that, the plant cells in contact with the hyphopodium go through cytoskeletal changes, creating a prepenetration apparatus (PPA) to facilitate mycorrhizal entry. The PPA is a thick cytoplasmic bridge that crosses the vacuole of the root cells. Mycorrhizal fungi then penetrate the host cell through the PPA. The mycorrhiza then pass into the cortex through the apoplast. Finally, mycorrhiza penetrate into the inner cells of the plant root cortex forming highly branched arbuscule structures. The arbuscules serve as an interface for nutrient exchange between the plant and the fungi (Parniske, 2008).

# 2 Early events in nodulation: signalling and the activation of gene expression

Over the last 10 years, plant genes in the nodulation signalling pathway have been identified mainly through forward genetics in both *M. truncatula* and *L. japonicus*, which are two widely used model legumes. The most upstream event in the nodulation signalling pathway is the perception of Nod factors. Two receptor-like kinases with *N*-acetylglucosamine binding lysine motifs (LysM) in the extracellular domain, (Bensmihen et al., 2011) were proposed as receptors because the LysM motif-containing receptor like kinase CERK1 has been shown to be involved in chitin signalling and to bind chitin (Petutschnig et al., 2010; Liu et al., 2012). In *L. japonicus*, two receptors were identified, both of which are required to initiate signalling, Nod Factor Receptor 1 (NFR1) and NFR5. In *M. truncatula*, Nod Factor Perception (NFP) is the ortholog of NFR5 (Besma Ben et al., 2003; Madsen et al., 2003; Radutoiu et al., 2003; Arrighi et al., 2006). Recently, NFR1 and NFR5 have been shown to directly bind Nod factors using multiple methods (Broghammer et al., 2012). As mentioned above, Nod factor specificity is mediated by these receptors as NFR1 and NFR5 cross-species domain swap experiments proved symbiont host range can be extended (Radutoiu et al., 2007). This was demonstrated using *Lotus filicaulis* which does not nodulate with the DZL strain of rhizobia. In *L. filicaulis* the extracellular domain of NFR1 and NFR5 fused with *L. japonicus* intracellular kinase domain of NFR1 and NFR5 was used to partially complement the *L. japonicus nfr1nfr5* mutant. Amino acid mutations in the *L. filicaulis* NFR5 extracellular domains to better match sequence from *L. japonicus* dramatically improved the complementation of the *L. japonicus nfr5* mutant inoculated with DZL strain (Radutoiu et al., 2007). This suggests that key amino acids in the NFR5 extracellular domain is necessary for nodulation specificity. The *M. truncatula* symbiont *S. meliloti nodFnodL* mutant which produces Nod factors that lack the C16:2 acyl chain aborts infection in the root hair curl (Limpens et al., 2003). Despite the abortion of rhizobial infection, cortical cell divisions were still induced leading to nodule organogenesis (Smit et al., 2007). This observation, that organogenesis requires less specificity than epidermal infection, have led to the proposal of a so-called entry receptor. LysM domain-containing receptor-like Kinase 3/4 (LYK3/4), orthologs of NFR1, have been hypothesised to be

the entry receptors (discussed in more detail below) (Limpens et al., 2003; Haney et al., 2011).

Nod factors induce calcium spiking (Ehrhardt et al., 1996), which is a key signature of the nodulation signalling pathway. Calcium spiking is observed both in and around the nucleus. The elements that transduce the signal from plasma membrane to nucleus to induce calcium spiking are: a Leucine-rich repeat receptor like kinase: LjSYMRK/MtDMI2 (for SYMbiosis Receptor-like Kinase/Does not Make Infection 2) (Endre et al., 2002; Stracke et al., 2002); three nucleoporins: NUcleoPorin 85 (LjNUP85) (Saito et al., 2007), NUcleoPorin 133 (LjNUP133) (Kanamori et al., 2006) and LjNENA (Groth et al., 2010); cation channels in the nucleus membrane: Does not make infections (MtDMI1) (Ane et al., 2004; Imaizumi-Anraku et al., 2005; Brendan et al., 2007; Edwards et al., 2007) in *M. truncatula*; LjPOLLUX and LjCASTOR (Charpentier et al., 2008) in *L. japonicus*. Evidence shows that LjPOLLUX and LjCASTOR are potassium channels, and they facilitate the pumping of calcium in and out of the nucleus (Charpentier et al., 2008). It has been considered there is probably a second messenger linking Nod factor signalling from cell plasma membrane to the events in the nucleus. Phospholipase C (PLC) functions to degrade plasma membrane phosphatidylinositol-4,5-bisphosphate to generate IP3 and diacylglycerol. Mobilization of IP3 links ligand perception at the plasma membrane and calcium changes in the cytosol (Singer et al., 1996; Sun et al., 2007). Nod factor is able to stimulate an increase in phosphatidic acid (PA) and diacylglycerol pyrophosphate, which is indicative of PLD or PLC activity in combination with diacylglycerol kinase (DGK) and PA kinase (den Hartog et al., 2001). Also, pharmacological effectors that inhibit PLD and PLC activities are able to block *ENOD11* gene activation (Charron et al., 2004). In another study, the use of the U-73122, which is the inhibitor of PLC, inhibits Nod factor induced calcium spiking (Engstrom et al., 2002). These studies strongly suggest PLC and PLD function to transmit the Nod factor signal from the cell plasma membrane to the nucleus to activate gene expression.

The calcium signature is thought to be perceived and transduced by the nuclear-localized CCaMK/DMI3 (for Does not Make Infection 3), a calcium- and calmodulin-dependent protein kinase (Levy et al., 2004; Mitra et al., 2004). Together with its interactors, one of which is CYCLOPS/IPD3 (for Interacting Protein of DMI3)

(Messinese et al., 2007; Yano et al., 2008; Horvath et al., 2011; Ovchinnikova et al., 2011), calcium signal is decoded and transmitted leading to the induction of gene expression. IPD3 was first identified as an interactor of CCaMK/DMI3 (Messinese et al., 2007), later the Lotus *cyclops* mutant which is defective in infection thread initiation was identified and found to be the ortholog of IPD3. It was demonstrated that CYCLOPS can be phosphorylated by CCaMK (Yano et al., 2008).

Several transcription factors act downstream of CCaMK. In *M. truncatula*, these include Nodulation Signalling Pathway 1 (NSP1) (Smit et al., 2005), NSP2 (Kalo et al., 2005), ERF Required for Nodulation (ERN 1) (Middleton et al., 2007) and Nodule Inception (NIN) (Schauser et al., 1999; Marsh et al., 2007). NSP1 and NSP2 are GRAS [for gibberellin insensitive (GAI), repressor of ga1-3 (RGA), SCARECROW (SCR)] family transcription factors (Hirsch and Oldroyd, 2009). During nodulation, NSP1 forms a heterodimer with NSP2 and binds to the *ENOD11* (for Early NODulation 11) and *NIN* promoters to induce their expression (Hirsch et al., 2009). ERN1 promotes *ENOD11* expression (Middleton et al., 2007) and NIN suppresses it (Marsh et al., 2007), also it has been hypothesised that ERN1 and NIN compete for the *ENOD11* promoter binding site to balance its expression. This group of transcription factors act together to orchestrate the gene expression required for rhizobial infection and nodule organogenesis. Another gene, *HAP2.1* encodes a HAP2-type transcription factor subunit, a component of the hetero-trimeric CCAAT-box-binding-factor complex. The gene expresses in the nodule meristem, knocking down *HAP2.1* results in smaller nodules that lack meristems. The expression domain of *HAP2.1* is tightly controlled by micro RNAs and alternative splicing (Combier et al., 2006; Combier et al., 2008).

# 3 Nodule organogenesis

## 3.1 Cytokinin's role

Cytokinins are a class of phytohormones that promote cell divisions. The predominant cytokinins in higher plants are isopentenyladenine, zeatin and dihydrozeatin (Sakakibara, 2006). Cytokinin homeostasis is regulated spatially and temporarily through synthesis and catabolism. Cytokinin signalling relies on a phosphorelay mechanism similar to the prokaryotic two-component system. In *Arabidopsis thaliana*, three transmembrane histidine kinases have been identified.

They are Arabidopsis HIS Kinase2 (AHK2), AHK3 and AHK4/CRE1. They function as cytokinin receptors. Through cytokinins perception, cytokinin receptors autophosphorylate and transmit the signal via phosphorelay to Arabidopsis HIS Phosphorelay transfer proteins (AHPs). The AHPs translocate to nucleus to phosphorylate members of the type-A and type-B response regulators (ARRs). Activated type-B ARRs act as transcription factors to regulate type-A ARRs and other signalling molecules. Activated type-A ARRs negatively regulate cytokinin signalling pathways (Perilli et al., 2010).

Two types of nodule development occur in legumes. In *M. truncatula*, the nodule meristem keeps dividing and nodules develop indeterminately. Whereas in *L. japonicus* determinate type-nodules no persistent nodule meristem is observed (Subramanian et al., 2007). The initiation of the nodule primordium and maintenance of the meristem requires cytokinin signalling. The first report of cytokinin involvement in nodulation dates to 1994 (Cooper and Long, 1994). A rhizobia strain carrying a constitutive trans-zeatin secretion gene from *Agrobacterium tumefaciens* T37 but lacking the a Nod factor synthesis gene was found to be able to induce nodules in *Medicago sativa* (Cooper and Long, 1994). Later a mutant for the cytokinin receptor LHK1/CRE1 was discovered to have a defect in nodulation, cortical cell divisions are initially absent, and after a delay, disorganized cell divisions occur, resulting in misformed nodules (Murray et al., 2007). Another mutation that produced a constitutively active form of this protein was sufficient to induce nodule organogenesis in absence of rhizobia (Gonzalez-Rizzo et al., 2006). MtRR4, a type A-response regulator is induced by cytokinin and also by rhizobia and this induction is dependent on the nodulation early signalling pathway (Gonzalez-Rizzo et al., 2006). *MtRR4* and *MtCRE1* are activated quite early upon rhizobial infection, 3 days post inoculation, their gene expression was observed in inner cortex and later their expression in the nodule primordium. In the mature nodule, *MtRR4* and *MtCRE1* mainly express in the nodule meristem (Plet et al., 2011), consistent with cytokinin's role in nodule development. Exogenous application of cytokinin has been reported to induce spontaneous nodules in a tissue culture system (Heckmann et al., 2011). The gain-of-function cytokinin receptor mutant has been useful in determining the genetic position of cytokinin responses in the nodulation signalling pathway. By introducing the gain-of-function mutation into different mutant backgrounds it was determined

that the induction of spontaneous nodules (Tirichine et al., 2007) depends on NSP1, NSP2 and NIN (Madsen et al., 2010). It has also been shown that cytokinin activates *NIN* expression (Gonzalez-Rizzo et al., 2006), and reciprocally that CRE1 signalling is needed for activation of *NIN* gene expression (Tirichine et al., 2007), suggesting that NIN is part of a feedback loop with that involves cytokinin signalling. The discovery of CRE1/LHK1 provides direct genetic evidence for cytokinin's function in nodule organogenesis. Interestingly, the *hyperinfected1* (*hit1*) mutant of LHK1/CRE1 was hyperinfected by rhizobia (Murray et al., 2007). This suggests a negative feed-back mechanism from the cortex to the epidermis in nodulation.

We have learned a lot more in cytokinin mediated nodule organogenesis over these few years. Some signalling molecules have been identified and the relationship with other hormones starts to be revealed.

Nodule organogenesis starts with cortical cell and pericycle cell activations right after Nod factor perception. In the indeterminate nodules of *M. truncatula* and *M. sativa*, cortical cell and pericycle cell divisions were observed 16-18 hours post rhizobial inoculation. Cell divisions start with anticlinal and followed by periclinal divisions. 24-48 hours post inoculation which lead to the formation of the nodule primordium, an inward gradient of differentiation was observed starting from the outer cortex. This differentiation in the outer cortex involves the formation of cytoplasmic bridges that align anticlinally and predict the path of the infection thread, called pre-infection threads (PIT), and are analogous to the PPA formed during mycorrhization. At 60-72 hours post inoculation the nodule meristem is formed (Timmers et al., 1999). At about 5-7 days after infection the rhizobia within the infection threads are released into the nodule cells and become surrounded in a plant derived membrane called the symbiosome membrane and then go through endoreduplication,differentiate into bacteroids, and begin to fix nitrogen. NCR peptides and DNF1 (a signal peptidase) have been identified to be required for bacterial differentiation (Van de Velde et al., 2010; Wang et al., 2010). By this stage the nodule has developed into different zones-the meristem (zone I), the rhizobial infection zone (zone II), the nitrogen fixation zone (zone III) and the senescence zone (zone IV). (Fig.1). In the infection zone, which is absent in mature determinate nodules, the differentiating cells produced by the meristem are invaded by infection threads where rhizobial release takes place. The cell containing the symbiosomes is called the nodule nitrogen

fixation zone. This is where $N_2$ is reduced to ammonia which is then taken up and assimilated by the plants. The plants produce an oxygen-binding protein called leghemoglobin which acts to lower the oxygen concentration in the bacteroids and is needed to keep the oxygen-sensitive nitrogenase functioning. Oxygen binding to the leghemoglobin heme cofactor leads to the characteristic red colour of nitrogen-fixing nodules (Long, 1989). In the mature nodule, bacteroids degenerate in the senescence zone and the zone is symbolized with a green colour due to breakdown of the leghemoglobin (Roponen, 1970).

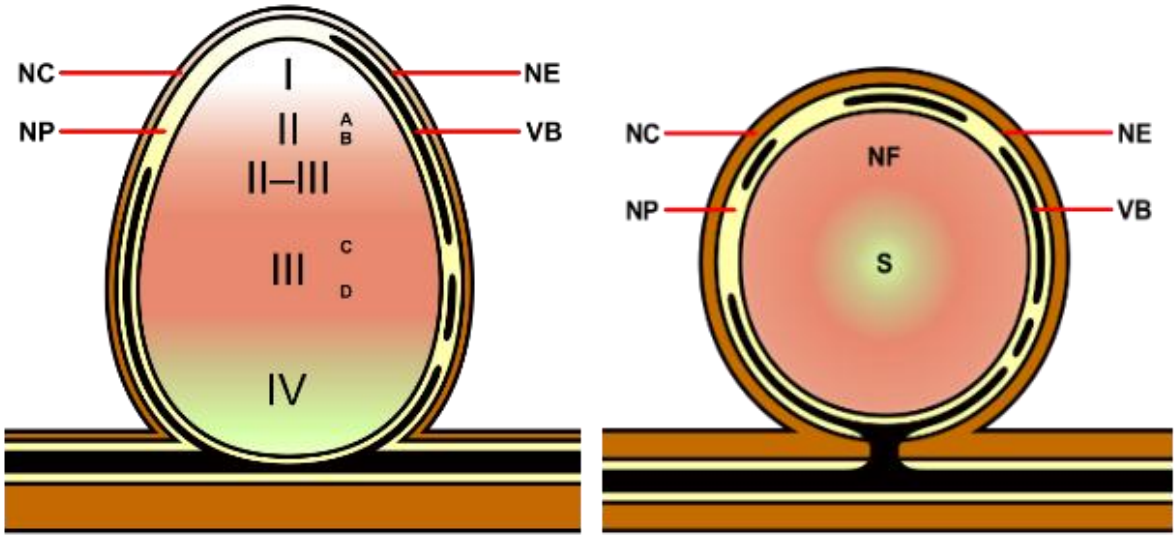


**Fig.1.** Indeterminate nodule (left) and determinate nodule (right) structure. I: meristem zone; II: infection zone; III: nitrogen fixation zone; IV: senescence zone. NC: nodule cortex; NP: nodule parenchyma; NE: nodule endodermis; VB: vascular bundle. NF: nitrogen fixing zone; S: senescence zone. Pictures taken from Wikimedia Commons.

## 3.2 The role of auxin

Auxin was the first major plant hormone identified. The first structure determined for it was indole-3-acetic acid (IAA). Auxin signal perception involves a protein turnover pathway. Auxin stabilises the interaction between the Aux/IAAs and TRANSPORT INHIBITOR RESPONSE1 (TIR1) or closely related proteins of the AUXIN SIGNALING F-BOX PROTEIN (AFB) family. TIR1 and the AFBs are alternative subunits of SCF-type protein-ubiquitin ligases, targeting ubiquitination of the Aux/IAAs, marking them for degradation by the 26S proteasome (Leyser, 2010). *GH3* has been shown to be specifically induced by the plant hormone auxin. The auxin-responsive *GH3* gene promoter is composed of multiple auxin response elements (AuxREs), and each AuxRE contributes incrementally to the strong auxin inducibility to the promoter (Walker and Estelle, 1998).

Through physiological studies a role for auxin in nodule organogenesis has been revealed. Using *GH3* as a marker, results indicate that 30 hours post inoculation by rhizobia, auxin signalling is present in all cortical cells and vascular bundles around the site of inoculation. Its expression then becomes more restricted, as the nodule develops it becomes prominent in the nodule vasculature when the nodule primordium begins to differentiate and expression is no longer seen in the centre of the primordium (Mathesius et al., 1998). Current studies suggest that changes in auxin transport are an important feature of nodulation. It was shown that Nod factors led to a reduction of auxin transport capacity in *Vicia sativa* (Boot et al., 1999). Also, rhizobial inhibition of acropetal auxin transport seems to be mediated by flavonoids, which act as natural auxin transport inhibitors (Wasson et al., 2006). These studies suggest during nodulation, there is a general repression of auxin transport, and that spatially, auxin signalling is more confined to where vasculature will be developing (Pacios-Bras et al., 2003; Takanashi et al., 2011). With the exception of the work on flavonoids, the surprisingly few genetic components involved in auxin related nodulation signalling and transport have been identified. One ABCB transporter that was demonstrated to have auxin transport activity and was reported to express in the uninfected nodule cells (Takanashi et al., 2012). One *Casuarina glauca* AUX1 has been shown to express in the plant cells infected by Frankia throughout the course of actinorhizal nodule development (Peret et al., 2007). So it remains an exciting area for future investigations. Another consideration is the possibility of interactions

between auxin transport and signalling and other hormones. In particular, the interaction of cytokinin and auxin in nodule organogenesis has recently been investigated. In the *cre1* mutant, auxin transport is not changed in the presence of the rhizobia, compared to the strong downregulation seen in wild type. This corresponds to an upregulation of PIN protein gene expression in the *cre1* mutant compared with WT (Plet et al., 2011).

### 3.3 Spontaneous nodulation

Genetics in *L. japonicus* has identified more several spontaneous nodulation mutants that nodulate in the absence of rhizobia. Two of the mutants were cloned and were found to be caused by gain-of-function mutations in CCaMK (*spontaneous nodule formation 1*; *SNF1*) and LHK1/CRE1 (*SNF2*).(Tirichine et al., 2006; Tirichine et al., 2007). *snf1* is caused by a mutation in the protein kinase domain and *snf2* is caused by a conserved leucine change to phenylalanine in the cytokinin-binding CHASE domain. Although spontaneous nodules are formed in these two mutants, some root epidermis markers (rhizobial infection marker genes) are not properly activated, so the signalling activation is not complete (Takeda et al., 2011).

## 4 Rhizobial infection

The legume plants secrete flavonoids into the rhizosphere to switch on the rhizobial *NodD* gene. NodD is a member of the LysR family of transcriptional regulators that act to increase expression of Nod factor biosynthetic genes (Peck et al., 2006). At some point the rhizobia must attach to the plant; it has been reported that rhizobial components, Nod factors, some secreted proteins and surface polysaccharides, function in rhizobial root hair attachment (Downie, 2010). However, it is not clear which plant components are required for root hair attachment. Nod factors can induce legume root hair swelling, branching, and spot application of Nod factors can induce changes in the direction of root hair growth (Esseling et al., 2003), implying that rhizobia direct root hairs to entrap them in the sealed root hair curl, the structure formed is called “shepherds crook” (Jones et al., 2007). The root hair cell walls then need to be degraded to let rhizobia enter either by the rhizobia or the plant or both. Recently, a cellulase from *Rhizobium trifolii* was reported to be required for rhizobial infection (Robledo et al., 2008). However, during its synthesis in bacteria, cellulose is continuously polymerized and then cleaved in the periplasm. The cellulase gene is

embedded within an operon involved in bacterial cellulose synthesis and the mutation of the gene may only affect cleavage of the cellulose. It is possible that uncleaved cellulose made by the cellulase mutant could inhibit bacterial infection and so it seems an open question as to whether rhizobial cellulase is required for infection (Xie et al., 2011). Very recently, a pectate lyase from *L. japonicus* has been found that functions to degrade the root hair cell wall during infection (Xie et al., 2011). However, it seems unlikely that this pectate lyase is the only component required to mediate this process since some infection threads do eventually form on the *npl* mutant, and the cell wall also contains other structural components in addition to pectin that would also need to be dealt with, namely cellulose and xyloglucan. The root hair membrane system is another obstacle to rhizobia, it has been hypothesized that rhizobial hydrated polysaccharides can increase the turgor pressure in the infection foci, pushing against the high pressure in the root hair to help the infection thread initiate and grow (Nagpal et al., 1992).

The infection thread is the apparatus that allows the rhizobia to enter the plant. It is an ingrowth of the root hair cell membrane and cell wall that forms a tubular structure which becomes colonized by rhizobia. The growth of the infection thread is proposed to be another form of tip growth and to be the result of reorganization of cellular polarity (Gage, 2004). Several phenomena have been found related to infection thread elongation, such as cytoplasmic streaming, and the rearrangement of microtubule arrays (Gage, 2004). With the help of genetics and the development of the cell biology, quite a few components have been identified to be associated with rhizobial infection from both the rhizobial and the plant sides.

## 4.1 The rhizobia

To this point, it is known that two key components in rhizobia are associated with rhizobial infection thread initiation and elongation. These are Nod factors and exopolysaccharides (EPSs).

Nod factors can induce root hair deformation and cortical cell divisions. The initiation of infection threads has been shown to have more stringent requirements for Nod factor structures than the cortical responses. Studies from several rhizobia species and their hosts show that the loss of the Nod factor decorations can result in rhizobial infection defects (Geurts et al., 1997). In *S. meliloti*, the Nod factor

backbone is made by the gene *NodABC*. *NodEF* make the N-linked acyl group, *NodL* makes the O-linked acetyl group and *NodH* is required for the addition of the sulphate group at the reducing end (Ardourel et al., 1994). The *S. meliloti nodF nodL* double mutant that produces Nod factors without acetyl decorations can't efficiently invade plant cells (Ardourel et al., 1994; Limpens et al., 2003). The *nodF nodL* double mutant can, induce nodule formation, however during infection only root hair curling is induced with a large microcolony in it, but no infection threads are initiated (Ardourel et al., 1994). It is also known that the *S. meliloti nodF nodL* double mutant can induce normal calcium spiking, however, the calcium flux that is considered to be related to rhizobial infection is different from that of the wild type strain (unpublished data in the lab). The fact that *LYK3* knockdown plants displays more severe rhizobial infection phenotype when inoculated with the *S. meliloti nodF nodE* double mutant than with the wild type rhizobium suggests that LYK3 functions as a rhizobial entry receptor (Limpens et al., 2003).

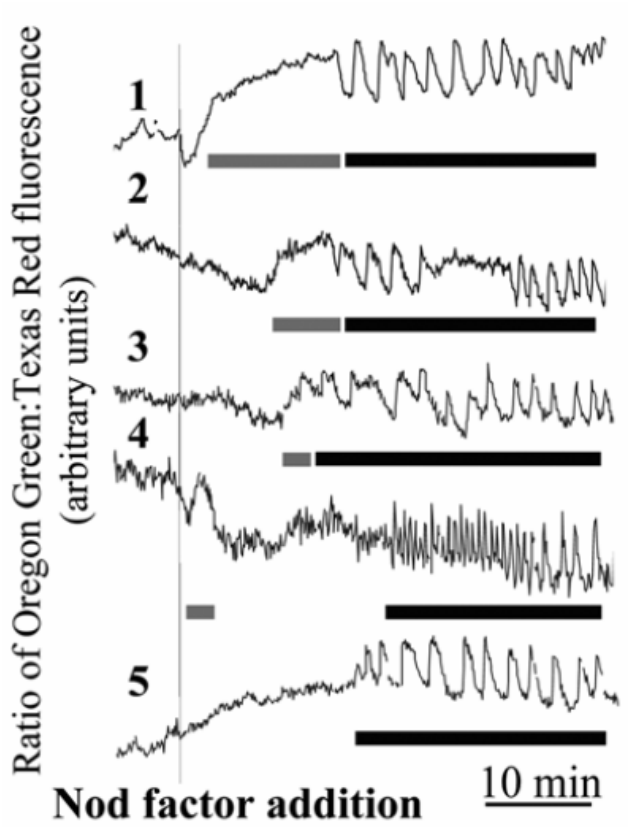


**Fig. 2.** Nod factor induced calcium flux and calcium spiking (Miwa et al., 2006). Grey bar: calcium flux; black bar: calcium spiking. The calcium spiking and calcium flux were monitored in roots hairs using using ratiometric fluorescence after microinjection with a mixture of dextran-linked Oregon Green and Texas Red.

Rhizobial extracellular polysaccharides or exopolysaccharides (EPS) have been well studied for their role in infection. They generally consist of monosaccharides and some non-carbohydrate substituents (such as acetate, pyruvate, succinate and phosphate) (Poli et al., 2011). They are secreted into the environment by most bacteria and are important for biofilm formation. In pathogenic bacteria, studies have shown a mild function for EPS in the suppression of plant defence (Aslam et al., 2008). An insight into the function of EPS in establishing pathogenesis compatibility was made when it was discovered that EPS can chelate calcium and that this chelation is associated with the suppression of the expression of defence genes (Aslam et al., 2008). However whether this effect is a direct result of calcium binding by the EPS is not clear. One thing worth noting is that the high-molecular-weight (HMW) bacterial EPSs have been linked with pathogenicity while in rhizobial infection, the low-molecular-weight (LMW) one is required for symbiosis.

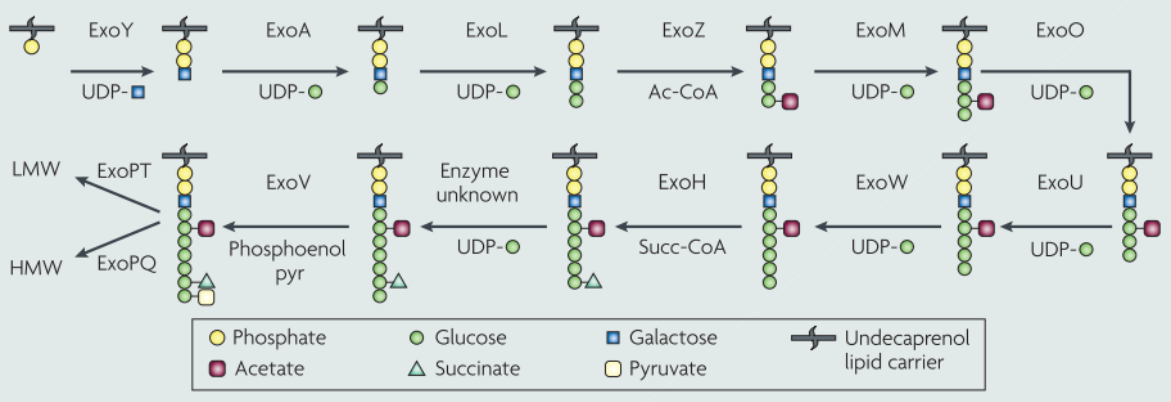


**Fig. 3.** *S. meliloti* succinoglycan biosynthesis pathway (Jones et al., 2007).

In rhizobia, EPS has been shown to have important functions in infection thread initiation and elongation. There are two functional LMW EPS identified, succinoglycan (EPS I) and galactoglucan (EPS II). Succinoglycan has been found to be more efficient than galactoglucan in mediating infection thread formation (Pellock et al., 2000). The *S. meliloti* 1021 lab strain used in this thesis does not have galactoglucan but still is effective at infecting *M. truncatula*. The biosynthetic pathway (Fig.3) for succinoglycan has been determined and ExoY (an adenylate cyclase) was shown to be the first enzyme in succinoglycan biosynthesis (Jones et al., 2007). The *exoH* gene is required for the succinyl modification. The *exoY* mutant aborts infection in the root hair curl and initiates very few infection threads (Cheng and Walker, 1998). In the *exoH* mutant the succinoglycan is not cropped so the LMW fraction is not produced (only HMW EPS is produced). The *exoH* mutant produces infection threads that abort in the cortex (Cheng and Walker, 1998). A constitutively active mutant of the transcriptional regulator *exoS* and a null mutant of the transcriptional regulator *exoR* both overproduce succinoglycan, and are defective in rhizobial infection. However, these two mutants also lack flagella, so the cause of the rhizobial infection defect is unclear (Yao et al., 2004).

Until now, there is still debate about whether EPS acts as a protective barrier shielding the bacteria from host defence or acts as a signalling molecule which is perceived by the plant. A microarray gene expression study was carried out to better understand the *exoY* infection phenotype. The study showed that two putative receptors are expressed more strongly inoculated with WT rhizobia compared with an *exoY* mutant. They were considered as possible succinoglycan receptors in the paper. The plant defence response genes were more strongly expressed in the *exoY* inoculated plants (Jones et al., 2008), implying plant defence is suppressed by the presence of EPS. Also, another paper states that rhizobial strain specificity on *M. truncatula* plants is correlated with succinoglycan oligosaccharide structure (Simsek et al., 2007). These suggest EPS may function as a signalling molecule.

K-antigen polysaccharide (KPS) is another type of secreted polysaccharide. It has a disaccharide repeating unit containing glucuronic acid and a modified pseudaminic acid residue. It is significantly less efficient than succinoglycan in mediating infection thread elongation but more efficient than galactoglucan (Pellock et al., 2000). Since the function is not crucial for nodulation, there have not been a lot of studies on it.

In addition to these polysaccharides and Nod factors some rhizobial metabolic genes are also required for rhizobial infection. Some *Rhizobium etli* mutants that are defective in anabolic pathways (such as biosynthesis of lysine or purine) abort rhizobial infection in the invaded root hairs (Ferraioli et al., 2004). However, the importance of these metabolites in rhizobial infection has been argued, because the infection phenotype may simply be due to a general decreased fitness of the rhizobia.

## 4.2 Plant control of rhizobial infection

In infection threads, the matrix inside the lumen of the infection thread contains material that is normally found as part of the extracellular matrix of the plant cell wall. It has been suggested that the infection matrix is made by hydrogen peroxide cross-linking the legume-specific arabinogalactan protein-extensins (AGPE) (Gage, 2004). Researchers have used immunogold to localize AGPEs and found there is an alteration of AGPEs in the infection thread matrix in *sym33* which blocks infection thread formation. The authors suggested this correlates with defect in endocytosis of rhizobia into the host cytoplasm (Tsyganova et al., 2009).

There have been several genes identified in legumes that function in rhizobial infection. They are *VAPYRIN* (Murray et al., 2011), *LIN/ Cerberus* (Kuppusamy et al., 2004; Kiss et al., 2009; Yano et al., 2009), *RIT1/ NAP1*, *PIR1*, *CRINKLE* (Tansengco et al., 2003; Yokota et al., 2009; Miyahara et al., 2010), *FLOTILLIN2 and FLOTILLIN4* (Haney and Long, 2010), *IPD3*/ *CYCLOPS* (Messinese et al., 2007; Yano et al., 2008; Horváth et al., 2011), *PUB1* (Mbengue et al., 2010), *RPG* (Arrighi et al., 2008), *REMORIN* (Lefebvre et al., 2010), *PECTATE LYASE* (Xie et al., 2011), *ALB1* (Imaizumi-anraku et al., 1997; Imaizumi-Anraku et al., 2000; Yano et al., 2006) and others (Table 1). The function of some of these genes is still unknown, but others have contributed to our understanding of rhizobial infection.

In emerging root hairs, microtubules are found parallel to the elongation axis of the cell with the nucleus close to the tip of the root hair (Timmers et al., 1999). Similar cytoskeletal rearrangements have been shown to be associated with infection thread formation. After activation by rhizobia, microtubules gradually concentrate to the tip of the root hair surrounding the nucleus (Timmers et al., 1999), this may lead to root hair swelling and branching. During root hair curling, microtubules organize into arrays and progressively converge to the curl centre (Timmers et al., 1999). During

infection thread progression, microtubules organise to form a dense network surrounding the growing infection thread and connect the nucleus to the growing tip. Microtubules accumulate at both sides of the adjacent cells when infection threads are about to cross between cells. Once the infection thread has penetrated into initial primordium cells, microtubules concentrate in the region of the cell facing the advancing thread and can't be observed in the cells through which the infection thread has already passed (Timmers et al., 1999). Actin rearrangement is a prerequisite for infection thread formation. Similar to microtubules, it was reported that the actin filaments localise in parallel to the elongation axis of the growing root hair cell. After application of Nod factors, fine actin filaments accumulate at the root hair tip. After continuous exposure to Nod factors, bundles of actin microfilaments reappear in the shank of the root hair (Crdenas et al., 1998). Mutants that have been identified as being defective in rhizobial infection have been shown to have actin rearrangement defects. NAP1 and PIR1 are components of the SCAR/WAVE complex (Yokota et al., 2009). ARPC1 is a subunit of ARP2/3 complex (Hossain et al., 2012). SCAR/WAVE complex is required to activate the ARP2/3 complex, which is necessary for actin filament formation and organisation (Smith and Oppenheimer, 2005). The *nap1* and *pir1* mutants abort rhizobial infection mostly in the epidermis. In elongating root hairs, these mutants form actin filaments that spiral along the root hairs instead of in parallel to the elongation axis as seen in the wild type. Also, after Nod factor application, there is no accumulation of the fine actin filaments in the root hair tip of *nap1* and *pir1* (Yokota et al., 2009). This latter change may directly result in the mutant rhizobial infection phenotype. The defects in these mutants are not specific to rhizobial infection; these mutants also displayed defects in trichome and root hair development (Yokota et al., 2009). The third component that has been proved to function in infection thread initiation is lipid rafts. These are glycolipoprotein microdomains that are composed of a combination of glycosphingolipids and protein receptors on the cell plasma membranes. These specialized membrane microdomains compartmentalize cellular processes by serving as organizing centres for the assembly of signalling molecules, influencing membrane fluidity and membrane protein trafficking and regulating neurotransmission and receptor trafficking (Pike, 2009). Two components have been identified to function in rhizobial infection: flotillins and remorins. Flotillins have been found to mediate membrane-shaping events including membrane budding, actin-

mediated neuronal differentiation and filopodia function (Haney and Long, 2010). There are 7 flotillins in *M. truncatula*, Flotillin2 (FLOT2) and Flotillin4 (FLOT4) have been found to have roles in rhizobial infection. Without rhizobia inoculation, FLOT2 and FLOT4 localise to punctate dots on the root hair membrane. Upon inoculation, FLOT4 relocalises to the periphery of the root hair cells and later surrounds the infection threads (Haney and Long, 2010). Also FLOT4 and LYK3 colocalization in the root hair cell increases significantly after rhizobia inoculation (Haney et al., 2011), implying a function for FLOT4 in organising Nod factor receptors in rhizobial infection.

Plant-specific remorin proteins don't contain transmembrane domains, but they have been found exclusively in detergent-insoluble membrane fractions prepared from plasma membrane extracts. Until recently, several remorin family members have been found to be differentially regulated during plant-microbe interactions but a clear role had not been demonstrated. A *M. truncatula* remorin MtSYMREM1 has been implicated both in nodule development and in rhizobial infection. The mutant displays sac-like and highly branched infection threads. MtSYMREM1 also localizes in the infection thread membranes and rhizobia release sites. It colocalizes with LYK3, NFP which are Nod factor receptors and DMI2 (Lefebvre et al., 2010), but has not yet been shown to localize to microdomains. One possibility is that FLOT2, FLOT4 and MtSYMREM1 are required for proper localization of the Nod factor receptor complex.

The fourth component required for infection is the ubiquitin protein degradation pathway. Ubiquitination is a post-translational modification carried out by a set of three enzymes, E1, E2 and E3. Ubiquitin is first activated by ubiquitin activating enzyme E1. The ubiquitin is then passed on to the second enzyme, ubiquitin conjugating enzyme E2. Then E3, the ubiquitin ligase recognises and binds to its target and labelling it with ubiquitin. The whole processes can be repeated until a chain of ubiquitin is formed and three or more ubiquitins usually target the substrate into the proteasomes (Kerscher et al., 2006). Substrate specificities are defined by E2 and E3 combinations. E2 enzymes share many well conserved catalytic domains, E3 ligases only share several conserved motifs, therefore they are quite specific (Kerscher et al., 2006). There have been several E3 ligases identified required for rhizobial infection. The most well studied one is PUB1. PUB1 functions negatively in nodulation. Evidence shows that the Nod factor receptor LYK3 phosphorylates PUB1

*in vitro*, and *PUB1* knockdown can partially recover the *lyk3* mutant infection phenotype (Haney et al., 2011). It would be informative to determine the LYK3 phosphorylation site of PUB1 and observe the phenotype of a point mutation in the PUB1 phosphorylation site. And it will be equally important to find out PUB1 targets to pull out components of the LYK3 related signalling pathway. Recently, a family of E3 ligases called SEVEN IN ABSENTIA (SINA) was identified in plants (Den Herder et al., 2008). SINA4 , which was shown to interact with and mediate the degradation of SYMRK, negatively regulates rhizobial infection (Den Herder et al., 2012). Opposite to PUB1, LIN, a putative E3 ligase, functions as a positive regulator to rhizobial infection. *lin* aborts infection in root epidermis (Kuppusamy et al., 2004), and it encodes a novel type of U-box/WD40 protein (Kiss et al., 2009). However, its function in rhizobial infection is not clear. These findings make it clear that protein turnover plays a key role in rhizobial infection.

Not surprisingly, hormones have important roles in rhizobial infection. What we know from literature very clearly is that ethylene represses infection. Ethylene also suppresses root hair responses to Nod factor and the maintenance of Nod factor induced calcium spiking (Oldroyd et al., 2001).The *M. truncatula sickle (skl)* mutant, the ortholog of *A. thaliana ein2,* which is insensitive to ethylene, is hyper-infected (Penmetsa and Cook, 1997; Varma Penmetsa et al., 2008). The infected root hair microarray in *sickle* shows that during infection most infection related genes are induced more strongly in *skl* compared with wild type (A. Breakspear unpublished data). Cytokinin may also play a negative role in rhizobial infection, because *hit1* which mutated in the cytokinin receptor LHK1/CRE1 is hyper-infected (Murray et al., 2007). However it may be caused by a positive feedback mechanism rather than be a direct effect of reduced cytokinin signaling since the *hit1* lacks cortical cell divisions. Combining *hit1-1* with the autoactive *CCaMK snf1* spontaneous nodulation mutant showed a similar nodulation phenotype as *hit1-1*, suggesting that LHK1/CRE1 acts downstream of CCaMK. So, as the case with auxin, there is no genetic evidence showing a direct role for cytokinin in infection. Recently, microarray from root hairs of infected plants has identified several auxin and cytokinin related signalling genes upregulated during rhizobial infection (Andy Breakspear unpublished data) leaving open the possibility that these hormones play direct roles in rhizobial infection.

In addition to the cytoskeleton rearrangements, protein turnover, lipid rafts, cell wall remodelling and hormones function in rhizobial infection, there are probably additional unknown processes related to infection thread initiation and elongation. Legume scientists are using genetics, microarrays, cell biology and other approaches, trying to identify them. I have used a molecular genetic approach to study infection thread development.

Concluding remark: Rhizobial infection has increasingly become an attractive topic in legume-rhizobia interaction. Researchers worldwide have been using forward and reverse genetics, transcriptome, protein-protein interactome and so on to try to identify new elements involved.

# 5 Coordination of nodule organogenesis and rhizobial infection

To make a functional nodule, the interconnection of rhizobial infection and nodule organogenesis is crucial. Nod factors induce root hair deformations at the same time as cortical cells are activated. Root hair cells entrap rhizobia inside the root hair curl, which is concomitant with cortical cell divisions. After that, the tube like structures which contains rhizobia, called the infection threads, form in the root hair and develop into the root to penetrate the nodule (Timmers et al., 1999; Kosuta et al., 2008). Nodules initiate opposite to the protoxylem poles. It is believed ethylene plays a role in this positional regulation. One of the evidences is in *sickle* mutant, this spatial regulation is completely lost (Penmetsa et al., 2003). Following the release of the rhizobia the nodule begins to develop and the meristem is established. As the nodule grows several vascular bundles develop from the stele and grow peripherally to serve in the exchange nutrients between roots and nodules (D'Haeseleer et al., 2010). Nod factor signalling mutants are defective for both organogenesis and infection thread development. In particular, CCaMK has been shown to coordinate rhizobial infection and nodule organogenesis (Madsen et al., 2010) maybe through the control of NIN.

Recently, there are two papers illustrating functions of the different domains of CCaMK in nodule organogenesis and rhizobial infection (Shimoda et al., 2012; Takeda et al., 2012). From these papers, it seems the CCaMK EF hands present in the C-terminal regulatory domain are required for rhizobial infection but are not as

important for organogenesis. Another interesting study showed when they transform *ccamk* with CCaMK driven by an epidermal specific promoter, rhizobial infection is complemented but no cortical cell division is observed. But when they transform the *nfp* mutant with epidermal specific promoter driving NFP, they observed cortical cell divisions (Rival et al., 2012). This implies that NFP is not required in the cortex whereas CCaMK is.

In this study, I found further evidence that specific events in the epidermis are needed to induce nodule organogenesis in the cortex. The details will be discussed in Chapter IV.

# 6 NIN

*NIN* was the first symbiosis gene cloned in 1999 in *L .japonicus* (Schauser et al., 1999). It's clear that *NIN* expression is an important output of the nodulation signalling pathway since the *nin* mutant cannot form infection threads and cannot initiate nodule organogenesis. Later, orthologous *nin* mutants were identified in *M. truncatula* and *Pisum sativum* (Borisov et al., 2003; Marsh et al., 2007). Despite this, the progress on NIN's function has been limited. Bioinformatics predicts it is a transcription factor with a predicted a DNA binding domain. There is a predicted nuclear localisation signal (NLS) in the middle of the protein, and a DNA binding domain and a transcription activation domain follow the NLS. As mentioned above, CRE1 perception of cytokinin then activates *NIN* expression in the cortex and leads to nodule organogenesis (Tirichine et al., 2007). Also, data in the lab show that NIN binds the *CRE1* promoter *in vivo* and trans-activates *CRE1* expression in *N. benthamiana*. However, the N-terminal region of NIN has no known function, and is the least conserved (Schauser et al., 2005). My unpublished data (CHAPTER II) show that NIN localises in the nucleus in *Nicotiana benthamiana*. Data in the lab shows that NIN has transcription activation function and it can bind to DNA *in vivo*, proving that NIN is indeed a transcription factor. NIN's role in organogenesis has been discussed in the section on cytokinin above, below I discuss its role in infection.

## 6.1 NIN's function in rhizobial infection and nodule organogenesis

*nin* has a unique infection-related phenotype as it shows excessive root hair curls (Borisov et al., 2003; Marsh et al., 2007) that only occasionally entrap very few

rhizobia (CHAPTER II). The possibilities are that *nin* can't entrap enough rhizobia to allow formation of the infection pocket or that NIN is required for repression of root hair growth genes. As a transcription factor, NIN is an attractive subject to study using root hair RNA microarrays to identify downstream genes in order to identify other processes in infection. Recently it was demonstrated that NIN transcriptionally regulates a nodule-specific pectate lyase (*LjNPL*) gene, which acts as an enzyme to degrade the cell wall in rhizobial infection (Xie et al., 2011).

# 7 Lateral root development

*Arabidopsis thaliana* is the most commonly used model in studying lateral root development. *A. thaliana* lateral roots originate exclusively from pericycle founder cells located opposite to xylem poles. Lateral roots are initiated either by one or several pericycle founder cells several rounds of anticlinal divisions, forming a single layered primordia composed of up to ten small cells of equal sizes (Malamy and Benfey, 1997). Next, the cells divide periclinally, creating two layers. Further anticlinal and periclinal divisions form a dome-shaped primordium that eventually emerges from the parent roots (Swarup et al., 2008).

Auxin initially accumulates in the lateral root primodium central cells and later at the tip of the lateral root primodium. There it targets the degradation of AUX/IAA proteins, and enables ARF proteins to transcribe genes that pattern the lateral root primordium (Okushima et al., 2007; De Smet et al., 2010) It was reported that auxin primes the pericycle founder cells to divide into a lateral root primordium (De Smet et al., 2007).The specification of xylem pole pericycle cell fate is controlled by the same genetic pathway determining diarch patterning of the underlying root vasculature. The cells at the phloem poles are analogous to quiescent centre cells in root development, the cells opposite to the xylem poles are competent to form lateral root primordial.

## 7.1 Hormonal control of lateral root development

Auxin has been studied extensively in lateral root development and it functions in different stages. Once it was thought that auxin specifies prebranch sites. This is from the observation that priming of pericycle founders cells is correlated with an oscillating auxin response (visualized using *DR5::GUS*) (De Smet et al., 2007).

However, later it was found that it was not auxin itself, but a more general oscillating gene expression process ─ biological clock that determines plants *in vivo* control of lateral root emergence sites (Moreno-Risueno et al., 2010). A lot of genetic components in the auxin signalling pathway have been identified to function in lateral root development. For example, IAA14 is one of the most important auxin signalling proteins regulating lateral root initiation (Fukaki et al., 2002). It belongs to a family of unstable AUX/IAA proteins that function to repress auxin-regulated transcription. A key step in lateral root initiation is the degradation of IAA14. The gain of function *iaa14*/*slr-1* mutant does not form lateral root primordium as a result of pericycle founder cells failing to undergo formative divisions (Péret et al., 2009).

Cytokinin has been considered as antagonising auxin in root development. In lateral root development, cytokinins influence lateral root primordium patterning, mainly through affecting lateral root founder cell identity, more mechanistically, through suppressing the expression of the gene's encoding the PIN proteins. And this inhibition effect can't be altered by the addition of auxin (Laplaze et al., 2007).

Ethylene has also been studied in lateral root development. Enhanced ethylene biosynthesis promotes lateral root primordial initiation. However, higher doses inhibit pericycle cells to initiate lateral root primodia, but promote the emergence of the existing lateral root primordia. Ethylene is not able to inhibit lateral root formation when the tissues formed before ethylene treatment, but is able to inhibit the ones formed after ethylene application (Lewis et al., 2011). Combined with genetics evidences (Negi et al., 2008; Lewis et al., 2011), all the results suggest there is a strong connection in auxin and ethylene function in lateral root formation.

## 7.2 Lateral root development in *M. truncatula*

Most lateral root development studies have used *A. thaliana* as a model plant. In Arabidopsis the lateral root primordia develop from pericycle cell layers. However, there are studies in other species including legumes that lateral root development involves cortical cell divisions (discussed in (Op den Camp et al., 2011)). These studies show that the hormonal control of lateral root development varies among plant species.

### 7.3 Interaction between nodule organogenesis and lateral root development

From the literature we know that nodules are initiated from cortical cell divisions and lateral roots are developed from pericycle cell divisions. The hormonal control of these two processes is opposite. Cytokinin is the driving force in nodule organogenesis, whereas auxin drives lateral root development. There are several interesting studies of alterations of the manner of cell divisions that occur in relation to changes in auxin transport and signalling. One of them is from studies using the auxin polar transport inhibitor NPA. The application of NPA causes spontaneous nodules in *M. truncatula* (Rightmyer and Long, 2011), *M. sativa* (Fang and Hirsch, 1998) and white clover (Wu et al., 1996), however these nodules either lack vascular bundles or develop abnormal central vasculature. In another study type-A cytokinin response regulator *MtRR9* was overexpressed and resulted in cell divisions leading to the formation of lateral root-like primordia (Op den Camp et al., 2011). The above two studies suggest that changes in either auxin or cytokinin signalling in legumes may result in different developmental outcomes.

## 8 Experimental approach

To study rhizobial infection in nodulation, I used two approaches. The first one is to make use of the *nin* mutant which aborts rhizobial infection in the root hair curl. I extracted *nin* root hair RNAs and carried out a microarray analysis to try to identify the genes NIN regulates in rhizobial infection. The second approach is to try to identify more genetic components involved in rhizobial infection using forward genetics. Both of these approaches proved to be quite effective and I have identified several components potentially involved in nodulation rhizobial infection.

# CHAPTER II NIN

## 1 Background

NIN is a putative transcription factor with an RWP-RK domain which is predicted to be involved in DNA binding and a PB1 domain which is involved in the heterodimerization with other PB1 domain containing proteins (Ponting et al., 2002). A nuclear localisation signal (NLS) is found in the middle of the protein (Fig. 1). However, the N-terminal part is of unknown function, contains two putative transmembrane domains, and has the lowest identity among gene family members (NIN-Like Proteins, NLPs). However, NIN is required for the expression of *NPL* and can bind its promoter *in vitro* (Xie et al., 2011). Here I show that NIN localises in the nucleus in *Nicotiana benthamiana* and that there a major changes in gene expression in the *nin* mutant background, suggesting that NIN is a transcription factor.

*NIN* was the first symbiosis gene cloned in 1999 in *Lotus japonicus* (Schauser et al., 1999). The *nin* mutant cannot form infection threads and cannot initiate nodule organogenesis. During infection, the *nin* mutant aborts rhizobial infection in the root hair curl, the root hair displays excess curling (Borisov et al., 2003; Marsh et al., 2007). Biochemical analysis shows *L. japonicus Nodulation Pectate Lyase* (*NPL*) which functions in infection thread initiation is under the direct control of NIN (Xie et al., 2011). However, this cannot be the only downstream target of NIN. Since the NIN phenotype is much stronger than *npl*, which eventually forms normal looking infection threads. Based on the strong *nin* phenotype, it should control additional earlier steps before infection thread initiation. Using genetics, we also know that NIN functions downstream of the cytokinin receptor in nodule organogenesis (Tirichine et al., 2007; Madsen et al., 2010). Interestingly, the *nin* mutant phenotype has never been fully complemented. There is one report using *pNIN*::*NIN* CDS to complement the *nin* mutant in *L. japonicus*, in which rhizobial infection was restored, but not cortical cell divisions (Yokota et al., 2010).

There are several different NIN like proteins (NLPs) in plants. Other than NIN itself, the best studied one is *Arabidopsis thaliana* NLP7. The *nlp7* mutant shows defect in

nitrate sensing, and nitrate assimilation. It also shows a phenotype in low nitrate growth condition (Loren et al., 2009). In this analysis, I attempt to investigate NLP protein family evolution to learn about NIN function from an evolutionary point.

# 2 Results

## 2.1 NIN localises in the nucleus

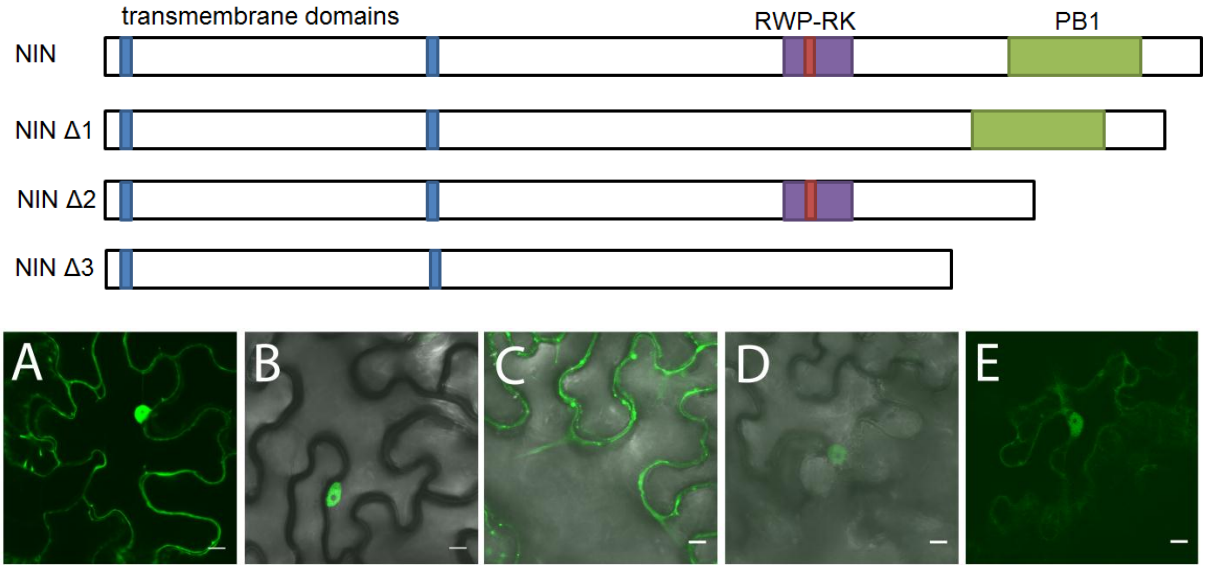


**Fig. 1.** MtNIN protein structures and different NIN deletion variants localisation in *Nicotiana benthamiana*. The Medicago truncatula NIN full length protein contains 933 amino acids (aa). The blue boxes show the predicted transmembrane domains (3 aa-22 aa and 318 aa-334 aa). The red box shows predicted nuclear localisation signal (608 aa-612 aa). The purple box shows RWP-RK domain (610 aa-664 aa). The green box shows the PB1 domain (832-913 aa). NINΔ1 represents NIN without RWP-RK domain (ΔRWP-RK), NINΔ2 represents NIN without PB1 domain (ΔPB1); NINΔ3 represents NIN without both RWP-RK and PB1 domains (ΔRWP-RK & ΔPB1). (A-E) NIN proteins localisation in *N. benthamiana*. (A) empty GFP; (B) NIN; (C) NINΔ1; (D) NINΔ2; (E) NINΔ3. Scale bar= 10 µm.

The full length *NIN* coding region was amplified and either N or C terminal fusions to GFP localized in the nucleus in *N. benthamiana* leaves (Fig. 1B). Without the RWP-RK domain (with NLS in it), the protein is excluded from the nucleus (Fig. 1C). The ΔPB1 variant still localises in the nucleus (Fig. 1D). When both domains are removed (ΔRWP-RK & ΔPB1), the fluorescence is observed in the cytoplasm and nucleus similar to free GFP (Fig. 1E). However, NIN-GFP was not detectable with a western using anti-GFP antibody. The anti-GFP antibody was used successfully to detect DMI3-GFP using the same system. Attempts to visualize NIN-GFP in *M. truncatula* roots with either the native promoter or 35S promoter were unsuccessful.

## 2.2 Overexpression of *NIN* suppresses nodulation

In order to try to complement the *nin* mutant phenotype, *NIN* was overexpressed using the *Agrobacterium rhizogenes* hairy root transformation system. The attempt at complementation was not successful, but remarkably, I observed repression of nodulation in the WT control plants overexpressing full length *NIN* (Fig. 4A). To investigate this phenomenon, I first confirmed that *NIN* transcripts were present in the *NIN* overexpression roots using QPCR (Fig. 4B). I then considered the possibility that overexpression of the NIN transcript may have induced post transcriptional gene silencing (PTGS) (Depicker and Montagu, 1997). To address this question, we obtained a *M. truncatula* RNA dependent RNA polymerase 6 (*rdr6*) mutant line from Dr. Martin Crespi. RDR6, also known as SDE1 and SGS2, is one of six RNA dependent RNA polymerases in RNA silencing machinery (Dalmay et al., 2000; Mourrain et al., 2000). The *rdr6* line is deficient for PTGS (Curaba and Chen, 2008). Unfortunately, when I introduced the *NIN* overexpression construct into the *rdr6* line, almost no transformed roots were obtained although normal numbers of transformed roots were observed using the empty vector control. Two independent experiments showed the same results. Therefore we cannot be totally sure that NIN repression of WT nodulation is not caused by gene silencing. However, this result may suggest that strong overexpression of the NIN protein may interfere with root growth or emergence, at least in the hairy root system. Since western blots of NIN had been unsuccessful in the past, we used another strategy to determine whether this phenomenon required expression of the NIN protein. To do this, I created constructs to express NIN variants lacking RWP-RK domain (ΔRWP-RK; NINΔ1); PB1 domain (ΔPB1; NINΔ2); and both together (ΔRWP-RK & ΔPB1; NINΔ3). These truncations were expressed fused to an N-terminal GFP tag. The effects of these constructs on nodulation were tested using the hairy root system. Results showed that all of the deletion constructs were able to suppress nodulation relative to the empty vector control (Fig. 4A). The –RWP-RK & –PB1 construct was less effective in repression nodulation than the other constructs. When marker genes were analyzed, the –RWP-RK & –PB1 had the strongest expression. However, 6 out of 11 plants failed to produce nodules (compared to 4 of 20 plants on the empty vector control) and the average nodule numbers are comparable to empty vector control (Fig. 2A). In the –RWP-RK construct, only 1 out of 13 plants produced nodules compared to the

complete repression of nodulation seen using the full length NIN construct. This indicates that the DNA binding function of NIN may not be required for repression of nodulation, making PTGS mechanism seem likely.

Strangely, the phenomenon of NIN repressing nodulation is not consistent across labs. Another lab showed that p*35S*::*NIN* coding sequence (CDS) did not block WT nodulation in *M. truncatula* in (personal communication, Rene Geurts). Also, in recent experiments in our lab using a different construct it was found that pUbiquitin:: *NIN* genomic sequence does not block WT nodulation in *M. truncatula*. However, we learned that p*Ubiquitin*:: *NIN* genomic sequence or p*Ubiquitin*:: *NIN* CDS blocks WT nodulation in *L. japonicus* (personal communication, Makoto Hayashi). This is an interesting phenomenon, but it will be difficult to investigate the mechanism involved, so for now we still don't have a clear explanation about why NIN overexpression can suppress WT nodulation.

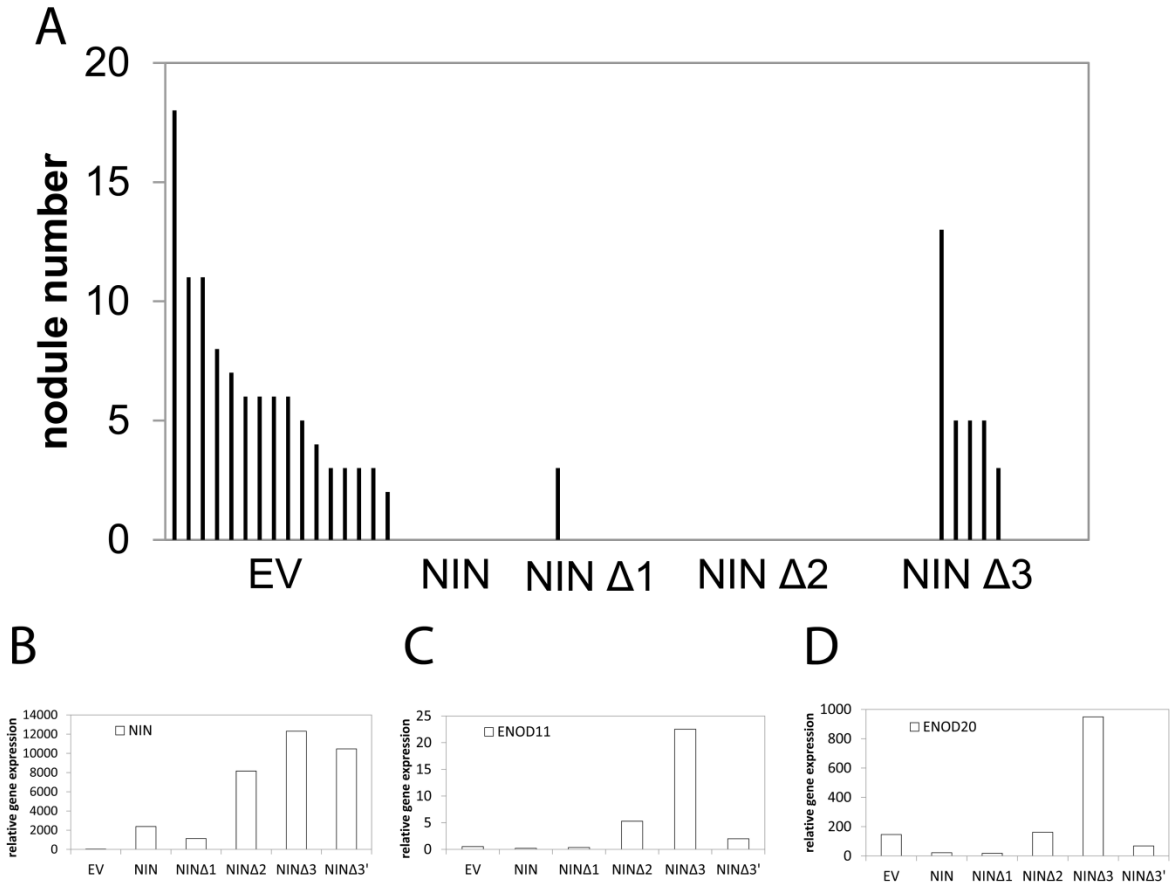


**Fig. 2.** *MtNIN* overexpression represses nodulation in WT. (A) *MtNIN* deletion construct overexpression nodule numbers in transformed WT hairy-root roots. Each column represents one single plant. (B) *MtNIN* gene expression in the different domain deletion overexpression hairy root transformants. (C-D) Marker genes *MtENOD11* (C) and *MtENOD20* (D) gene expression in *MtNIN* different domain deletion overexpression hairy root transformants. (B-D) QPCR were done with several plants bulk materials. EV: empty vector; NIN: *MtNIN* genomic full length; NINΔ1: *MtNIN* genomic full length (ΔRWP-RK); NINΔ2: *MtNIN* genomic full length (ΔPB1); NINΔ3 in (A): *MtNIN* genomic full length (ΔRWP-RK & ΔPB1); NINΔ3 in (B-D): *MtNIN* genomic full length (ΔRWP-RK & ΔPB1) with nodules; NINΔ3’ in (B-D): *MtNIN* genomic full length (ΔRWP-RK & ΔPB1) without nodules.

## 2.3 *nin* root hair microarray

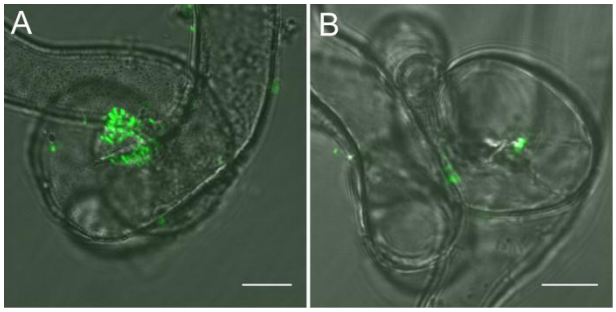


**Fig. 3.** *nin* mutant rhizobial infection phenotype. (A) WT and (B) *nin* mutant root hair infection phenotype. Pictures were taken 7 days post *S. meliloti* 1021 inoculation on BNM plates. Some rhizobial entrapment is seen, but no normal size microcolonies within infection pockets were seen. Green fluorescence indicates rhizobia. Scale bar= 10 µm.

A

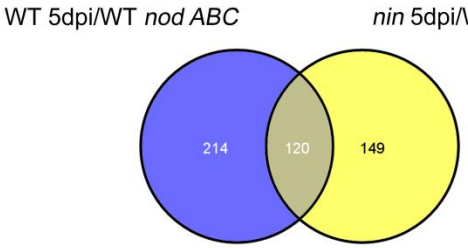


B

| sym genes induced in A17 5dpi, repressed in *nin* 5dpi VS A17 5dpi | |
|---|---|
| *RPG* | Mtr.1440.1.S1_at |
| *CBS1* | Mtr.23516.1.S1_at |
| *Pectate Lyase* | Mtr.26489.1.S1_at |
| *MtANN1* | Mtr.14183.1.S1_at |
| *MtHAP2.1* | Mtr.43750.1.S1_at |
| *RIP1* | Mtr.25211.1.S1_at |
| *ENOD40* | Mtr.12359.1.S1_at |
| *RIP1* | Mtr.25211.1.S1_s_at |

C

| myccorhization genes induced in *nin* 5dpi VS A17 5dpi | |
|---|---|
| *Lectin like kinase* | Mtr.7279.1.S1_s_at |
| *HAP3 (NFYB)* | Mtr.4282.1.S1_at |
| *Catalase* | Mtr.35719.1.S1_at |
| *HAP5 (NFYC)* | Mtr.51511.1.S1_at |
| *H+-ATPase* | Mtr.43470.1.S1_at |
| *serine/threonin protein kinase* | Mtr.50698.1.S1_at |
| *nucleoside phosphorylase* | Mtr.40235.1.S1_at |
| *Cytochrome P450* | Mtr.23217.1.S1_at |

D

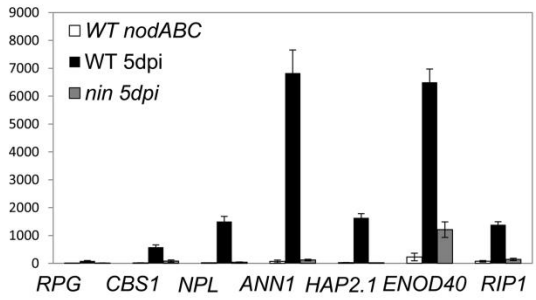


E

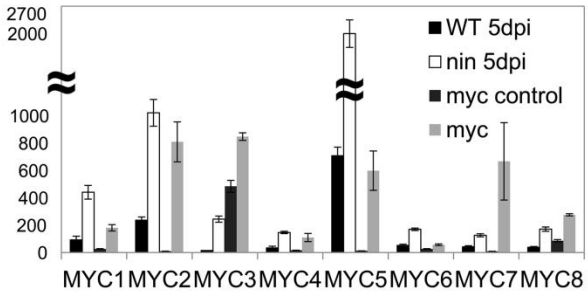


**Fig. 4.** Summary of *nin* root hair microarray results. (A) Blue circle: Probe sets number (214) induced 3 fold in WT *S. meliloti* 1021 5dpi compared with WT *S. meliloti* 1021 *nodABC* control. Yellow circle: Probe sets number repressed 3 fold in *nin* mutant *S. meliloti* 1021 5 dpi (149) compared with WT *S. meliloti* 1021 5 dpi. Shared: Probe sets number (120) of genes that are required for NIN induction during rhizobial infection. An MeV (MultiExperiment viewer, used for microarray analysis) Delta threshold value of 2.8 (statistical analysis) was used as an additional criterion. (B,D) Eight symbiotic genes probe sets required for NIN induction during rhizobial infection (down regulated in *nin S. meliloti* 1021 5dpi compared with WT *S. meliloti* 1021 5dpi). (B) Symbiotic genes probe sets and (D) symbiotic genes expression from root hair microarray in 3 biological replicates. (C,E) 8 gene probe sets induced in mycorrhization and more than 3 fold induced in *nin S. meliloti* 1021 5 dpi compared with WT *S. meliloti* 1021 5 dpi. (C) Mycorrhization induced genes probe sets and (E) mycorrhization induced genes expression from root hair microarray in 3

biological replicates and *Medicago truncatula* Gene Atlas (myc control and myc). All error bars show standard deviation (n=3); dpi: days post inoculation; myc: mycorrhization.

In *M. truncatula*, rhizobial infection occurs through root hairs. To learn more about rhizobial infection, it is important to know which gene transcripts change their level of expression in the root hairs during rhizobial infection. Rhizobial infection occurs in isolated root hair cells surrounded by non-infected cells. Previous microarray analysis used whole root systems which was not sensitive enough to study rhizobial infection. For this purpose, Dr. Andy Breakspear in the lab developed a root hair isolation method in which root hairs were removed from plants by brushing using liquid nitrogen. Using this method, he was able to isolate enough root hairs RNA for microarray analysis. He analysed samples from WT plants 3 dpi and 5 dpi *Sinorhizobium meliloti* carrying the *hemA*::*lacZ* fusion or a *S. meliloti nodABC* (non-Nod factor producing mutant) as a control. The result was very informative; some known rhizobial infection genes were upregulated quite dramatically and some unknown genes were identified, and some processes that may be involved in rhizobial infection were also revealed. NIN is a key component in rhizobial infection. *nin* mutants has defects in infection foci formation, with very few rhizobia entrapped (Fig. 3). To better understand NIN's function, I studied gene expression in *nin* root hairs 5 days post inoculation with *S. meliloti* 1021 following Dr. Breakspear's protocol. Using three fold cut off, 120 genes were downregulated in the *nin* mutant (Fig. 4A) (appendix Table 4). The *nin* root hair microarray confirmed previous biochemical experiments that showed that *NPL* is a direct target of NIN (Fig. 4D). The data also revealed that in *nin* root hairs, *HAP2.1* gene expression is not induced, suggesting *HAP2.1* may be another direct target of NIN. No *hap2.1* mutant has yet been reported so its effect on infection is unknown. At the same time, more candidate targets have been identified (Fig. 4B and D). *ENOD40* has been reported to be induced in the cells surrounding vascular bundles associated with nodulation (Yang et al., 1993). It's function in rhizobial infection or the gene expression in the epidermis has not been reported. In the root hair microarray, it has been identified that ENOD40 is induced in WT during rhizobial infection and the gene expression is under NIN control. Interestingly, the newly identified *CBS1* (CHAPTER III) acts downstream of NIN in rhizobial infection (Fig. 4D).

In addition to the many genes downregulated by NIN, a smaller set of 31 probesets were 3-fold increased compared to the WT control, suggesting NIN has a role in

gene repression. None of these genes have been previously studied, but they include an $H^+$-ATPase, several regulatory genes (transcription factors and kinases) and some genes encoding proteins with roles in secondary metabolism.

Remarkably, 8 of the 31 probesets are significantly induced primarily during mycorrhization, having no expression in nodules or other tissues (Fig. 4C and E).

## 2.4 NLPs phylogenetic analysis

NIN belongs to a small gene family of NLPs (NIN-like proteins) characterized by the presence of RWP-RK and PB1 domains (Schauser et al., 1999; Schauser et al., 2005). Using a BLAST search of the Phytozome database (www.phytozome.net), 4 NLPs in *M. truncatula* were retrieved. Expression profiles of these NLPs were investigated using *Medicago truncatula* Gene Expression Atlas and this surprisingly revealed a second NLP, in addition to NIN, that is specifically expressed in nodules (probeset number Mtr.29529.1.S1_at, gene ID Medtr4g092610.1). This gene, which I designate *NLP1* is not induced at 4 dpi, but is highly expressed at 10 dpi and later nodule time points, coinciding with the onset of nitrogen fixation (Fig. 5). This is quite an interesting finding because there is no mention of any other NIN-like genes involved in nodulation in the literature, other than mention of two NLPs (*LjNLP1*, *LjNLP2*) isolated from nodule cDNA libraries in *L. japonicus*. (Schauser et al., 2005).

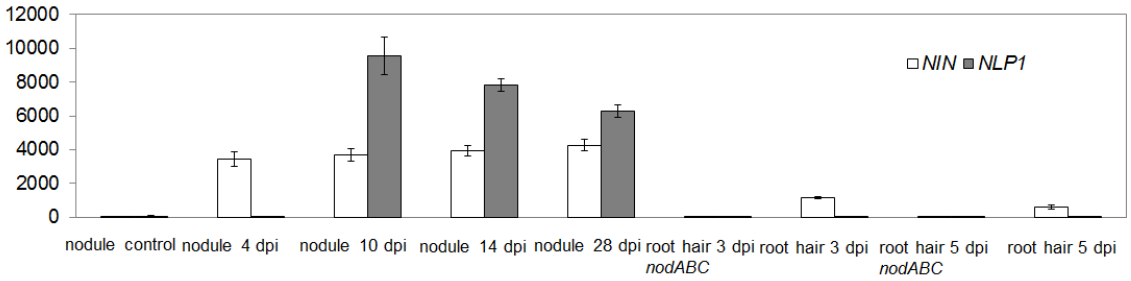


**Fig. 5.** *NIN* and *NLP1* gene expression in nodules and root hairs.

Gene expression data obtained from *Medicago truncatula* Gene Expression Atlas. Error bars represent standard deviation.

Using the maximum likelihood method, a phylogenetic tree was created using NLPs from *M. truncatula*, *Populus trichocarpa, Phaseolus vulgaris*, *Glycine max*, *Arabidopsis thaliana*, *Oryza sativa*, *L. japonicus* and *P. sativum* (Fig. 6). *NIN* (Medtr5g106690.1) and *NLP1* (Medtr4g092610.1) cluster separately suggesting they are not very closely related. Comparing the two clades, it seems NIN evolved earlier than NLP1. Interestingly, AtNLP7 which was earlier reported to function in nitrate signalling (Loren et al., 2009) is in the same clade as NLP1.

Based on *NLP1* gene expression, and the NLP1 clade in the phylogenetic tree, we can postulate how NLPs evolved. The ancestor of NIN and NLP1 split at one point and this leads to the separate evolution of NIN and NLP1. Probably, NIN first evolved, functioning in both rhizobial infection and nodule organogenesis and NLP1 may have an important role in nitrogen fixation, consistent with its expression at 10 dpi.

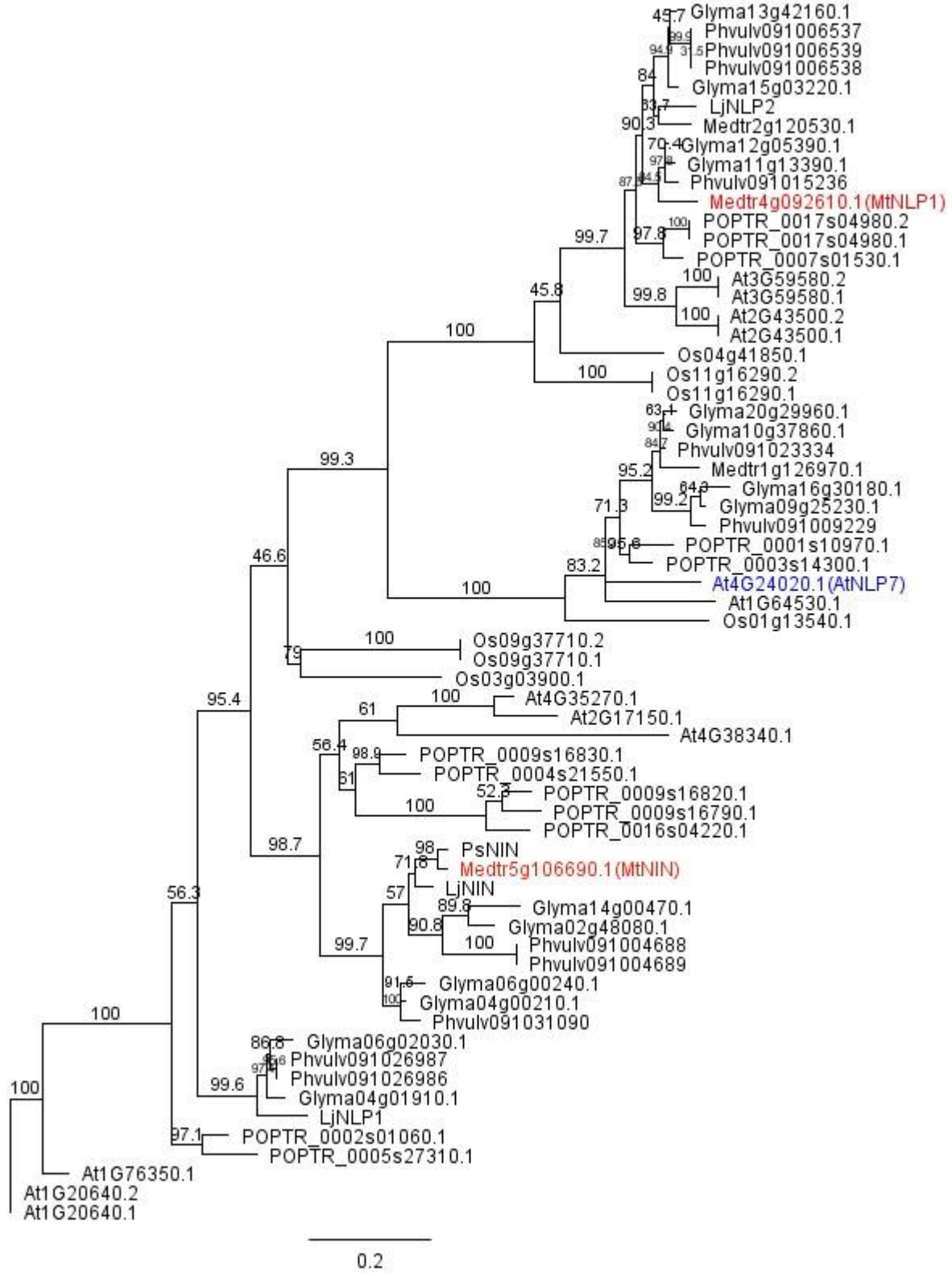


**Fig. 6.** Phylogenetic tree of NLPs.

The tree was created using PHYMaximum Likelihood method. 8 species are included in the tree construction. At: *A. thaliana*; Os: *O. sativa*; Glyma: *G. max*; Mt: *M. truncatula*; Lj: *L. japonicus*; Ps: *P. sativum*; Phvulv: *P. vulgaris*; POPTR: *P. trichocarpa*. The numbers above the branches show the confidence value. Red texts highlight *M. truncatula* NIN and NLP1. Blue texts highlight *A. thaliana* NLP7. The scale below the tree shows divergence time.

# 3 Discussion

*NIN* appears to be a primary target of the symbiosis signalling pathway (Schauser et al., 1999; Marsh et al., 2007) and is an essential gene for nodule organogenesis and bacterial infection. The *nin* mutant blocks rhizobial infection in the root hair curl, entrapping very few rhizobia and showing no infection foci or infection threads. Considering that *NIN* encodes a transcription factors I assessed *NIN* function during rhizobial infection using a root hair microarray. The results suggest that *NIN* has a very important function in rhizobial infection by regulating several key infection related processes and some known rhizobial infection-associated genes. Interestingly, the microarray data suggested that *NIN* may function to suppress mycorrhization, through the suppression of mycorrhizal-associated transcription factors and this is discussed in more detail in the general discussion along with a detailed discussion of the *NIN* targets (CHAPTER V).

## 3.1 *NIN* overexpression represses WT nodulation

Surprisingly, the overexpression of *NIN* appears to suppress nodulation. Using different *NIN* deletions I show that the RWP-RK domain plays an important role in this suppressive function. However, the RWP-RK domain alone is not sufficient for nodulation suppression. The suppressive affect may be the result of silencing or the action of the NIN protein. My analyses indicate that the levels of *NIN* transcripts are high in the *NIN* overexpression lines, suggesting that any affect cannot be the result of RNA silencing. However, gene silencing also functions at a post transcriptional level (Depicker and Montagu, 1997). RNA dependent RNA polymerase 6 (RDR6) functions in post transcriptional gene silencing (Dalmay et al., 2000; Mourrain et al., 2000) and the *rdr6* mutant line is deficient in post transcriptional gene silencing (Curaba and Chen, 2008). Unfortunately overexpression of *NIN* in the *rdr6* line resulted in no hairy root transformants, making it difficult to use this genetic material and suggesting that *NIN* overexpression may have a detrimental effect on root development.

The suppressive effect of *NIN* overexpression may be the result of NIN action. The fact that *NIN* can act as a transcriptional repressor on symbiotic gene expression (Marsh et al., 2007) is supportive of this idea. If this were the case then I would predict that the N terminus has this suppressive effect. To test this I suggest

assessing the effect of a *NIN* N terminal deletion on the nodulation suppressive phenotype. The detailed study of this phenomenon may help unravel some important aspects of regulation in nodulation.

## 3.2 A close homolog of *NIN* expressed during nodulation

NIN is expressed in the root epidermis, the root cortex and in infected and uninfected cells of the nodule central tissue (Schauser et al., 1999; Kosuta et al., 2011). This suggests its function in rhizobial infection, nodule organogenesis and nitrogen fixation. Through phylogenetic analysis, a new NIN-like protein (*NLP1*) has been identified which clusters quite distinctly from NIN, in a separate group to the NLP family. Surprisingly, *NLP1* is specifically induced in nodulation (dramatically induced in nitrogen fixing nodules) but not induced at early stages of infection or in root hairs. From the phylogenetic tree created using a PHYMaximum Likelihood method, *NLP1* evolved later than *NIN*. Interestingly a second NLP sequence clusters quite close to *NLP1* in the phylogenetic tree. This *NLP* is induced during nodulation and in root hair cells, but the gene expression is not limited to nodulation.

An analysis of *NLP1* revealed homology to β-galactosidases. These constitute a large family of enzymes characterized by their ability to hydrolyze terminal, nonreducing β-D-galactosyl residues from β-D-galactosides. Several β-galactosidases, sometimes referred to as *exo*-galactanases, have been purified from plants and shown to possess *in vitro* activity against extracted cell wall material via the release of galactose from wall polymers containing β(1→4)-D-galactan (Smith et al., 1998). The closeness of *NLP1* and this β-galactosidase suggests *NLP1* may have β-galactosidase activity and this may provide an additional clue to *NIN* function.

This discovery of *NLP1* could open up several new lines of research. Most important is to determine the *NLP1* function during nodule development. RNAi knockdown of *NLP1* could be used to check for a nodulation phenotype, or a reverse screen could be carried out by TILLING or PCR screening the *Tnt1* retrotransposon mutant population (Tadege et al., 2008; Pislariu et al., 2012). Promoter GUS analysis p*NLP1*::GUS and p*NLP1*::GFP will be useful to check where *NLP1* gene expression is induced in the nodule and may help answer whether it has a role in nitrogen fixation or infection. It will be interesting to see whether *NLP1* has a role during nodulation and whether this function overlaps with that of *NIN*.

# 4 Materials and methods

## 4.1 Protein subcellular localization in *N. benthamiana*

The different *MtNIN* constructs, and a pCH32-C58C1 containing p*35S*::p19, were transformed into competent *A. tumefaciens* strain pCH32-C58C1 . Overnight cultures of pCH32-C58C1 with grown at 28 °C (< 20 h). Cells were harvested by centrifugation at 5000 g for 15 min at room temperature (RT) and thenresuspended in 10 mM $MgCl_2$ and 150 µg/mL acetosyringone (4'-Hydroxy-3,5-dimethoxyacetophenone) to an $OD_{600}$ of 0.22. *A. tumefaciens* cells transformed with *MtNIN* construct and p19 were then mixed and left in this medium for about 2 hours at RT. Young fully expanded leaves of 2-3-weeks-old *N. benthamiana* plants were then injected with this mixture. Fluorescence was then assayed: taking leaf discs 48-72 h after infiltration, and placing them between slides in water. Fluorescence was then observed using a Zeiss 510 Meta Confocal microscope.

## 4.2 *nin* mutant infection phenotype observation

A17 and *nin-1* mutant plants were germinated on BNM square plates (100 mm x 100 mm) containing 0.1 µM Aminoethoxyvinylglycine (AVG). After growing for 2 days, the seedlings were flood inoculated with *S. meliloti* 1021 expressing GFP. 5 days post inoculation, the rhizobial infection phenotype was checked under a Zeiss 510 Meta Confocal microscope.

## 4.3 *nin* root hair extraction and RNA purification

For each biological replicate, 200 *nin* mutant plants were used. After the seeds were germinated upside down on agarose plates and grown overnight to allow the radicles to emerge straight, the seedlings were put on DWA (1.5% agrose)+0.1 µM AVG plates (8 seedlings per plate). The medium in each plate has been pre-covered with a white filter paper.The seedlings were then placed on top of a filter paper with the radicles pointed down. After that, take another filter paper sprayed with 500 µL OD 0.05 *S. meliloti*. A Mucosal Atomisation Device (Intavent Direct) to spray. The filter paper was then placed on top of the seedlings. The plates were then placed upright,

being careful not to let the seedlings fall. 5 days later, the seedlings were individually removed from the plates and root hairs were removed by brushing in liquid nitrogen. The brush used was size 4 paint brush. A28 cm x 13 cm non-stick baking tin was used to hold the liquid nitrogen. In the process of brushing, the paint brush and the baking tin were kept cooled all times to prevent ice formation. The liquid nitrogen containing the root hairs were then poured into a conical bottom 45 mL PTFE centrifuge tube with a screw cap (VWR Cat. 525-0191) and stored in a -80 °C freezer for later RNA extraction. The Qiagen RNeasy Micro kit was used to extract RNA from the root hair cells.

## 4.4 *nin* root hair microarray

(performed by Christian Rogers)

After RNA extraction, RNA quality was checked using a BioAnalyser (Agilent). The microarray probe was made using the Affymetrix GeneChip® 3' IVT Express Kit. Following the GeneChip® 3' IVT Express Protocol, 50 ng RNA was used for reverse transcription to synthesize first-strand cDNA. This cDNA was then converted into a double-stranded DNA template for *in vitro* transcription to synthesize aRNA with incorporated a biotin-conjugated nucleotides (cRNA is also known as amplified RNA or aRNA). The aRNA was then purified to remove unincorporated NTPs, salts, enzymes, and inorganic phosphate. The biotin-labelled aRNA sample was then fragmented for hybridization onto GeneChip 3' expression arrays. The GeneChip® hybridization wash and stain kit and the Affymetrix® GeneChip® fluidics station 450 instrument was then used. After washing and staining, the Affymetrix® GeneChip® Scanner 3000 was used to scan the cartridge by laser light to obtain fluorescence intensity data. The microarray results were normalised together with WT (A17) 3 days post inoculation, 5 days post inoculation data sets in GeneSpring GX software. The microarray results were analysed in MultiExperiment Viewer (MeV) using Significance Analysis of Microarray to do significance test, using a delta value of 2.8.

## 4.5 Gene cloning

The full length *NIN* genomic sequence without the stop codon was amplified using Phusion high fidelity DNA polymerase with attB1 and attB2 tagged primers from a *M. truncatula* BAC containing the *NIN* gene. Gateway entry vector were then constructed by BP reactions of pDONR207 vector and each of those attB1 and attB2 tagged fragments respectively. Gateway® BP Clonase® II enzyme mix (Invitrogen, 11789-020) was used with standard protocols on product manual. The construct sequence was confirmed before the next step. The entry vector for *NIN* genomic full length was generated by adding stop codon TAG using QuikChange® XL Site-Directed Mutagenesis Kit.The expression constructs were generated by LR reactions of various entry vectors and destination vectors (Table 2.4.6). Gateway® LR Clonase® II enzyme mix kit (Invitrogen, 11791-100) was used with standard protocols on product manual.

**Vectors and constructs**

| constructs | Vector used |
|---|---|
| *pEXPANSIN7-NIN* genomic full length-GFP | pK7FWG2 (*p35S* is replaced by *pEXPANSIN7*) |
| *NIN* genomic full length (domain deletions) over expression | pK7WG2R |
| *GFP-NIN* genomic full length (domain deletions) | pK7WGF2 |
| *NIN* genomic full length-GFP | pK7FWG2 |
| *pNIN-NIN* genomic full length-GFP | pK7FWG2 (*p35S* is replaced by *pNIN*) |

**Primers**

| | |
|---|---|
| MtNIN pDONR F | 5’-GGGGACAAGTTTGTACAAAAAAGCAGGCTTCATGGAATATGGTGGTGGGTTAGT-3’ |
| MtNIN pDONR R without stop codon | 5’-GGGGACCACTTTGTACAAGAAAGCTGGGTTGGAGGATGGACTGCTGCTGCTGCTG-3’ |
| MtNIN_ins_3nt_after_2799 | 5’-AGCAGTCCATCCTCCTAGGACCCAGCTTTCTTG-3’ |
| ins_3nt_after_2799-antisense | 5’-TCGTCAGGTAGGAGGATCCTGGGTCGAAAGAAC-3’ |
| MtNIN site directed mutagenesis (-RWP-RK domain) F | 5’-AAGAAGCTACAACTTGTGATTGAT-3’ |
| MtNIN site directed mutagenesis (-RWP-RK domain) R | 5’-ACACACTGTATCACAAAATTATTA-3’ |

| | |
|---|---|
| NIN site directed mutagenesis (-PB1) F | 5’-TGTAAAGACTTGCACACATCATCT-3’ |
| NIN site directed mutagenesis (-PB1) R | 5’-TTCTAGGAGTGTTGATGATGAAGA-3’ |

## 4.6 NLP sequence collection

MtNIN protein sequence was used to search phytozome using BLASTP to search *P. trichocarpa, P. vulgaris*, *G. max*, *A. thaliana* and *O. sativa* sequences. The *L. japonicus* and *P. sativum* whole genome sequences are still not available, so a BLAST of MtNIN in the NCBI Genbank database was done to obtained NLPs from those two species. Only NLP protein sequences with both RWP-RK and PB1 domains were used.

## 4.7 Multiple alignment and phylogenetic tree construction

NLP sequences were imported into Geneious Pro (ver. 5.6.5). Multiple alignment was done under MUSCLE (Edgar, 2004) using default parameters. The result was exported in FASTA format. To refine the alignments for phylogenetic analysis, Gblocks server (http://www.phylogeny.fr/version2_cgi/one_task.cgi?task_type=gblocks) (Castresana, 2000) was used to eliminate poorly aligned positions and divergent regions of protein alignment. The trimmed sequences (221 amino acids for each NLP including RWP-RK and PB1 domains) were used for tree construction. The text file with trimmed NLPs was imported into Geneious, and used to create both Neighbor-Joining tree build method and PHYML (PHYMaximum likelihood) (Guindon et al., 2005; Guindon et al., 2009; Guindon et al., 2010) to build phylogenetic trees. To determine confidence levels for tree branches in the Neighbor-Joining method, a Bootstrap resampling method as statistical analysis was used, the number of replicates was 1000. In the PHYML (it is in the Genenious Pro plugin) method, the Jones-Taylor-Thorton (JTT) as the substitution model was used, and Bootstrap was used as the branch support (n= 1000) using default settings.

# CHAPTER III New *M. truncatula* rhizobial infection mutants

## 1 Background

Forward genetic screens have been applied in nodulation studies for several years to unravel gene functions. From 1999, which saw the identification of the first nodulation gene *NIN*, several genes in the symbiotic pathway have been cloned. These mutants were identified for their inability to form nodules. More recent studies have focussed on mutants that can form white nodules; this has included some rhizobial infection mutants and nitrogen fixation mutants. At the time this work was begun in 2009, the genes proved to be required for rhizobial infection were *CCaMK*, *NSP1*, *NSP2*, *NIN*, *ERN1*, *CYCLOPS*, *LIN*, *NAP1*, *PIR1*, *RPG* and *VAPYRIN*, and several of them are also required for nodule organogenesis. In order to discover more processes involved, we applied a forward genetics approach. The *Tnt1* transposon tagging system is a powerful tool to generate mutants. *Tnt1* has no unique target site specificity, but prefers to transpose into coding exons (Tadege et al., 2008). *Tnt1* transposon mutants have been widely used in both forward and reverse genetic screens, and several mutants with interesting nodulation phenotypes have been isolated (Lefebvre et al., 2010; Murray et al., 2011; Pislariu et al., 2012). These mutants were made using the *M. truncatula* ecotype R108. Each line contains an estimated average of 25 insertions, most of which are in gene-rich regions of the genome (Tadege et al., 2008). Indeed, the *Tnt1* mutant population has used similarly to the *A. thaliana* T-DNA insertion mutant collections. Here I describe two new mutants identified from this population.

## 2 Results

A group of 48 lines of *Medicago truncatula* putative nodulation mutants were obtained from forward genetics screens carried out at the Samuel Roberts Noble Foundation. The majority of these lines were selected as putative mutants because they produced white bumps after 3-4 weeks inoculation with *S. meliloti*. To re-screen these lines for rhizobial infection mutants, an *S. meliloti* 1021 expressing the *lacZ*

gene was used to help visualize the infection threads. The rhizobial infection phenotype was checked at 8 days post inoculation (dpi) and 11dpi. Phenotypes were recorded, including whether the mutants develop bumps; whether infection threads were present; whether the bumps were colonized by rhizobia, or any other interesting features (appendix Table 1). Two mutants (line numbers NF0457-3 and NF1268-1) were chosen for further study. These two mutants developed bumps and had some infection events, but did not develop rhizobia-colonized nodules.

## 2.1 A novel infection mutant with a potential role in ROS homeostasis

Plants of line NF0457-3 were defective in nodule formation, forming nodules later than WT (Fig. 1A and B). Also the mutant displayed a delay in infection thread initiation and a low percentage of success in infection thread formation (Fig. 1F). Despite these impediments in infection the mutant eventually developed similar numbers of nodules compared with WT (Fig. 1G), but the nodules were defective. The mutant nodules were colonized by rhizobia, but fewer symbiosomes formed (Fig. 1C-E) and no nitrogen fixation was detected (Fig. 1H).

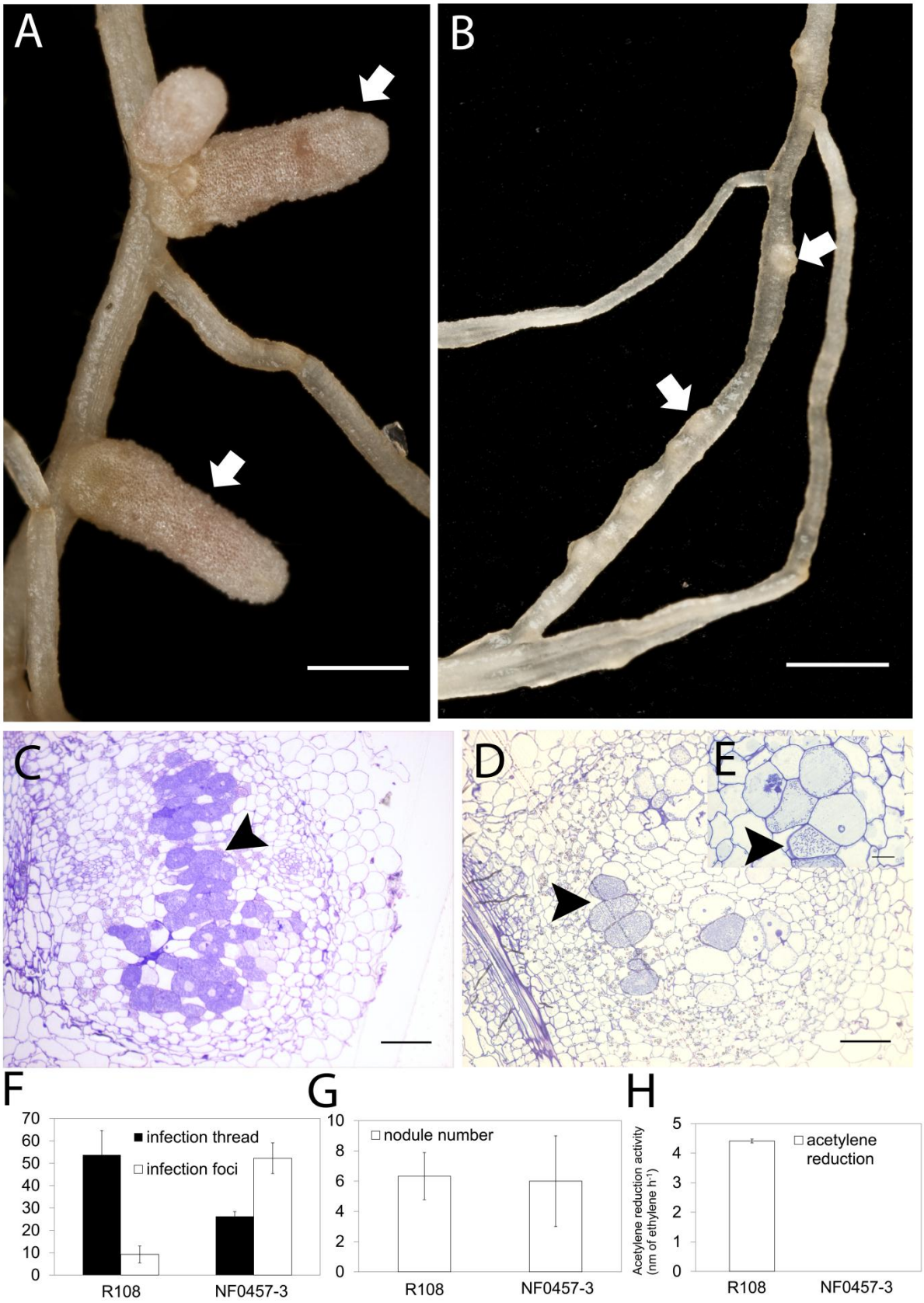


**Fig. 1.** NF0457-3 nodulation phenotype. (A and B) WT (A) and NF0457-3 (B) roots with nodules 1 month post inoculation. Arrows show nodules (A) and bumps (B). (C,

D and E) WT (C) and *cbs1* (D and E) nodule sections visualised with toluidine blue. Arrow heads show symbiosomes. (F) Infection events quantification in WT (R108) and *cbs1* 14 days post inoculation. (G) Nodule number quantification in WT (R108) and *cbs1* 14 days post inoculation. (H) Acetylene reduction in WT (R108) and *cbs1* 2 months post inoculation. The value was measured per plant. Scale bars in (A) and (B) are 5 mm, in (C) and (D) are 100 µm, in (E) is 25 µm.

Using inverse PCR, four *Tnt1* insertion flanking sequences were identified. Among them, one candidate encoding a Cystathionine Beta-Synthase (CBS) domain-containing protein had increased gene expression in nodules (MtGEA). The segregation of this insertion was tested in the backcross BC1F2 population (by my colleague Dr. Chengwu Liu) and it was found this *Tnt1* insertion cosegregated with the mutant phenotype. At this time we became aware that a group in the USA had identified a mutant with a similar phenotype with an insertion in the same gene (which they have designated as *CBS1*). They confirmed it was causing the nodulation phenotype by using the *Agrobacterium rhizogenes* hairy root transformation to complement the mutant. Interestingly, the nitrogen fixation defect in *cbs1* is not apparent when using rhizobium strains other than *S. meliloti* (personal communication, Senjuti Sinharoy). We consider the existence of two independent alleles with the same phenotype, the co-segregation analysis and complementation as proof that the mutation of *CBS1* results in the observed infection defect. Interestingly *CBS1* has a close homolog *CBS2* which is found adjacent to it in the genome and is induced in mycorrhization. These proteins have a carboxy-terminal CBS domain and an N-terminal Domain of Unknown Function 21(DUF21) domain.

## 2.2 Towards cloning a novel infection mutant with a block in infection thread initiation

The second mutant identified in the screen (line NF1268-1) was found to form normal infection pockets containing rhizobial microcolonies, but failed to initiate infection threads. Therefore the locus was named as *Knocks but Can't Enter* (*KCE*).

The phenotypic analysis will be presented in Chapter IV. This section will describe the efforts to identify the KCE locus. Inverse PCR was used to attempt to identify the causal mutation through identification of *Tnt1*-transposon flanking sequence tags (FSTs) in the parental line NF1268-1. Thermal asymmetric interlaced (TAIL) PCR was used in the BC1F2 population with six plants with the mutant phenotype. Inverse PCR was not successful in identifying a single *Tnt1* insertion. Using TAIL PCR, 20 *Tnt1* insertions were identified. PCR-based markers were developed for each FST and their cosegregation with the phenotype in the BC1F2 population was tested.

A *Tnt1* insertion in *FLOT6* in chromosome Chr. 1 was found to have 6 recombinants in the population of 86 F2 individuals ($\chi^2$=18.586, P<0.0003). *FLOT6* locates on the Chr. 1 lower arm. Since no FSTs perfectly cosegregated with the phenotype and a mapping population was not yet available, Illumina paired-end sequencing was used to identify additional *Tnt1* FSTs. Nuclear DNA isolated from a pool of 21 mutants from a BC1F2 population was used as a template.

The sequencing results were analysed by Dr. Nick Krom (Noble Foundation). A *de novo* assembly was carried out using Velvet 1.1.05, and the results are summarized in (Table 1).

**Table 1.** Sequencing assembly statistics for pooled *kce* mutants

| | |
|---|---|
| Total contigs | 1082012 |
| N50* | 3930bp |
| Longest contig | 38467 |
| Total base pair in assembly | 298370140 |
| Average coverage depth | 6.65x |
| Reads used in assembly | 65341336 out of 79650496 reads |
| Read data retained after quality trimming | 95.3% |

*N50 length is defined as the length N for which 50% of all bases in the sequences are in a sequence of length L < N.

After *de novo* assembly into contigs, *Tnt1* transposon sequence and *MERE1* transposon sequence were used to BLAST the assembled genome. The reason *MERE1* transposons were also checked that it has been found that *MERE1* transposons are also activated by tissue culture (Rakocevic et al., 2009). A total of 67 *Tnt1* insertions were identified, and 13 of them locate on Chromosome 1 (appendix Table 2). 19 of them locate on Illumina contigs that have not been positioned on any chromosome (appendix Table 2). There are 38 *MERE1* transposons identified with 5 of them locate on chromosome 1 (appendix Table 3). The cosegregation of these insertions with the phenotype was tested and a single FST with sequence homology to human Werner syndrome DNA helicase was found to cosegregate 100% (no recombinants) with the mutant phenotype. During the preparation of this thesis the ongoing map based cloning using new markers and an F2 (*kce* (R108) x A17) mapping population this candidate gene was excluded (population developed by me and mapping was done by Dr. Chengwu Liu). However, the *LIN* gene locus is 3 Mb away from the DNA helicase locus and the *lin* mutant phenotype is similar as *kce*. So *LIN* was tested by sequencing and a stop codon was found in the coding sequence (Fig. 2; appendix 5).

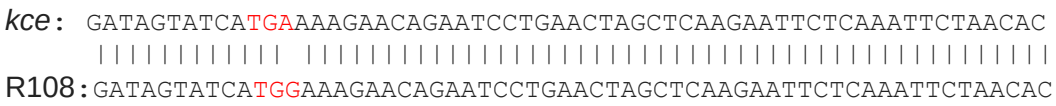


**Fig. 2.** LIN sequence comparison between *kce* and R108. TGA in *kce* encodes a stop codon.

# 3 Discussion

In my studies, I made use of 48 *M. truncatula* putative nitrogen fixation defective lines which I rescreened for rhizobial infection defective mutants. Two mutants were chosen for further study. For one of them, *cbs1* (NF0457-3), the relevant insertion was readily identified using inverse PCR. However for *kce* (NF1268-1), neither inverse PCR nor TAIL PCR was successful in identifying the underlying mutation. In a further effort to identify *Tnt1* transposition events causing the phenotype whole genome deep sequencing was used on a bulk of 21 BC1F2 segregants. Surprisingly, a total of 67 FSTs were identified, much higher than expected based on current surveys using TAIL-PCR. It's possible therefore that the *Tnt1* lines harbour many more transposition events than previously thought, or it could be that NF1268 is not representative, more lines will need to be sequenced to discriminate between these possibilities. Since the whole genome sequencing is not yet complete, there are many gaps in the assembly and many sequences are still not mapped to the genome. 19 FSTs were identified that corresponded to unmapped short contigs from the most recent Illumina assembly of the Medicago genome v3.5 (Young et al., 2011). These unmapped FSTs are a source of candidate genes and efforts are now underway to develop markers to test cosegregation of these genes with the *KCE* locus. Although a 6.65X genome coverage was achieved, the key transposition event may still have been missed. It's also possible that the mutation responsible for the *kce* phenotype is not a *Tnt1* insertion. Spontaneous single base pair mutations created in tissue culture system could contribute to the mutant phenotype and it's known that native transposons, like *MERE1* can be active in a tissue culture system. In the Jemalong A17 background, it was reported that one copy of *MERE1* can actively transpose during regeneration from tissue culture (Rakocevic et al., 2009). Therefore, the mapping population I developed between the *kce* mutant (R108 background) and Jemalong A17 in combination with the FSTs identified by deep sequencing should be a valuable resource for the identification of the *kce* mutation.

Previously in Arabidopsis, two related CBS domain-containing proteins, CBSX1 and CBSX2, were found to have a role in the regulation of reactive oxygen species (ROS). These proteins differ from CBS1 in that they do not contain a DUF21 domain.

CBSX1 and CBSX2 were found to be localised in the chloroplast where they appear to regulate thioredoxins (Trxs) in the ferridoxin-Trx system. A third family member, CBSX3, localised in the mitochondria, was found to regulate Trxs in the NADP-Trx system. CBSX1 is believed to regulate $H_2O_2$ levels through its direct interaction with Trxs. *CBSX1* overexpression causes decrease in $H_2O_2$ levels, resulting in the failure of secondary wall thickening in the anther endothecium (Yoo et al., 2011). The follow-up functional studies on *cbs1* have been carried on by Dr. Chengwu Liu.

From the studies in *A. thaliana*, CBS1 may be involved in decreasing $H_2O_2$ in rhizobial infection. Data in the lab has already suggested this. Interestingly *CBS1* has been found to be downregulated in *nin* mutant root hairs during rhizobial infection compared with WT (details are in Chapter II). Suggested experiments have been mentioned in Chapter II. ROS function in nodulation has not been well studied. Details will be discussed in the general discussion (CHAPTER V).

*kce* mutant aborts rhizobial infection in the root hair curl. The *KCE* locus is close to *LIN* (Fig.2), which is a rhizobial infection locus identified before. Although the rhizobial infection phenotype is not the same in these mutants, *kce* mutant is of a different background from *lin*. There have been evidences mutants in different background produce different phenotypes. *vapyrin* mutant in A17 background produce infected nodules, whereas *vapyrin* in R108 background produce non-infected nodules. Therefore it is necessary to exclude *LIN* in the *kce* mutant. After directly sequencing *LIN* gene, a stop codon was found in *kce* mutant, therefore it is highly likely *kce* is a new allele of *lin*.

# 4 Materials and methods

## 4.1 *M. truncatula* leaf genomic DNA purification

One trifoliate was collected for each sample, and the Sigma GenElute$^{TM}$ Plant Genomic DNA miniprep Kit was used to purify DNA.

## 4.2 TAIL PCR

For TAIL PCR, the PCR reactions were carried out as follows. The Primary PCR reaction used 200 ng of genomic DNA as a template. For the Secondary PCR reaction, 2 µL 100xdiluted PCR primary product was used as a template, and for the Tertiary PCR reaction 3 µL of 100xdiluted PCR secondary product was used. ,The PCR reactions each contained the following: 10x Invitrogen Taq DNA Polymerase buffer, 3 mM $MgCl_2$, 312.5 µM dNTPs 1.6 µL, 2 µM Tnt1 forward primer, 3 µM AD2, 0.4 UInvitrogen Taq DNA polymerase.

The TAIL PCR conditions were as follows: Primary PCR reaction 1:93°C, 1 min; 95°C, 1 min, 1 cycle; 94°C, 30 sec; 62°C, 1 min; 72°C, 2.5 min, 5 cycles; 94°C, 30 sec; 25°C, 3 min; 72°C, 2.5 min, 1 cycle; 94°C, 30 sec; 68°C, 1 min; 72°C, 2.5 min, 94°C, 30 sec; 68°C, 1 min; 72°C, 2.5 min, 94°C, 30 sec; 44°C, 1 min; 72°C, 2.5 min 15 cycles; 72°C, 5 min, 1 cycle. Secondary PCR reaction 2: 94°C, 30 sec; 64°C, 1 min; 72°C, 2.5 min, 94°C, 30 sec; 64°C, 1 min; 72°C, 2.5 min, 94°C, 30 sec; 44°C, 1 min; 72°C, 2.5 min, 12 cycles; 72°C, 5 min, 1 cycle. Tertiary PCR reaction 3:94°C, 60 sec; 44°C, 1 min; 72°C, 2.5 min, 20 cycles; 72°C, 5 min, 1 cycle.

The PCR products were purified using the QIAquick PCR purification kit. Purified PCR products (≈30 ng $\mu L^{-1}$) were ligated to pGEM®-T easy vector and LacZ blue white screening was used to select the colony with insertions in the pGEM®-T easy vector. More than 48 clones were sequenced to identify the *Tnt1* transposon flanking sequences.

**Primers**:

| | |
|---|---|
| Tnt1 forward | 5’-TCCTTGTTGGATTGGTAGCC-3’ |
| LTR3 | 5’-AGTTGCTCCTCTCGGGGTCGTGGTT-3’ |

| | |
|---|---|
| LTR7 | 5’-TATTATTCCGCTTTATTACCGTGA-3’ |
| AD1 | 5’-NTCGA(G/C)T(A/T)T(G/C)G(A/T)GTT-3’ |
| AD2 | 5’-NGTCGA(G/C)(A/T)GANA(A/T)GAA-3’ |
| AD3 | 5’- (A/T)GTGNAG(A/T)ANCANAGA-3’ |

## 4.3 Inverse PCR

1 µg of DNA was digested with 10 units of EcoRI and MfeI or AseI (Roche) in a 50 µl reaction volume at 37 °C overnight, then incubated at 65 °C for 20 min to deactivate the enzyme.

The digested DNA was purified with a phenol-chloroform extraction and then 6 units T4 DNA ligase (Promega) was used for self-ligation at 4 °C overnight after which the ligated products were purified using phenol-chloroform.

The inverse PCR conditions were as follows: First PCR: using ≈80 ng of *kce* genomic DNA as template the PCR reaction contained the following ingredients: 10x Invitrogen Taq DNA Polymerase buffer, 3 mM $MgCl_2$, 312.5 µM dNTPs 1.6 µL, 2 µM LTR3, 2 µM LTR5, 0.4 U Invitrogen Taq DNA polymerase.

The Secondary PCR used the same conditions except that 2 µL of a 100x dilution of first round PCR product was used as a template and LTR4 and LTR6 were replaced the LTR3 and LTR5 primers.

The Inverse PCR conditions were as follows: 95°C, 5 min, 1 cycle; 95°C, 15 sec; 65°C, 20 sec; 72°C, 3 min, 30 cycles; 72°C, 5 min, 1 cycle.

**Primers**:

| | |
|---|---|
| LTR5 | 5’-GCCAAAGCTTCACCCTCTAAAGCCT-3’ |
| LTR4 | 5’-TACCGTATCTCGGTGCTACA-3’ |
| LTR6 | 5’-GCTACCAACCAAACCAAGTCAA-3’ |

## 4.4 Phenol-chloroform DNA precipitation

For phenol chloroform extractions $H_2O$ was added to a final volume of 200 µL. An equal volume of phenol chloroform was then added and mixed and vortexed vigorously and then Centrifuged for 8 min at 14000 rpm. The supernatant was removed (≈200 µL), 2x volume of 95% ethanol (along with 1/10 volume of 3M sodium acetate) was added. It was then placed in -20°C freezer for 30 min and centrifuged for 10 min at 14000 rpm. The supernatant was then discarded and the pellet was washed with 70% ethanol. It was then centrifuged for 5 min, and the supernatant was removed after which the sample was dried in the flow hood before re-suspension in water.

## 4.5 Deep sequencing nuclear DNA preparation

This was carried out by Khuat Huu Trung, and Nguyen Thi Phuong Doai.

Buffer recipes (appendix)

Nuclear DNA Isolation Protocol

5 g of young trifoliate leaves from a bulk of *M. truncatula kce* BC1F2 mutant plants were harvested into a clean container and wrapped in aluminium foil and frozen in liquid nitrogen. The tissue was stored at -80$^{o}$C.

The tissue was then ground in liquid nitrogen. The powder was then transferred to cold SEB-M and incubated on ice for 10 min, with stirring. The mixture was then filtered through Miracloth and 1/20 volume SEB-MT containing Triton was added. It was then incubated on ice for 10 minutes with 20 seconds of swirling every 2 minutes followed by centrifugation at 650 g, for 10 min at 4$^{o}$C in 250 mL polypropylene tubes. The supernatant was then gently pipetted off using a 25 mL pipette, then a 3 mL Pasteur pipette. The pelleted nuclei were then gently resuspend in 1 mL SEB-M. More SEB-M was added to 20 mL in total. This centrifugation step was then repeated. Finally, the pelleted nuclei were resuspended in 1 mL SEB-M then more SEB-M was added to 7.5 mL in total. A 20% aqueous SDS (w/v) was added to a final concentration of 2% (w/v). This was mixed by gentle inversion to lyse the nuclei. The sample was then incubated in a water bath at 60$^{o}$C for 10 min, then cooled to room temperature (20$^{o}$C). When it became cool, 5 M sodium perchlorate (20$^{o}$C) was added to a final concentration of 1 M, to break up protein/DNA interaction. It was then centrifuged at 400 g for 20 min to pellet starch grains. The supernatant was then transferred to a new 15 mL falcon tube using a 1 mL pipette. The DNA sample was then extracted twice with an equal volume of Phenol/Chloroform/Isoamyl alcohol (25:24:1). The aqueous phase of the sample was then dialysed in TE (pH 7.0) at 4$^{o}$C overnight.

The next day, the dialysed was placed sample into a 15 mL falcon tube. RNase T1 was added to 50U mL$^{-1}$ and RNase A to 50 µg ml$^{-1}$ respectively and incubated at 37$^{o}$C for 45 minutes. Proteinase K was added to a concentration of 150 µg mL$^{-1}$ and incubated at 37$^{o}$C for 45 minutes. The DNA sample was then extracted twice with an equal volume of Phenol/Chloroform/Isoamyl alcohol (25:24:1). The upper aqueous phase was transferred into a new 15 mL tube. A1/10 volume of 3 M sodium acetate (pH 5.2) was added and 10 mL was transferred into a corning centrifuge tube. 2.5-3.0 volumes 100% ethanol (-20$^{o}$C) was added and mixed thoroughly. It was then stored at -20$^{o}$C overnight. The sample was then centrifuged at 14,000 rpm for 30

minutes at 4$^{o}$C. 1 mL of 70% ethanol was added and centrifuged again at 14,000 rpm for 15 minutes. The supernatant was decanted and air dryed for 1 hour. The dry pellet was redissolved in 500 µL $H_2O$.

After purifying the nuclear DNA, DNA was given to the Sainsbury lab, where Jodie Pike did the sequencing library construction and ran the HiSeq Illumina sequencing machine.

# CHAPTER IV Rhizobial infection abortion in the root hair curl induces centrally vascularized nodules

## 1 Background

Nodulation comprises two developmental programmes, infection and organogenesis. The symbiosis is initiated first by the host legume, which constantly secretes flavonoid and isoflavonoid compounds from its roots into the rhizosphere. Rhizobial Nodulation (Nod) factors are synthesised and secreted after sensing these signals (Wasson et al., 2006; Subramanian et al., 2007). In *Medicago truncatula*, the nodulation signalling pathway that transduces the signal consists of the Nod factor receptors NFP(Amor et al., 2003; Arrighi et al., 2006), and LYK3 (Limpens et al., 2003); a receptor-like kinase DMI2 (Endre et al., 2002); components involved in calcium signal transmission DMI1 (Ane et al., 2004), MCA8 (Capoen et al., 2011); and nuclear proteins that decode the calcium signal, CCaMK (Gleason et al., 2006) and CYCLOPS (Yano et al., 2008). This pathway acts through a suite of transcription factors NSP1 (Smit et al., 2005), NSP2 (Kalo et al., 2005), NIN (Marsh et al., 2007), ERN1 (Middleton et al., 2007) leading to the outputs of rhizobial infection and nodule organogenesis. These four transcription factors are each required for the initiation of both infection and organogenesis.

In rhizobial infection, genetic studies have identified genes involved in several key processes (Murray, 2011), namely cytoskeletal rearrangements PIR1, NAP1 (Yokota et al., 2009), RIT1 (Miyahara et al., 2010); cell wall degradation NPL (Xie et al., 2011), CelC2 (Robledo et al., 2008); protein turnover LIN (Kuppusamy et al., 2004; Kiss et al., 2009), PUB1 (Mbengue et al., 2010), SINA4 (Den Herder et al., 2012); and also proteins of unknown function VAPYRIN (Murray et al., 2011), RPG (Arrighi et al., 2008). From the standpoint of the rhizobia, the production of Nod factors (Ardourel et al., 1994; Geurts and Bisseling, 2002) and exopolysaccharides (Cheng and Walker, 1998) are essential for infection. The *Sinorhizobium meliloti exoY* mutant mutated in the gene encoding the first enzyme in the EPS biosynthesis pathway blocks rhizobial infection in the root hair curl (Cheng and Walker, 1998).

Infection and organogenesis develop synchronously. Addition of Nod factors induces root hair deformation and cortical cell divisions at the same time. In a similar manner, during nodulation, root hair cells entrap rhizobia inside the root hair curl, which is concomitant with cell divisions in the underlying cortex. After that, a tube-like structure which contains rhizobia, called the infection thread initiates in the root hair and then penetrates into the nodule (Timmers et al., 1999; Kosuta et al., 2008). The rhizobia are then released from the infection thread into the developing nodule cells.

In nodule organogenesis, the first cell divisions occur in the cortex followed soon after by divisions in the pericycle cells within one day after infection. Additional cortical divisions occurring 1 or 2 days after inoculation give rise to the nodule primordium. Simultaneously to the formation of initial primordium, from the outer cortex an inward gradient of differentiation is observed, preceding rhizobial infection. Later at about 3 days after inoculation the nodule meristem appears (Timmers et al., 1999). The nodule vascular bundles develop peripherally to exchange nutrients between roots and nodules (D'Haeseleer et al., 2010). The development of nodule vascular bundles is not well studied, only a bHLH transcription factor has been clearly shown to function in this process (Godiard et al., 2011). The nodule vascular bundles consist of xylem and phloem vessels in nodule parenchyma cells surrounded by a pericycle cell layer and an endodermis, which constitutes an apoplastic barrier for the vascular bundles and the central tissues of the nodule (Godiard et al., 2011).

Cytokinin is a key component in nodule organogenesis (Murray et al., 2007). A loss-of-function mutant in the cytokinin receptor *LHK1/CRE1* (Murray et al., 2007; Tirichine et al., 2007) results in cortical cell division defects. Few cortical cell divisions occur quite late and wired nodules form eventually. The gain-of-function allele of the cytokinin receptor *cre1* was able to induce spontaneous nodules without rhizobial infection (Tirichine et al., 2007). A rhizobial mutant that does not produce Nod factors carrying a constitutive trans-zeatin secretion gene was able to stimulates nodule-like structures (Cooper and Long, 1994). Also treatment with cytokinin was able to induce spontaneous nodules in *Lotus. japonicus* (Heckmann et al., 2011). So

cytokinin is both sufficient and necessary in nodule organogenesis. Also, it may have a negative effect on rhizobial infection (Murray et al., 2007).

Rhizobial infection and nodule organogenesis are tightly coordinated. Using the gain-of-function CCaMK isoform, it has been shown that CCaMK is involved in the coordination of these two processes (Madsen et al., 2010). Recent work shows that the main purpose of the nodulation signalling pathway is to activate CCaMK. In double mutants that combine *snf1* mutant (gain of function CCaMK) with either the *nfr1*, *nfr5*, or *symrk* mutants, nodules can be formed and a portion of these nodules can be infected (Madsen et al., 2010). Previous studies showed that within indeterminate nodules rhizobial infection progression is necessary to maintain the nodule apical meristem (Yang et al., 1992; Voroshilova et al., 2009). We used the *kce* mutant to uncouple infection and organogenesis to study the interconnectedness of this two programmes. We show that in the case of rhizobial infection blockage in the root hair curl, the nodule develops into a lateral root like structure.

# 2 Results

## 2.1 *kce* aborts rhizobial infection in the root hair curl

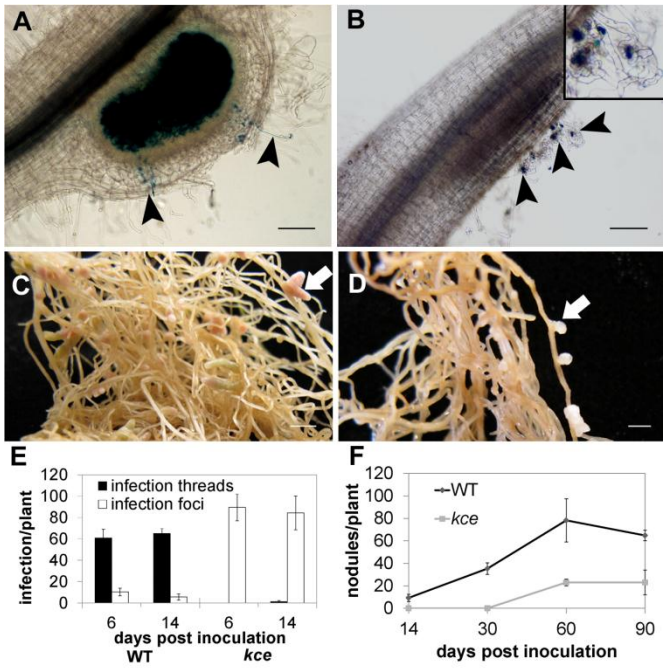


**Fig. 1.** *kce* nodulation phenotype. (A and B) nodules with associated infection threads in WT (A) and infection foci in *kce* (B) after inoculation with *S. meliloti* 1021 carrying *lacZ*, visualized using X-gal staining. Inset in B shows close-up of infection pockets. The black arrowheads in A and B highlight infection events.(C and D) Nodules of WT (C) and *kce* (D) 80 dpi with *S. meliloti* 1021. The white arrows in (C) and (D) highlight nodules. (E) Mean (± SD) number of infection threads and infection foci of WT and *kce* 6 and 14 dpi with *lacZ*-tagged *S. meliloti* 1021. (F) Mean (± SD) number of nodules of WT and *kce* 14,30,60 and 90 dpi with *S.meliloti* 1021. (n=8). Scale Bars in (A) and (B) are 0.2 mm; in (C) and (D) are 5 mm.

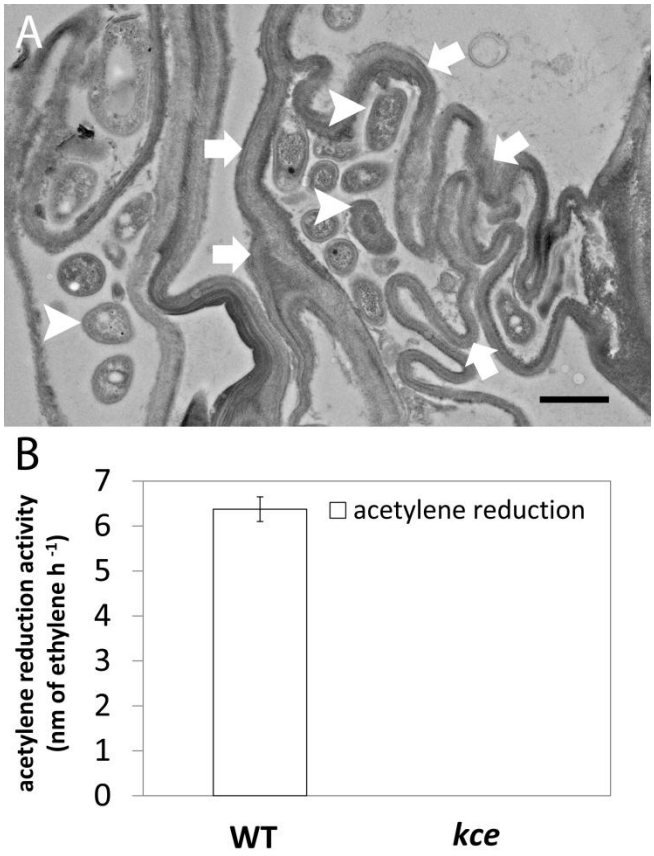


**Fig. 2.** Nodule phenotype of *kce*. A scanning electron micrograph of a *kce* nodule 500nm cross section (A) and acetylene reduction assay (B) 3 months post inoculation. White arrow heads show bacterial cells. White arrows show plant cell walls. Scale bar is 500 nm.

A *M. truncatula* mutant defective for infection by *S. meliloti* was identified from a population of *Tnt1* transposon tagged plants (ecotype R108). The mutant was found to abort rhizobial infection in the root hair curl (Fig. 1B). Rare infection threads did initiate but they were short, and never progressed across the root epidermis. So we named the mutant *Knocks but Can't Enter* (*kce*). When quantified, *kce* had more infection events than in the wild type (Fig. 1E). *kce* nodule development was delayed, with some white bumps starting to emerge 60 days post inoculation (Fig. 1F). At 90 days post inoculation, *kce* nodules remained as white bumps (Fig. 1D), compared with wild type nodules that were red and long. It is worth noticing that the early cortical cell divisions in *kce* nodule development are disorganised (Fig. 3B) compared to WT (Fig. 3A) and these cell divisions happen very late. TEM of *kce* nodule sections revealed some bacteria in the extracellular compartment, however, it is not clear whether they were rhizobia, and no infection threads were seen (Fig. 2A). *kce* nodules were deficient in nitrogen fixation (Fig. 5C, 2B), and plants showed nitrogen deficiency symptoms after 3 months growing in the sand. Genetic mapping data indicates that *kce* represents a novel symbiotic gene (Chapter III).

## 2.2 *kce* nodules are centrally vascularized

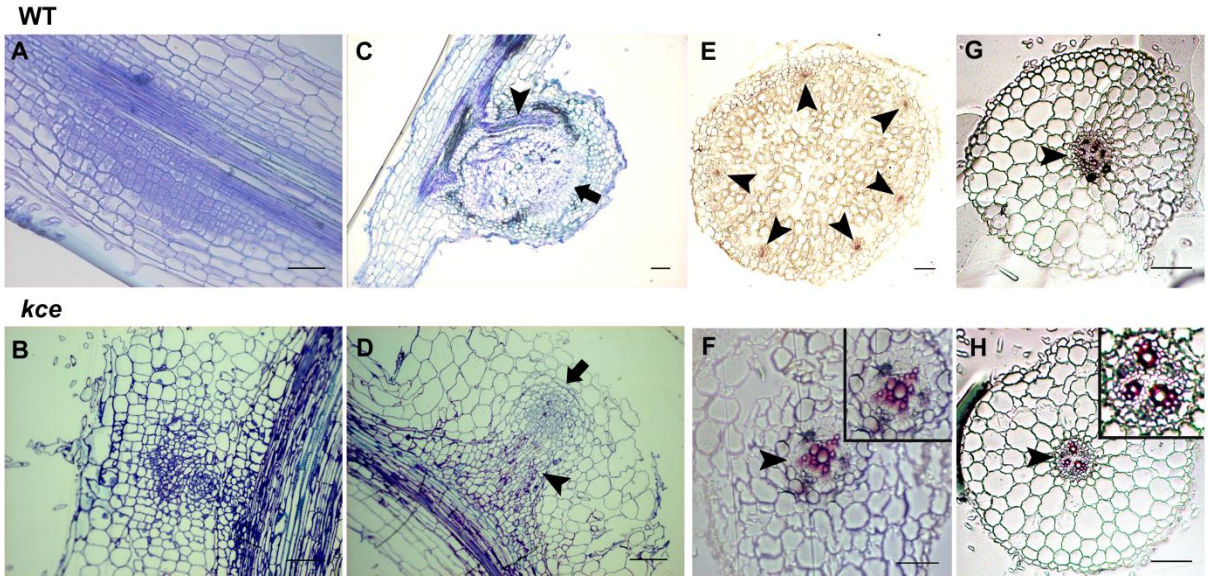


**Fig. 3.** *kce* nodule vascular bundles are central. (A and B) Early cell divisions in WT (A) 3 dpi and *kce* (B) 14 dpi longitudinal sections after *S. meliloti* 1021 inoculation. (C and D) Longitudinal sections of WT (C) 14 dpi and *kce* (D) 80 dpi nodules, the black arrows highlight nodule meristems. The sections (A-D) are stained with toluidine blue. (E and F) Phloroglucinol staining of WT (E) and *kce* (F) nodule cross sections. (G and H) Phloroglucinol staining of WT (G) and *kce* (H) lateral root cross sections. The black arrowheads highlight vascular bundles. Scale bars are 100 µm.

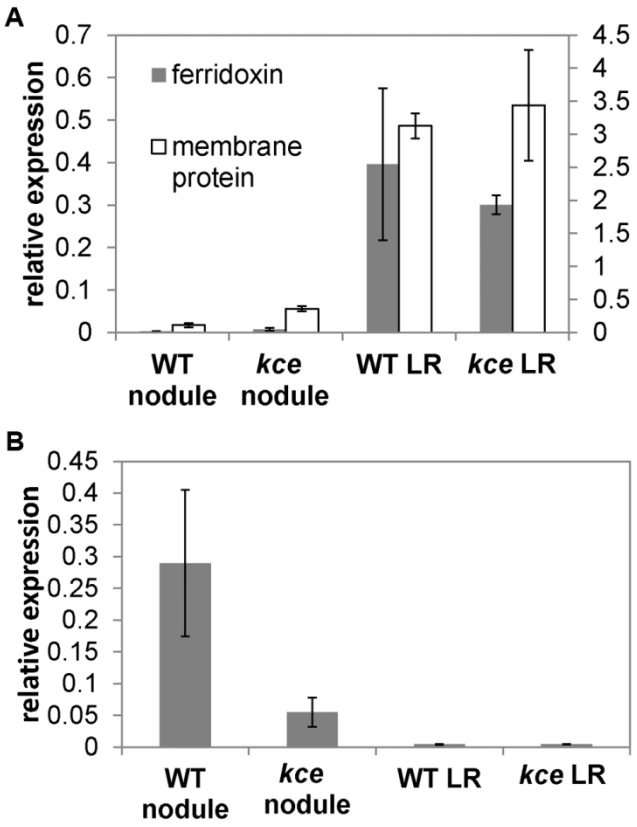


**Fig. 4.** *kce* nodules resemble nodules more than lateral roots based on marker gene expression. (A) Root-tip marker gene expression in WT and in size-matched *kce* nodules and lateral roots measured by quantitative PCR normalized using *EF1α*. Marker genes are *ferridoxin I* (Medtr2g006290) and a plant integral membrane protein (Medtr7g011090). (B) *NIN* gene expresion in WT and *kce* nodules and lateral roots measured by quantitative RT-PCR normalized using *MtEF-1α*. The results represent three biological replicates (±SD). LR: lateral roots.

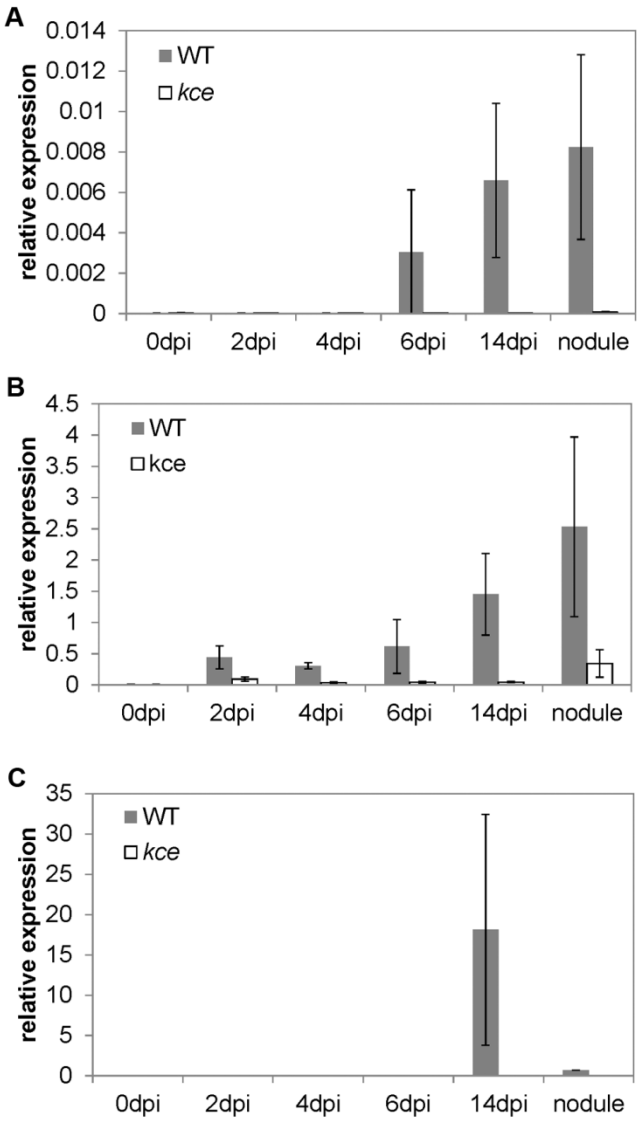


**Fig. 5.** *kce* mutant develops abnormal nodules. Nodulation marker gene (*ENOD20* in A, *HAP2.1* in B, *leghemoglobin* in C) expression in WT and *kce* spot inoculated roots(0, 2, 4, 6, 14 dpi) and excised size-matched nodules measured by quantitative RT-PCR normalized using *MtEF-1α*. Results represent three biological replicates (± SD).

WT nodules have vascular bundles which originate from the root stele and branch at the nodule base and then extend towards the nodule apex along the nodule periphery (Fig. 3C, E). *kce* nodule sections surprisingly revealed central vascular bundles (Fig. 3D, F), which resemble the vascular bundles of lateral roots (Fig. 3G, H). However, using phloroglucinol staining the xylem, it is obvious that the *kce* nodule vascular strand organization is different from that of the lateral roots (Fig. 3F, H). In particular the *kce* nodule distal part was not as sharp as a lateral root and lacked a quiescent centre (Fig. 1D). To determine whether these structures were more similar to lateral roots or nodules, two marker genes (Medtr2g006290, Medtr7g011090) specifically expressed in root tips were identified using the *Medicago truncatula* Gene Expression Atlas (MtGEA) database and the expression levels of these genes were compared between emergent lateral roots and *kce* nodules using quantitative RT-PCR (QPCR). The result shows that *kce* nodules don't express these root tip marker genes (Fig. 4A). In addition to that, I checked *NIN* gene expression. *NIN* encodes a nodulation specific transcription factor that is expressed throughout nodule development (Schauser et al., 1999; Marsh et al., 2007). *NIN* gene expression was reduced in *kce* nodules compared with WT nodules, but was much higher than in the lateral roots. I also checked the relative expression levels of some other nodulation marker genes in *kce* nodule development. *ENOD20* is induced in cortical cell divisions, infection threads, and later in the nodule infection zone and nitrogen fixation zone (Vernoud et al., 1999). *HAP2.1* is reported to express in the nodule meristem (Combier et al., 2006; Combier et al., 2008). Leghemoglobin is an oxygen carrying heme protein and is induced in nitrogen fixation. The expression of the nodulation marker genes *ENOD20*, *HAP2.1* and *leghemoglobin* in *kce* nodule development was much lower compared with WT (Fig. 5). This indicates that the nodules developing on *kce* are abnormal and is consistent with their delayed development and lack of nitrogen fixation ability. Together these results suggest that these structures are aberrant nodules rather than lateral roots.

## 2.3 Abortion of rhizobial infection in the root hair curl leads to aberrant nodule formation

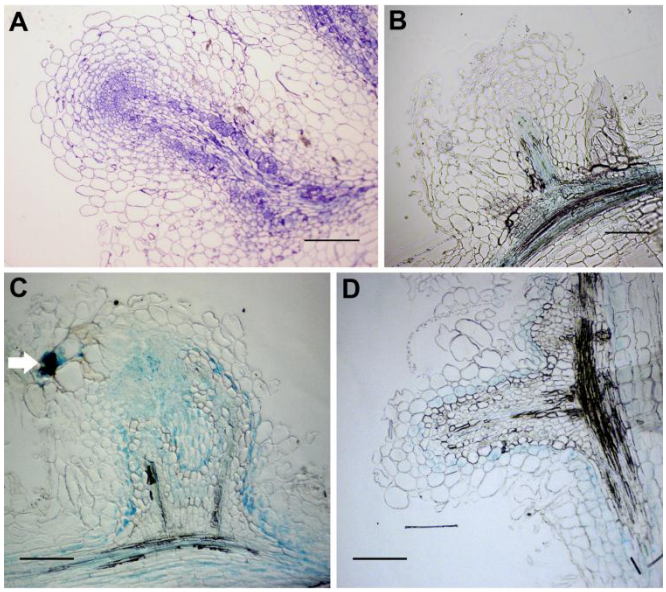


**Fig. 6.** Rhizobial infections that abort in the root hair curl lead to abnomal nodule organogenesis featuring a central vascular bundle. Nodules were harvested at 60 dpi. Longitudinal nodule sections of 10 µM thickness are shown. (A) A *vpy-2* nodule. The section is stained with toluidine blue. (B) An *S. meliloti* 1021 *exoY* mutant-induced nodule on WT (ecotype R108). (C and D) *lin-1* forms two types of nodules: (C) nodules with branched, peripheral vascular bundles; and (D) nodules with central vascular bundles. Note the thickened infection thread in the nodule outer cortex (white arrow, panel C) visualised by X-gal staining. Scale bars are 200 µm.

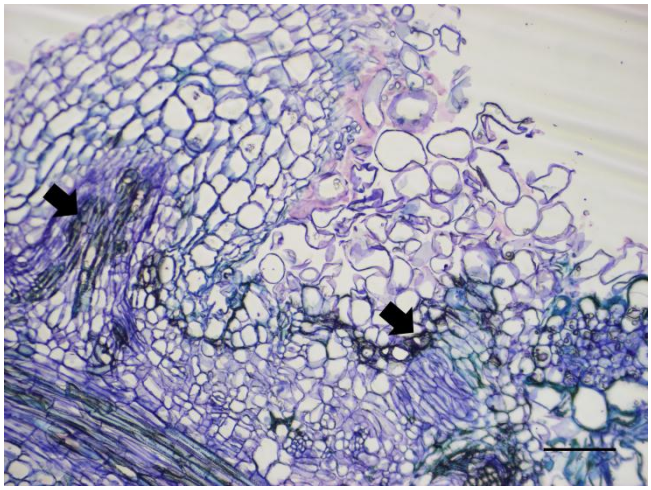

**Fig. 7.** Spontaneous nodule with periphery vascular bundles induced in *kce* transformed with CCaMK kinase domain construct. Black arrow heads show the vascular bundles. Scale bar is 200 µm.

To test whether it is the rhizobial infection defect in *kce* mutant that results in central vascular bundle (CVB) nodule structure, other rhizobial infection mutants in which rhizobial infection aborted at a similar stage as *kce* were examined. We included the *M. truncatula vapyrin* (R108 allele; *vpy*-2), the *lin* mutant (A17 allele; *lin*-1), and the *S. meliloti exoY* mutant. For the *vpy* mutant, in cases where infection arrested early, CVB nodules were also observed (Fig 6A). The medicago *lin* mutant formed a mixture of peripheral vascular bundle (PVB) and CVB nodules. In the *lin* mutant, we noticed both PVB nodules (Fig. 6C), and CVB nodules (Fig. 6D) were formed. The normal PVB nodules are almost always (19 of 20 events observed) associated with a thickened infection thread in the nodule outer cortex. On the CVB nodules, infection threads were never found. This indicates a relationship between the stage rhizobial infection abortion and the development of nodule vasculature. The *S. meliloti exoY* mutant is blocked in the first step in exopolysaccharide biosynthesis, which leads to abortion of rhizobial infection in the root hair curl. In *exoY* there were occasional infection threads that initiated and then aborted in the root epidermis. Nodules formed on *exoY* had vascular bundles that formed centrally (Fig 6B).

To further test the hypothesis that it's the rhizobial infection defect in *kce* that results in CVB nodules, I transformed the gain-of-function CCaMK under the *CCaMK* native promoter (CCaMK kinase only) (Gleason et al., 2006) into *kce*. This was done to determine whether activation of Nod factor signalling could lead to normal nodules in the *kce* mutant. I observed a mixture of CVB and PVB spontaneous nodules (Fig. 7) demonstrating that the *kce* mutant is able to make nodules with normal vascular architecture.

## 2.4 Cytokinin signalling is not maintained in *kce* nodule development

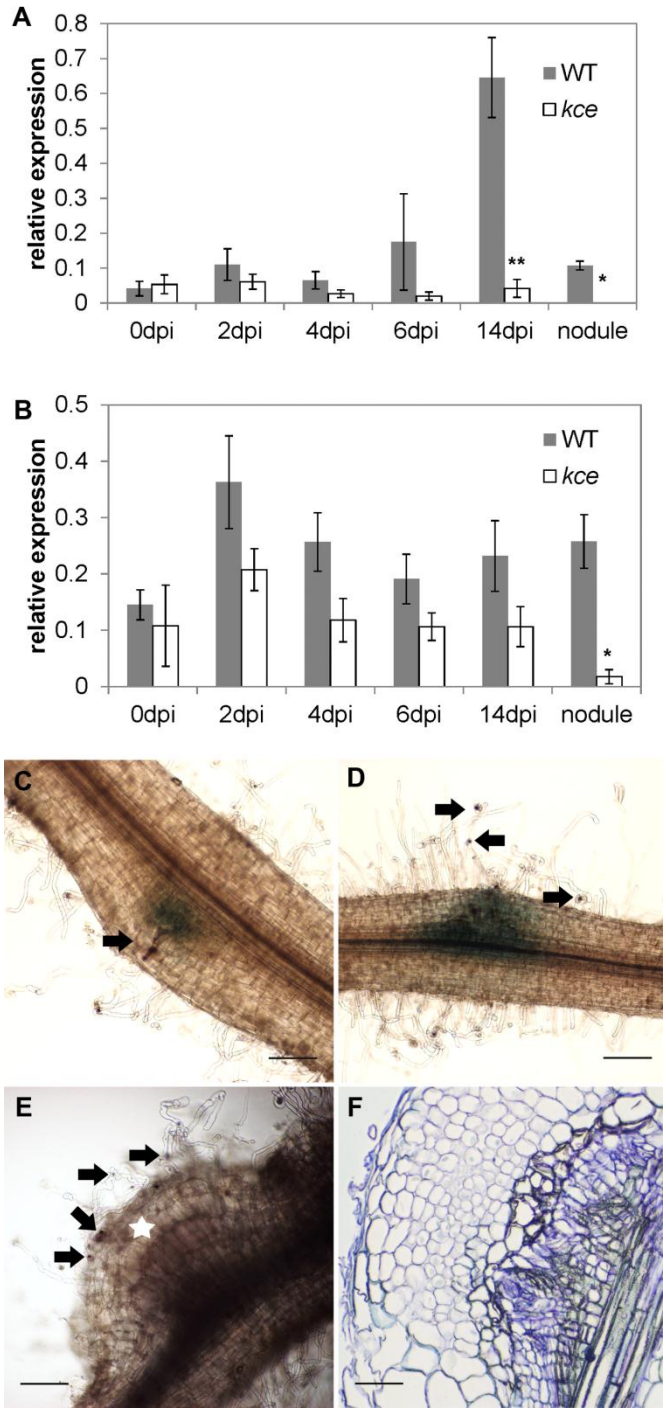


**Fig. 8.** Cytokinin signalling is not maintained in *kce* nodule organogenesis. (A and B) *MtRR4* (A) and *MtCRE1* (B) gene expression in WT and *kce* spot inoculated roots (0, 2, 4, 6, 14 dpi) and excised size-matched nodules (see materials and methods) measured by quantitative RT-PCR normalized using *MtEF-1α*. Results represent three biological replicates (±SD). * P<0.05;** P<0.01 (Welch's *t*-test). (C-F) WT (C) and *kce* (D-F) transformed with *pMtCRE1::GUS* using the hairy root transformation system. (C and D) 6 dpi with *S. meliloti* carrying *lacZ*. (E) 45 dpi with *S. meliloti*

carrying *lacZ*. (F) section of (E) stained with toluidine blue. X-Gluc was used to stain for GUS activity in (C-E), seen as blue in (C) and (D). Infection foci and infection threads containing rhizobia were detected by LacZ activity using Magenta-gal (indicated by the black arrows). The white star represents where *MtCRE1* expresses in a WT nodule at the same developmental stage (Plet et al., 2011).Scale bars in C-E, 200 µM, in F, 100 µM.

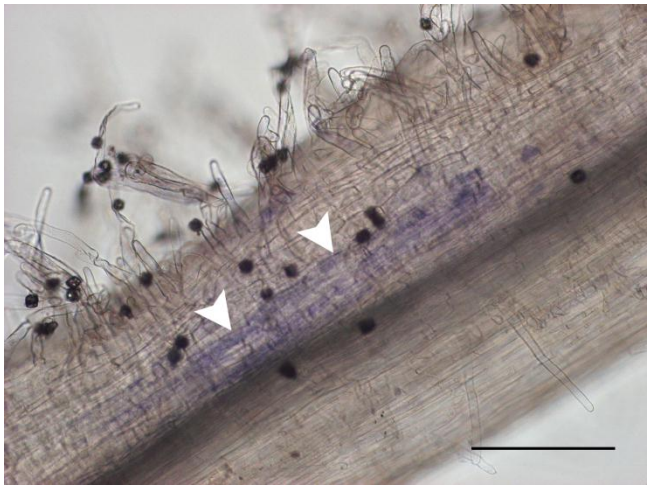

**Fig. 9.** *kce* 4 days post inoculation *in situ* with *RR4* probe. White arrow heads show *RR4* expresses in *kce* root inner cortex. Scale bar is 100 µm.

During nodulation, cytokinin signalling is activated within a three days (Gonzalez-Rizzo et al., 2006; Plet et al., 2011). Later on, cytokinin signalling, as indicated by p*RR4*::*GUS* is maintained in the nodule meristem (Plet et al., 2011). To test whether cytokinin signalling is activated in the *kce* mutant, the expression of two cytokinin marker genes, *CRE1* and *RR4* were analysed. It was found that the expression of the cytokinin receptor *CRE1* and the response regulator *RR4* were induced to a similar level as in the WT (Fig. 8C, D, and Fig. 9), indicating that in *kce*, early cytokinin signalling is activated normally in terms of timing and location. However, in late nodule development, 45 days post inoculation, *CRE1* gene expression was not detectable in the nodule apex (Plet et al., 2011). This is consistent with QPCR result (Fig. 8A and B), where *CRE1* and *RR4* gene expression is not maintained in *kce* late nodule development.

# 3 Discussion

## 3.1 Nodule identity

In the *L. japonicus alb1* mutant, there were two forms of nodules observed. The CVB nodules were not infected by rhizobia, whereas the PVB nodules were infected (Imaizumi-Anraku et al., 2000; Yano et al., 2006). In the PVB type nodules, which account for the majority part, there are no infected cells, and rhizobia are packed in enlarged infection threads which reside in the intracellular space; whereas in the CVB type nodules, the bacteria enter the nodule at a very low frequency (Imaizumi-anraku et al., 1997).

*kce* nodules lacked expression of lateral root marker genes. However the expression of nodule-specific genes is also weak. This could be because the nodulation marker genes used are associated with cortical cell divisions and rhizobial infection (*ENOD20*), the nodule meristem (*HAP2.1*), and nitrogen fixation (leghemoglobin), processes which are either absent or weak in *kce* nodules.

## 3.2 The coordination of rhizobial infection and nodule organogenesis

The coordination of rhizobial infection and nodule organogenesis is necessary to make a functional nodule. In this study, we found that a defect in rhizobial infection progression leads to the development of nodules that have central rather than peripheral vascular bundles. Plant mutant *ipd3* (Ovchinnikova et al., 2011) and rhizobium mutant *bacA* (Oldroyd et al., 2011) which support normal infection thread growth but fail to form symbiosomes have normal nodule architecture. The coordination between infection thread progression and nodule development has been suggested before. In the literature, it has been reported that a defect in rhizobial infection progression within the nodule can prevent the nodule apical meristem formation (Yang et al., 1992; Voroshilova et al., 2009) The finding that in the *hit1* mutant, which was blocked in early cortical cell divisions, more infection threads were observed (Murray et al., 2007). This suggests that cytokinin signalling activation is important for the synchronisation of rhizobial infection and nodule organogenesis. From these pieces of evidence, it can be seen that the degree of rhizobial infection progression correlates with that of nodule organogenesis in a step by step manner.

## 3.3 In *kce* nodule development, auxin and cytokinin balance is disrupted

In the legume-rhizobia symbioses, Nod factors suppress polar auxin transport through induction of flavonoid production (Boot et al., 1999; Wasson et al., 2006). Flavonoids are suggested to function as natural inhibitors of polar auxin transport (PAT) (Taylor and Grotewold, 2005). The auxin efflux inhibitor NPA was found to induce spontaneous CVB nodules or nodules lacking vascular bundles in *M. truncatula* and *Medicago sativa* (Hirsch et al., 1989; Fang and Hirsch, 1998; Rightmyer and Long, 2011). One possibility is that in the absence of sufficient Nod factor production in the correct location (the nodule cortex), cytokinin signalling is not maintained and polar auxin transport is not suppressed. In this model if the infection thread didn't progress into the nodule cortex, there would be insufficient Nod factor signalling to cause the appropriate changes in auxin transport in the nodule and

nearby vascular tissues. This alteration in the spatial balance between auxin and cytokinin signalling would lead to altered nodule architecture.

## 3.4 Nod factor dependent signalling is essential for peripheral vascular development in nodules

It was reported that *S. meliloti* Nod factors are able to induce two types of nodules, normal or centrally vascularized in *M. sativa* roots (Truchet et al., 1991; Grosjean and Huguet, 1997). This may suggest that different concentrations of Nod factors taken up by the plant may lead to these different developmental outcomes. In the WT plant situation, infection threads deliver rhizobia which constantly secret Nod factors, which maintains cytokinin levels. But in the *kce* mutant case, infection blocks in the infection foci, Nod factor concentration is not enough to maintain the level of cytokinin induced cortical cell divisions, resulting in CVB nodules.

In actinorhizal plants, the formation of the nodule primordium and vascular bundle development are spatially and temporally separate processes (Gualtieri and Bisseling, 2000). In actinorhizal plants, Frankia first induces a few root cortical cell divisions, forming a nodule primordium-like structure called prenodule that becomes invaded by an infection thread, later away from the cortical cell division site, pericycle cell divisions occur that develop into a lateral root, and the cortex in the emergent lateral root becomes infected via the pre-nodule. Both the pre-nodule and lateral root-like nodule structures are infected and contain nitrogen fixing cells (Gualtieri and Bisseling, 2000). In the parasponia-rhizobia symbiosis, similar nodule structures are formed as actinorhizal plants (Bender et al., 1987; Bender et al., 1987).

It has been argued that legume-type nodulation may have evolved from the older actinorhizal nodulation (Gualtieri and Bisseling, 2000). In actinorhizal plants-Frankia symbiosis, it’s believed that the signalling molecule that Frankia secretes is not Nod factor-like (personal communication, Jongho Sun). Similarly, in the parasponia-rhizobia symbiosis, the rhizobia mode of infection is intercellular first, which is a Nod factor independent mode of infection. Only when rhizobia reach the nodule primordia, intracelluar infection happens (Streng et al., 2011). In non-legume nodulation, which does not involve or require Nod factors, invasion results in CVB nodules (actinorhizal

nodules and parasponia nodules) (Gualtieri and Bisseling, 2000; Madsen et al., 2010; Streng et al., 2011). All the above supports the hypothesis that the presence of the Nod factors produced by rhizobia within cortical infection threads is required for normal peripheral vascular nodule development.

# 4 Materials and methods

## 4.1 Marker gene Q-PCR assay

### Plant materials and bacteria strains

The *Medicago truncatula* cv Jemalong A17, *lin-1* and *M. truncatula* R108, *vapyrin-2*, and *kce* mutants were used for the experiments described. For hairy root transformation, *M. truncatula* seedlings were transformed with *Agrobacterium rhizogenes* strain *ARqua1* carrying the appropriate binary vector using standard protocols (Boisson-Dernier et al., 2001), see modified protocol below. For nodulation assays, either *S. meliloti* 1021, *S. meliloti* 1021 pXLGD4 or *S. meliloti* Rm7210 *exoY210*::Tn*5* (Leigh et al., 1985) strain was used.

### Material preparation (spot inoculation)

The germinated *M. truncatula* plants were placed on Buffered Nodulation Medium (BNM) solid medium containing 0.1 µM 2-aminoethoxyvinylglycine (AVG) for 2 days until the main roots grow to a length about 3 cm. The seedlings were spot inoculated on the part of the root where root hair were initiating (the differentiation zone) with *S. meliloti* 1021 OD≈0.2. The inoculated region was marked on the back of the plate. The inoculated part was excised at different time points post inoculation. For each time point, more than 6 pieces of material were obtained and the material was placed in a 2ml eppendorf tube in liquid nitrogen before RNA extraction.

### RNA extraction

The sample was ground in a precooled (name the shaker equipment) in eppendorf tubes at 5000rpm shaking for 1 min. After disruption the samples, immediately placed on dry ice. The Qiagen RNeasy plant micro kit was to extract RNA according

to the kit handbook. After RNA extraction, RNA concentration was measured using a Nanodrop spectrophotometer.

**cDNA synthesis**

cDNA was synthesized using SuperScript™ II RT according to the manufacturer's instructions.

**Real-time PCR**

qRT PCR was carried out on a LightCycler® 480 SYBR GREEN I master mix on a LightCycler® 480 Multiwell Plate 384. 2µl of cDNA (1:3 diluted) was added as template and the reaction were carried outusing a LightCycler® 480 System thermocycler (Roche Applied Science Ltd (using the following cycling parameters:

| | Target (°C) | Acq Mode | Time | Ramp | Acq (per °C) | Sec Target | Step Size | Step Delay |
|---|---|---|---|---|---|---|---|---|
| Preincubation | 95 | None | 2 min | 4.8 | 5 | 0 | 0 | 0 |
| Amplification | 95 | None | 25 sec | 4.8 | 5 | 0 | 0 | 0 |
| | 58 | None | 25 sec | 2.5 | 5 | 0 | 0 | 0 |
| | 72 | Single | 40 sec | 4.8 | 5 | 0 | 0 | 0 |
| Melting curve | 95 | None | 5 sec | 4.8 | 5 | 0 | 0 | 0 |
| | 65 | None | 1 min | 2.5 | 5 | 0 | 0 | 0 |
| | 97 | Cons | 0 sec | 0.11 | 5 | 0 | 0 | 0 |

QPCR primer sets used : *ENOD20*: 5'-CTCTTATTCCACATCTATC-3'; 5'-ACCCGTTGGGCCTCTAACT-3'. *HAP2.1*: 5'-AAAATATGGCTATGCAACCTGTTTA-3'; 5'-CAACTGACATCTTACAATCATCTGG-3'. *MtRR4*: 5'-ATGCTTTTGTTCCGGGTTTA-3'; 5'-CTGCACCTTCCTCCAAACAT-3'. *MtCRE1*: 5'-CACCACCCTTTGGCTTCTAA-3'; 5'-CACTAAGTAGCGGCCTTTCG-3'. *MtGH3*: 5'-ACTTAACGGTGCCACTGACC-3'; 5'-AACTGACGACGGTCCATTTC-3'. *MtNIN*: 5'-CAGGACTACCATCAGCTGCA-3'; 5'-CCACAGTTGGTCTTGGAGGT-3'. Root specific ferridoxin: 5'-GCAACCACACCTGCTTTGTA-3'; 5'-GTGGTGGTGCTGATTGACAC-3'. Root specific membrane protein: 5'-AGGAGCAGTGCTGGAATGAC-3'; 5'-TGCTGACAAAAAGCAAACCA-3'. *MtEF-1α*: 5'-ATTCCAAAGGCGGCTGCATA-3'; 5'-CTTTGCTTGGTGCTGTTTAGATGG-3'

**Q-PCR data analysis**

The raw (not baseline-corrected) PCR data was transferred into LinRegPCR (156) software. The baseline fluorescence and PCR efficiency of individual PCR reaction were calculated based on the kinetic model of each PCR reaction in this software. The mean PCR efficiency of each amplicon, $C_t$ threshold and $C_t$ value of each PCR reaction were then calculated based on the baseline fluorescence and individual PCR efficiency. The start concentration value (N0) of each well was calculated based on the mean PCR efficiency and $C_t$ value finally. N0 values were then transferred into Excel 2007 (Microsoft, USA) software to calculate the relative cDNA amounts of each sample (containing three technical replicates) by dividing the mean N0 values of target gene cDNA with the mean N0 values of reference gene cDNA. The fold changes of expression increase/reduction were calculated by dividing the relative cDNA amounts of two target genes. The standard Deviation (SD) values were given by Excel 2007 software.

## 4.2 *M. truncatula* seeds germination

Seeds were scarified with sulphuric acid for about 10 mins after which seeds were rinsed with $dH_2O$ 5 times. Seeds were then sterilized for 2 min in 100% bleach and then rinsed seeds 8 times with sterile water. Seeds were then imbibed in 2-3 times of water for 4-6 hours at room temperature and then placed on Distilled Water (DWA) plates which were then sealed with foil, and incubated at 4°C for 1 day. The plates were then taken out of 4°C and left at 23°C overnight, until seedlings were about 1-2 cm in length.

## 4.3 Rhizogenes transformation

Overnight cultures of *Agrobacterium Rhizogenes* were started one day before the transformation in 5mL TY broth with appropriate antibiotics. They were then grown overnight at 28°C with shaking. Seeds to be transformed were imbibed and placed in a dark, 23°C cabinet.

On the day of transformation the overnight Arqua-1 culture was spun down for about 10 minutes 4000 rpm using a table top centrifuge and resuspended in 5 mL TY broth. In the flow hood, about 3 mm was cut off from the root tip of each seedling and the cut end dipped into the Arqua-1 culture. The seedlings were then placed on a Petri dish containing agar with modified Fahraeus medium and the plates were sealed with micropore tape and incubated upright in 21°C growth cabinet.7 days after transformation the growing roots were cut out from the seedlings, and placed on modified Fahraeus medium with appropriate antibiotics. These plates were poured at an angle so that the stem/leaves were in the air. One piece of filter paper was placed on the medium before putting the plants on to keep the plants from growing into the medium. Hairy roots will be examined after three weeks.

## 4.4 Nodulation assay

*M. truncatula* seeding were grown in a p40 tray with terragreen and sand 1:1 mixture for 7 days. The seedlings were then inoculated with 3 mL of OD600≈0.02 *S. meliloti* (resuspended in Buffered Nodulation Medium). Nodules and infection events are counted several time points post inoculation.

## 4.5 GUS staining followed with LacZ staining

GUS staining

GUS staining solution was freshly made as follows: 1 mM 5-bromo-4-chloro-3-indolyl-beta-glucuronic acid (X-Gluc); 5 mM Na-EDTA; 0.5 mM potassium ferrocyanide; 0.5 mM potassium ferricyanide; 0.1 M potassium phosphate pH 7.0.

The plant material was immersed in the GUS staining solution and incubated in a 37°C incubator, and the staining checked at one hour intervals and stoped using three washes of Z buffer when appropriate. Samples were fixed by immersing plant material in Z buffer with 2.5% glutaraldehyde, after which a 15 to 20 minutes vacuum was applied. Fresh glutaraldehyde was then to the material and left at least 1 hour at room temperature in the fume hood.

After fixing, Z buffer was used to wash the material for three times, each time for 5 minutes.

To stain the samples X-Gal staining solution was made as follows:, for 1 mL: 930 µL Z buffer; 25 µL 200 mM potassium ferricyanure; 25 µL 200 mM potassium ferrocyanure; 20 µL 4% 5-bromo-4-chloro-3-indolyl-beta-D-galactopyranosid (X-gal).

The staining solution was pipetted into the material and left in a 28°C incubator overnight.

The next morning, Z buffer was used to wash the material, one quick wash followed by one for an hour. The stained material was then stored with Z buffer with 2-3 drops of 0.5M Na-EDTA to avoid fungal contamination.

Z buffer was made as follows: 100 mM $Na_3PO_4$ pH 7.0 (use the combination of $Na_2HPO_4$ and $NaH_2PO_4$ to make it); 10 mM KCl; 1 mM $MgCl_2$.

## 4.6 Technovit imbedding, sectioning and phloroglucinol staining

Tissues were fixed using 2.5% glutaraldehyde as described previously. After changing the fresh fixation solutions, the material was placed at 4°C overnight.

The next day, the tissues were dehydrated with an ethanol series: 30% ethanol for 45 minutes; 50% ethanol for 45 minutes; 70% ethanol for 45 minutes; 90% ethanol for 45 minutes; 100% ethanol for 45 minutes.

The tissue was then pre-infiltrated with 50% ethanol/50% base liquid Technovit 7100 for 2 hours. The tissue was then positioned in the blocks and 200µl of polymerization solution was put into each block, covering the block using cling film to exclude air. The specimen were left to cure for 2 days.

The blocks were then trimmed and mounted on Perspex rods, and cut dry with a glass knife on a microtome. After sectioning, sections were placed on a drop of water on uncoated slides to stretch, and dried at 40°C.

**Phloroglucinol staining**

Phloroglucinol solution was made fresh as follows: 20% HCl: 37.5 mL distilled water; 62.5 mL concentrated HCl. 20 mg/mL phloroglucinol solution using 20% HCl. The phloroglucinol solution was applied on each section on the slides, and fine forceps were used to get rid of the bubbles, and pictures taken soon after.

## 4.7 RNA *In situ* hybridization in *M. truncatula* roots

**Fixation and embedding**

Fixation solution was freshly prepared (4% formaldehyde in DEPC-treated PBS). After transferring 1 cm pieces of roots to the fixative in the small bijous, vacuum immediately applied, and then slowly bleed, this was repeated until all the material sank to the bottom of the cup. At this point the fixation solution was exchanged and allowed to fix at 4 $^{o}$C for 6 hours. After fixaton, the sample was transferred into 75% ethanol, then the samples were put in the VIP machine for wax embedding. For sectioning, 8µm sections were made and then mounted on SuperFrost Plus slides and left at 42 $^{o}$C (air bath) overnight.

**Probe preparation**

*In situ* probes were cloned the into the pGEM®-T Easy vector that allows for *in vitro* transcription using a bacteriophage RNA-polymerase, such as T3, T7 or SP6 RNA-polymerase. The plasmid was linearized by digesting with Spe I or Nco I that left a 5’ overhang and cuts on the far side of the insert, relative to the promotor for *in vitro* transcription. About 10 µg plasmid was digested with 50U enzyme in 100 µL and then extracted with phenol/chloroform/IAA DNA precipitation (method in CHAPTER III). For the *in vitro* transcription reaction, the protocols in the Roche SP6 RNA

Polymerase, Roche T7 RNA Polymerase and Roche DIG RNA Labeling Mix manuals were followed. 0.5 µL of the *in vitro* transcription reaction was checked on a standard agarose gel (150V, 15 min). If the reaction was specific, the reaction volume was increased to 100 µL with water. 100 µL 2x Carbonate-buffer (80 mM $NaHCO_3$, 120 mM $Na_2CO_3$) was then added and the sample was incubated at 60$^{o}$C for x minutes.

$$X = \frac{\text{Original length of probe (kb)} - \text{desired length (0.15} - \text{0.2 kb)}}{\text{0.11 x original length x desired length}}$$

10 µL 10% acetic acid was added. The probe was precipitated with 0.1 volume 3 M NaOAc, 2.5 volume ethanol. The sample was stored at -20 $^{o}$C for 1h to overnight, and spun at 13000 rpm, 4$^{o}$C for 20 min. The pellet was washed with 70% ethanol and air dried and was then resuspended in 80µl 50% formamide. 2 µL of the probe was then checked on an agarose gel and the concentration was measured using the NanoDrop spectrophotometer. Probes were stored at -80 $^{o}$C until use. For an original probe length of 1kb, use between 80 and 800 ng of labelled RNA was used per slide, depending on the expression strength of the gene.

RR4 probe sequence:

TTGTTCCGGGTTTAAAGGTGGATCTAGTAATTACAGATTATTGCATGCCAGGAAT
GACTGGTTATGAGTTGCTTAAGAAAATCAAGGAATCAACCACTTTTAGAGCAATT
CCAGTAGTGATTATGTCTTCTGAAAATATCTTGCCACGCATTGACAGATGTTTGG
AGGAAGGTGCAGAGGATTTTATAGTGAAGCCAGTGAAATTATCTGACGTGAAAC
GTTTGAAGGGTTACATGACAACTAAGGAGGTTAATGTGGGAAGCCAAGACACT
GAAGTTATCGTTACCAACAATGTTGGTAACGATAACGATGGTGATGGTGTAGGG
ATAGGTATCAACAACAAAAGGAAGTTAGAAGAAGCATCTGATCTATCATCATCTG
AACCATCAATTTCATCATCGACACTTTCATCACCATCATCATCACCGTCACCTTC
ATCATCACCGTTGTCTTCACCCGACGTTCTTGAT

***In situ* hybridization**

Preparing the slides

The following solution was freshly prepared: 250 mL 0.85% NaCl (w/v); 250 mL 0.2% glycine in 1x PBS; 250 mL Pronase buffer (50 mM Tris-HCl, pH 7.5, 5 mM EDTA); 250 mL 4% formaldehyde in PBS, freshly prepared; 250 mL TEA buffer (0.1 M triethanolamine, pH 8.0; weigh 3.75 g triethanolamine into an RNAse-free bottle, add 250 mL water, shake to dissolve, adjust pH with approximately 700 µL concentrated HCl); 750 mL 1x PBS.

The slides were placed in a glass-rack and the following solutions were applied: Histoclear 10 min; Histoclear (fresh) 10 min; 100% ethanol 1 min; 100% ethanol; 95% ethanol (the rack was submersed about 15 times, goes for all the EtOH steps that follow) 1 min; 85% ethanol 1 min; 75% ethanol 1 min; 50% ethanol 1 min; 30% ethanol 1 min; 0.85% NaCl 30 sec; PBS 2 min; 0.125 mg/mL Pronase (782 µL stock for 250 mL buffer) 10 min; 0.2% glycine in PBS 1 min; 1x PBS (same as above) 1 min; 4% formaldehyde (keep on ice until used) 10 min; 1x PBS (same as above) 1 min; 1x PBS (fresh) 1 min; Acetic anhydride (1.25 mL per 250 mL TEA buffer; after adding the acetic anhydride, the sample was stirred vigorously and immediately put in the glass-rack with the slides.) 10 min; 1x PBS 1 min; 0.85% NaCl 1 min; ethanol series as above in the inverse order; after the “old” 100% ethanol, changed again to fresh 100% ethanol; left slides in this until the hybridization solution was applied (up to 2 hours).

Hybridization

A hybridization solution was made as follows: 8 µL 10x salts (3 M NaCl, 100 mM Tris-HCl pH 6.8, 100 mM $NaHPO_4$ pH 6.8, 50 mM EDTA); 33.6 µL formamide; 16 µL 50% dextrane sulphate; 1.6 µL 50x Denhardt’s solution; 8 µL 10 mg/mL tRNA. 12.8 µL of the probe in 50% formamide was denatured at 80$^{o}$C for 2’ and then added to the hybrization solution and placed on ice. 80-90 µL was then applied as one continuous band along the middle of the slide and a coverslip was carefully placed on top and then placed in a humid chamber at 55$^{o}$C overnight. Washing and detection

The slides were taken out of the humid chamber, held vertically to allow coverslip to slide off. The slides were then placed in glass-rack, in a container with wash buffer (0.2x SSC) and washed for 1 hour at 55$^{o}$C with gentle shaking, and then repeat with fresh 0.2x SSC. Blocking solution was prepared as follows (0.5% Blocking reagent [Roche Diagnostics, Cat.no. 1 096 176] in 1x TBS [100 mM Tris-HCl pH 7.5, 150 mM NaCl]; dissolved by shaking/rotating for 1h at 60$^{o}$C; prepare 1.1 mL per slide) and antibody buffer (1% BSA in 1x TBS, 0.3% Triton X-100). Slides were rinsed in 1x PBS for 2 min and then placed on plastic rack in humid chamber. 1 mL blocking solution was applied per slide, trying to cover all the tissue. The slide was then incubated at room temperature (RT) for 45 min with gentle shaking. The blocking solution was blotted off and 0.5 mL antibody buffer was applied and then the sample was incubated at RT for 15 min. Excess antibody buffer was then blotted off.80 µL of anti-Digoxygenin Fab-fragments (coupled to alkaline phosphatase; Roche Diagnostics, Cat.no 1 093 274) diluted 1:1250 in antibody buffer were then applied. A coverslip was put on and the sample was incubated in a humid chamber at RT for 2 hours after which the coverslip was removed as above, this time dipping in 1x PBS, if required. The slides were then washed 4 times with 0.5 mL antibody buffer each for 20 min followed by two rinses in detection buffer (100 mM Tris-HCl pH 9.5, 50 mM $MgCl_2$, 100 mM NaCl; prepare freshly each time) for 5 min each. Excess detection buffer was blotted off and 80 µL WesternBlue (Promega, Cat.no. S3841) was applied per slide, a coverslip put on, and the sample was incubated at RT in a dark humid chamber overnight or until staining developed. When staining is finished, the coverslip was removed, and 50 µL 50% glycerine was put on another coverslip put on the slides were stored at 4$^{o}$C.

## 4.8 Whole mount RNA *in situ* hybridization

(This protocol is described in detail in the thesis of Dr. Yiliang Ding)

# CHAPTER V General Discussion

## 1 Nodulation and mycorrhization crosstalk in symbiosis signalling

Legumes are capable of forming symbiotic associations with rhizobial bacteria leading to nodulation and arbuscular mycorrhizal fungi leading to extensive fungal colonisation of the root cortex. From genetic and biochemical analyses, it is known that nodulation and mycorrhization share a common signalling pathway. Rhizobial bacteria release a diffusible signal, termed Nod factor, that possesses a chitin backbone with an N-linked fatty acid moiety attached to the nonreducing terminal sugar and additional modifications to this basic structure (Denarie et al., 1996). Recognition of Nod factor involves the Nod factor receptors NFR5/NFP (Amor et al., 2003; Radutoiu et al., 2003), NFR1/LYK3 (Limpens et al., 2003; Radutoiu et al., 2003), that encode LysM domain receptor like kinases. This recognition induces calcium oscillations in the nuclear region requiring plasma membrane localised receptor like kinase SYMRK/DMI2 (Endre et al., 2002; Stracke et al., 2002; Madsen et al., 2003), components in nuclear pore NUP85, NUP133, NENA (Kanamori et al., 2006; Saito et al., 2007; Groth et al., 2010), nuclear ion channels DMI1, CASTOR, POLLUX (Ane et al., 2004; Charpentier et al., 2008) and the calcium ATPase MCA8 (Capoen et al., 2011). Perception of the calcium oscillations is mediated by a calcium and calmodulin dependent protein kinase (CCaMK) (Gleason et al., 2006; Tirichine et al., 2006) and its interacting partner CYCLOPS/IPD3 (Messinese et al., 2007; Yano et al., 2008). CCaMK phosphorylates CYCLOPS *in vitro* (Yano et al., 2008). Downstream of the signalling pathway, the GRAS proteins NSP1 and NSP2 (Kalo et al., 2005; Smit et al., 2005) form a heterodimer that coordinates nodulation gene expression (Hirsch et al., 2009). NSP1 binds the promoter of *NIN* and activates *NIN* expression (Hirsch et al., 2009). *NIN* is a nodulation specific target of the symbiosis signalling pathway that acts as a transcription factor to coordinate bacterial infection and nodule organogenesis (Schauser et al., 1999). Parallel to *NIN*, *ERN1* also functions to activate downstream rhizobial infection and nodule organogenesis (Middleton et al., 2007).

It has recently been revealed that mycorrhizal fungi also produce lipochitoolygosaccharides similar to Nod factors (Maillet et al., 2011), and these are likely to be perceived by the LysM motif receptor like kinase NFP in *Parasponia andersonii* (Op den Camp et al., 2010). It is still unclear how these LCOs are perceived in legumes and the role of the Nod factor receptors in the recognition of these mycorrhizal LCOs. Calcium oscillations are also induced in the nuclear region by mycorrhizal fungi (Kosuta et al., 2008). And mycorrhizal LCOs require *SYMRK* (Maillet et al., 2011), the nuclear pore complexes and the nuclear ion channels. Both CCaMK and CYCLOPS are also associated with mycorrhizal signalling (Yano et al., 2008). Specificity in symbiosis signalling appears to reside in the GRAS protein transcription factors with *NSP2* and *Reduced arbuscular mycorrhization* (*RAM1*) acting in mycorrhizal signalling downstream of the common symbiosis signalling pathway (Maillet et al., 2011; Gobbato et al., 2012). RAM1 binds the promoter of *RAM2* and activates its expression. *RAM2* is a mycorrhization specific target of the symbiosis signalling pathway. We know several components are shared between nodulation and mycorrhizal signalling and there is bifurcation leading to symbiotic specific outputs appears to occur between NSP2 and its interacting GRAS proteins NSP1 and RAM1. However, it is not clear how the decision to activate one pathway over the other is made and whether any positive of negative feedback is involved. In my studies, I found that NIN may function as a crosstalk that activates nodulation but suppresses mycorrhization.

## 1.1 NIN suppresses mycorrhizal signalling

In the *nin* mutant root hair microarray analysis, several mycorrhization genes are significantly induced as compared with WT. These genes appear to have a specific symbiotic function in mycorrhization, since they appear to be induced during mycorrhizal colonisation, but not during rhizobial infection. This excess mycorrhizal-associated gene induction implies that NIN may function to suppress the mycorrhizal signalling component of the symbiosis signalling pathway, once nodulation has been induced.

This finding is consistent with previous studies revealing a suppressive function for *NIN* in the regulation of the rhizobial and mycorrhizal reporter *ENOD11*. It has been

shown that in the *nin* mutant *ENOD11* gene expression is extended in the root compared with *ENOD11* expression in WT plants that shows a restricted range of gene induction (Marsh et al., 2007). *ENOD11* is not only induced in nodulation, but also induced in mycorrhization (Journet et al., 2001) and it is possible that the extended range of *ENOD11* expression in the *nin* mutant represents induction of this gene associated with its mycorrhization function. Thus NIN is a transcription factor that appears to have both activation and repressive activity, and it has been shown that NIN is able to bind the *ENOD11* gene promoter and negatively regulate its expression (Kim et al manuscript in preparation). Therefore, NIN may act to spatially regulate gene induction involving the negative control of mycorrhization-associated genes and the positive control of rhizobial infection genes. This hypothesis can be supported by the fact that two different NF-Y complexes are under differential regulation of *NIN* in the root hair microarray. One is under the positive regulation of *NIN* (*HAP2.1*) and this transcription factor is induced during rhizobial infection; while two other CCAAT transcription factors are under the negative regulation of *NIN* (*HAP3* and *HAP5*) and these components are induced during mycorrhization. Rhizobial infection occurs through trichoblast cells (root hair cells), whereas mycorrhizal invasion occurs through atrichoblast cells (non-root hair cells) and it will be interesting to test whether this differential regulation of symbiotic gene expression by *NIN* is associated with this cell-type specific mode of infection.

Considering that symbiosis signalling involves a conserved signalling pathway it seems apparent that once a cell is committed to one symbiotic process, there should be a mechanism to suppress the alternate process. *NIN* is a primary target for the nodulation-specific branch of the symbiosis signalling pathway and this gene negatively regulates mycorrhization-associated gene expression. Thus it appears that *NIN* could be a key component in locking the decision to nodulate, by blocking the activation of mycorrhizal associated responses. Even though the nodulation and mycorrhization signalling pathway bifurcates before the induction of *NIN*, the symbiotic signalling processes may not be sufficiently tight to ensure a singular mode of signalling. The suppression of mycorrhization after the bifurcation of nodulation and mycorrhizal signalling may function to fulfil this purpose. In the same way, if the hypothesis is correct, there should be a mechanism existing to suppress nodulation once the cell has committed to mycorrhization.

It seems likely that NF-Y transcription factors are a target for NIN and the differential regulation of nodulation and mycorrhizal associated NF-Y factors is particularly interesting. The spatial expression pattern of the nodulation specific NF-Y complex genes and the mycorrhization specific NF-Y complex genes needs to be assessed and it will be particularly interesting to see how *NIN* affects these patterns of gene expression. Furthermore, if this hypothesis is correct then overexpression of *NIN* should inhibit mycorrhization, while the loss of function *nin* mutants may show enhanced mycorrhizal colonisation. These should be tested to further validate this discovery.

## 1.2 NIN induction of rhizobial infection genes

### The *nin* mutant rhizobial infection phenotype

Previous results have shown that the *nin* mutant cannot support infection threads and the root hairs display excessive curling in response to rhizobial bacteria and Nod factor (Schauser et al., 1999; Marsh et al., 2007). From these studies it is unclear whether *nin* mutants could form infection foci, i.e. the entrapment of bacteria within a curled root hair. Using GFP labelled *Sinorhizobium meliloti*, I have shown that rhizobia are entrapped in the root hair curl of *nin* mutants, but no bacterial division appears to occur, leading to an absence of an infection focus. This indicates that *NIN* is required to allow bacterial replication in the root hair curl and this absence of bacterial replication may explain the lack infection threads developing in *nin* mutants.

### NIN coordinates rhizobial infection related genes expression

In the initial cloning of *NIN* it was postulated that NIN may be associated with the plasma membrane and may function in a manner analogous to Notch which translocates from the plasma membrane to the nucleus (Schauser et al., 1999). However, my research has shown that NIN localises to the nucleus and this is apparent with both N and C terminal fusions to GFP. The fact that NIN is present in the nucleus is consistent with its predicted function as a transcription factor.

The *nin* root hair microarray indicates that NIN coordinates rhizobial infection related gene expression. NIN regulates several genes that have already been identified to

have a function in rhizobial infection. NIN regulates *Nodulation pectate lyase* (*NPL*) that was identified in *Lotus japonicus* to function in degrading the cell wall during rhizobial infection. Such a function is necessary to allow the penetration of the infection thread. The *npl* mutant blocks rhizobial infection mostly in the root hair curl, but occasionally infection threads form and these rare infection threads are able to penetrate the nodule. It has been shown that NIN binds the *NPL* promoter and is necessary for its induction (Xie et al., 2011). From the *nin* root hair microarray, there are other cell wall related genes that are under the control of *NIN*, such as *Cellulose 5* (*CEL5*) and Pectin acetyl esterase family proteins. These may be associated with cell wall modifications associated with the penetration of the infection thread, or the production of new cell wall material that is required for infection thread growth.

In addition, *NIN* regulates *Rhizobium-directed polar growth* (*RPG*), mutants of which display inadequate root hair curling, slow progression of infection threads and balloon shaped infection threads that develop in the root cortex. Rare pink nodules can be found on *rpg* mutants and more patchy infection threads compared with WT. RPG encodes a putative long coiled-coil protein with an unknown function (Arrighi et al., 2008). *NIN* also regulates a Cystathionine Beta-Synthase domain containing protein (*CBS1*). It has been suggested that CBS-domain containing proteins function in the homeostasis of reactive oxygen species (ROS). The gene function will be discussed in a later section. There are other ROS related genes that are under the control of *NIN*, including two peroxidases. Whether these genes are primary targets of NIN or secondary affects of NIN action remains to be tested.

NIN coordinates the expression of a number of transcription factors, including *HAP2.1*. This gene is a member of the NF-YA family, a component of the NF-Y heterotrimer complex. Previously *HAP2.1* was identified due to its expression in the nodule meristem. *HAP2.1* silenced plants display small nodules lacking the meristem (Combier et al., 2006; Combier et al., 2008). No rhizobial infection phenotype has yet been reported, but recently analysis of a *hap2.1* stable mutant indicates this gene does function during rhizobial infection (personal communication, Andy Breakspear). In addition to *HAP2.1*, there are other transcription factors regulated by NIN. These include a basic helix-loop-helix (bHLH) DNA binding protein, a basic domain leucine

zipper (bZip) transcription factor, two members of the DREB subfamily A-6 of the ERF/AP2 transcription factor family, a member of the ERF (ethylene response factor) subfamily B-5 of ERF/AP2 transcription factor family and a MYB-like transcription factor family protein. The fact that NIN controls several transcription factors suggests that it controls more processes than those currently known.

Besides the known rhizobial infection genes that are under the control of *NIN*, processes such as hormone regulation also appear to be coordinated. Four gibberellin biosynthetic pathway proteins, a SAUR like auxin responsive protein and a cytokinin glycosyl hydrolase 9C3 (GH9C3) are all downregulated in the *nin* mutant. Gibberellin has not been shown to function in rhizobial infection, but this may be due to the high redundancy for gibberellin biosynthetic pathway genes. *NIN* control of gibberellin biosynthesis implies a gibberellin function in the root epidermis during rhizobial infection.

The gene profiling indicates a range of processes regulated by NIN. The simplest explanation is that NIN coordinates the expression of a number of transcription factors that then go on to activate the range of processes observed. However, the evidence for direct control of NPL by NIN (Xie et al., 2011) indicates that NIN does coordinate genes directly associated with the developmental processes required for bacterial infection. The fact that NIN is required for induction of a number of genes whose mutant phenotypes indicate a role during rhizobial infection highlights the importance of NIN at this stage. It will be interesting to discriminate the direct targets of NIN from those that are regulated as a result of NIN action and the best means to assess this will be a ChIP-seq approach using NIN antibodies or a NIN-antigen fusion.

**Section summary**

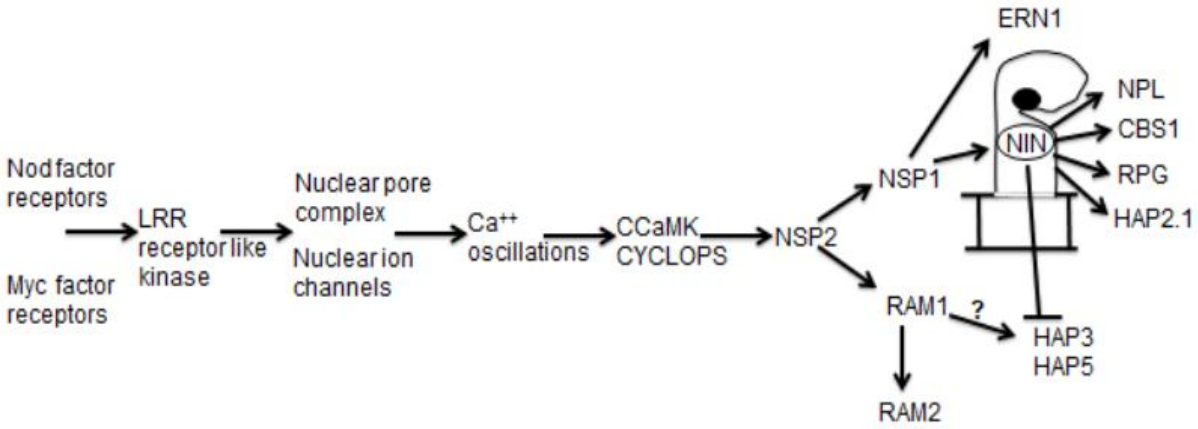


**Fig. 1.** Summary of nodulation and mycorrhization signalling pathways.

As indicated in Figure 1, there are several components shared in nodulation and mycorrhization signalling. Nodulation and mycorrhization signalling bifurcates through the NSP2 interaction with different GRAS proteins (NSP1 leading to nodulation; RAM1 leading to mycorrhization). *NIN* is specifically induced during nodulation by NSP1. *NIN* regulates a suite of important factors involved in rhizobial infection which include *NPL*, *CBS1*, *RPG* and *HAP2.1*. Probably there are other unknown processes also under the control of *NIN*. NIN also functions in nodulation as a feedback mechanism to block mycorrhizal signalling and this regulation may act through *HAP3* and *HAP5* transcription factors. Such a feedback mechanism may help to improve the nodulation efficiency, by inhibiting mycorrhizal processes being activated in the same cell.

# 2 New rhizobial infection mutants

## 2.1 Specific Nod factor signalling is critical for rhizobial infection

Symbiosis signalling, in particular activation by Nod factor, is critical for rhizobial infection. This is most apparent from studies of *S. meliloti nodF*/*nodL* double mutants, which produce a Nod factor lacking the acetyl decoration and an altered N-acyl group on the non-reducing end of the molecule. These mutants show a block in rhizobial infection in the root hair curl, with only very rare infection threads. Cortical cell divisions do happen leading to the formation of small bumps (Ardourel et al., 1994). Induction of calcium spiking is altered in *nodF*/*nodL* Nod factor (Oldroyd et al., 2001) and furthermore the induction of the calcium flux is mostly absent with this mutant Nod factor.

LYK3, that encodes a LysM receptor-like kinase, is considered as a potential Nod factor entry receptor. *lyk3*-1 (*hcl*) mutant (the *lyk3* mutant strong allele) cannot support rhizobial infection and the root hairs display hypercurls (Smit et al., 2007). In *LYK3* knockdown plants, the majority of the infection events result in aborted infection threads. In about 20% of the cases, tubes containing sac-like structures were observed (Limpens et al., 2003). *LYK3* knockdown plants inoculated with *S. meliloti nodF/nodE* mutants (defective in the *N-acyl* moiety) were still able to trap bacteria within curled root hairs. However, the number of infection threads was

markedly reduced. Most infections were arrested at the microcolony stage, with infection thread-like structures developing but these were aborted in the root hair and had aberrant morphologies that consisted of tube- and sac-like structures. On the control plants, the majority of the infection threads result in tubular structure (Limpens et al., 2003). Considering the infection phenotypes of the *S. meliloti nodF/nodL* mutant and the *M. truncatula lyk3* mutants, and the interplay between *S. meliloti* Nod factor mutants and *lyk3* mutants, it has been hypothesised that a greater stringency of Nod factor recognition occurs during bacterial infection and that *LYK3* may act in this stringent Nod factor recognition. LYK3 has punctate distribution on the cell periphery consistent with a plasma membrane or membrane-tethered vesicle localisation. In uninoculated roots, LYK3 localisation appears to be dynamic. However, upon rhizobia treatment, LYK3 localisation becomes more stable and this stability is dependent on the Nod factor non-reducing end decorations (*nodF/nodL*) (Haney et al., 2011). The dynamics of LYK3 localisation is further consistent with it acting as a Nod factor 'entry receptor', providing an additional barrier to bacterial entry.

Microdomains (lipid rafts) have recently been discovered to associate with Nod factor receptors either through colocalization or through interaction. Flotillins (FLOTs) are known to define a clathrin-independent, caveolin-independent endocytic pathway required for endocytosis of cholera toxin (Haney and Long, 2010). *FLOT2* and *FLOT4* have been found to function in rhizobial infection through knock down experiments. And it has been indicated that *FLOT2* and *FLOT4* induction during rhizobial infection is dependent on *NIN*. FLOT4 localises to infection thread membrane (Haney and Long, 2010) and interestingly, FLOT4 also changes its localisation in root hairs upon rhizobia inoculation, in a similar pattern as LYK3. LYK3 and FLOT4 colocalize after rhizobia inoculation and the dynamics of FLOT4 localisation is altered specifically in *LYK3* kinase inactive mutants (*lyk3*-1) (Haney et al., 2011). All the above suggests that FLOT4 either interacts with LYK3 upon rhizobial infection or is present in the same complex as LYK3. The work on FLOT4 and LYK3 is intriguing, with the dynamic localisation of these two proteins modulated by Nod factor recognition. This dynamic localisation may be associated with the conglomeration of the receptor during rhizobial infection may facilitate a heightened

level of signal transduction, or alternatively this change in localisation may facilitate the specific recognition of rhizobial Nod factors.

A second microdomain-associated protein, *symbiotic remorin* 1 (*SYMREM1*) has been found to function in rhizobial infection. SYMREM1 localises on the infection thread plasma membrane and the symbiosome membrane. Plants mutated for *SYMREM1* show reduced nodule numbers and infection threads in the nodule zone II appear to be greatly enlarged and highly branched. Bacterial liberation from ITs was greatly reduced or completely absent, reflected by the lack of symbiosomes in the nodule. SYMREM1 interacts with LYK3, NFP and DMI2 in *Nicotiana benthamiana*, suggesting a possible role for this protein in the localisation of these symbiotic receptors. These results show the importance of SYMREM1 in nodulation, however there are as yet no biological relevance shown for interaction with the receptors (Lefebvre et al., 2010).

Both FLOTs and remorins have provided evidence that plant plasma membrane microdomains supply Nod factor receptors a platform to move and interact with different partners and may also drive endocytosis of these receptors. This membrane fluidity control mechanism appears to play an important role in regulating the symbiotic receptors, but the precise role remains to be determined.

PUB1 is another LYK3 regulator that functions in rhizobial infection, that was identified due to its interaction with LYK3. PUB1 is a U-box dependent E3 ubiquitin ligase that is phosphorylated by LYK3. The interaction between PUB1 and LYK3 is specific, with no interaction between PUB1 and other LysM receptor like kinases tested. *PUB1* knockdowns revealed little nodulation defects, whereas *PUB1* overexpression suppresses WT nodulation. The genetic interaction between PUB1 and LYK3 was shown with the knockdown of *PUB1* in a *lyk3-4* mutant (a weak *Lyk3* allele). The *PUB1* knockdown overcame the *lyk3*-4 infection phenotype (Mbengue et al., 2010). PUB1 does not appear to ubiquitinate LYK3 and this implies that after phosphorylation by LYK3, PUB1 may interact with other proteins to regulate the signalling pathway. Protein interaction screens for PUB1 will be useful in addressing the role of this protein in symbiosis signalling. Different from the *PUB1* suppressive

function in rhizobial infection, *Lumpy infection* (*LIN*) a novel type U-box containing E3 ligase functions positively during infection (Kiss et al., 2009). *lin* mutants block rhizobial infection with abortions mostly in the root hair cell (Kuppusamy et al., 2004). The strong phenotype implies its importance during rhizobial infection. However its function has not yet been revealed. The WD40 repeats present in LIN suggests a function in protein-protein interactions (Smith et al., 1999), but the interacting partners have yet to be identified. E3 ligases have specificity in ubiquitination, so it will be easy to imagine there should be a variety of E3 ligases functioning in nodulation signalling pathway that may act as feedback mechanisms or may control aspects of signalling or development.

Exopolysaccharides (EPS) have an important function in rhizobial infection. *S. meliloti exoY* mutants, with defects in the first step of EPS biosynthesis, show blocks in infection in the root hair curl with occasional infection threads initiated, but never penetrate into the root cortex (Cheng and Walker, 1998). It has been argued that EPS may act as defence barrier for the bacteria or may act as a signalling molecule. Microarrays in *M. truncatula* using *exoY* mutants show reduction of two putative receptors compared with treatments of the WT strain (Jones et al., 2008). In addition the specificity of rhizobial strain interactions in *M. truncatula* is correlated with the succinoglycan oligosaccharide structure (Simsek et al., 2007). These studies suggest that EPS may function as a signalling molecule. However, an EPS signalling pathway has not been identified and efforts are underway to identify the EPS receptors and signalling components in the plant.

## 2.2 Cell wall remodelling is important during rhizobial infection

To allow rhizobial infection of legume roots, plant cell walls must be locally degraded for plant-made infection threads (ITs) to be formed. *Bradyrhizobium japonicum* has seed-exudate inducible genes encoding pectin methyl esterase and polygalacturonase (Wei et al., 2008), but database searches indicate these genes are relatively rare in rhizobia and absent from *M. loti* (Xie et al., 2011). Components in cell wall modification have been found to be required for successful rhizobial infection. *NPL* encodes a pectate lyase that is induced during rhizobial infection. The mutant blocks infection in the root hair curl with occasional infection thread initiation.

In addition to pectate lyases there are several pectin methyl esterases and polygalacturonases that could play a role in degradation of the cell-wall pectin. Also, a predicted polygalacturonase and a pectin methyl esterase are induced during nodulation which has been suggested to account for the *npl* leaky phenotype during rhizobial infection (Xie et al., 2011).

## 2.3 Rhizobial infection control of ROS regulation

ROS, mainly hydrogen peroxide ($H_2O_2$), superoxide ($O^{2-}$) and the hydroxyl radical ($OH^-$) are the highly reactive by-products of oxygen reduction. ROS production in cells can result in cytotoxicity but it can act as signalling molecules in many cellular processes. Both rapid generation of superoxide and accumulation of $H_2O_2$ are characteristic early features of the hypersensitive response following perception of pathogen avirulence signals. The oxidants are not only direct protective agents against pathogens, but $H_2O_2$ also functions as a substrate for oxidative cross-linking in the cell wall, as a threshold trigger for hypersensitive cell death, and as a diffusible signal for induction of cellular protectant genes in surrounding cells (Lamb and Dixon, 1997). ROS changes in the legume rhizobia symbiosis has remained an open question. NFs have been shown to both induce and suppress ROS, this probably depends on the timing of the observation (Ramu et al., 2002; Shaw and Long, 2003). Observation showed that suppression of ROS efflux occurred 30-90 min after treatment *of M. truncatula* roots with Nod factors, while the defence elicitor polygalacturonic acid (PGA), strongly increased $H_2O_2$ efflux. They further showed *M. truncatula* roots pretreated with PGA significantly decreased $H_2O_2$ efflux by Nod factors. This suggests that one aspect of Nod factors' response is to suppress defence-response related ROS. Interestingly, the suppression of $H_2O_2$ efflux is dependent on the Nod factor receptor *NFP*, but not on the downstream signalling components *DMI1 and DMI2*. This may imply that Nod factor suppression of ROS efflux is related to root hair responses leading to rhizobial infection instead of being a part in the common signalling pathway. Peroxidases degrade $H_2O_2$ to superoxide. Except being involved in initial Nod factor induced responses, ROS has also been detected in the cell-wall like matrix of the infection threads, where a role in cross-linking to promote hardening of the infection matrix has been proposed (Santos et al., 2001). Transcriptional studies of infected root hairs show *RIP1* and three other

peroxidases are induced at five days post infection by rhizobia. This time point corresponds with the onset of infection threads. *RIP1* and two of these peroxidases require *NIN* for appropriate induction.

Rhizobial mutant studies have provided evidence for ROS function in infection. Rhizobia produce several antioxidant enzymes. These include catalases that degrade $H_2O_2$ to $H_2O$ and $O_2$, and superoxide dismutase, which converts superoxide to $H_2O_2$ and $O_2$. Infection by the *S. meliloti* catalase genes (*katB katC*) double mutant and superoxide dismutase mutant (*sodA*) lead to root hair infection defects (Santos et al., 2000; Jamet et al., 2003). This indicates ROS levels must be limited in infection development. Interestingly, the *katB* overexpression also compromises root hair infection (Jamet et al., 2007), indicating a positive role of ROS in infection thread development. Together these data show that ROS changes during symbiont's epidermal infection are dynamic and its regulation is complex.

Forward genetic screens have been carried out using *Tnt1* transposon mutagenized *M. truncatula* plants for rhizobial infection mutants. One mutant that I characterised was found to encode *CBS1*. This gene encodes a Cystathionine Beta-Synthase (CBS) domain containing protein. *cbs1* is defective in infection thread initiation and infection thread progression. The *cbs1* mutant displays excess superoxide accumulation in root hair curls and infection threads, indicated by Nitroblue tetrazolium NBT staining (follow on work by Dr. Chengwu Liu). Previous work on CBS domain-containing proteins of *Arabidopsis*, CBSX1 and CBSX2, revealed a localisation in the chloroplast and a role in the regulation of thioredoxins (Trxs) in the ferridoxin-Trx system. CBSX3, that localises in the mitochondria, regulates Trxs in the NADP-Trx system. CBSX1 directly interacts with Trxs and therefore regulates $H_2O_2$ levels. *CBSX1* overexpression causes decreases in $H_2O_2$ levels, resulting in the failure of secondary wall thickening in the anther endothecium (Yoo et al., 2011). Based on this work, CBS1 may also be involved in interaction with Trxs and may negatively regulate ROS levels during rhizobial infection. Interestingly *CBS1* has a close homolog *CBS2* which is found adjacent to it in the genome and is induced during mycorrhization. This raises the question how these genes evolved. Most likely *CBS2* evolved first to function in mycorrhization and then at some point during the

emergence of legumes, CBS1 was created by tandem duplication after which it was recruited to function in rhizobial infection, possibly through neofunctionalization of its promoter.

### 2.4 *KCE* is required during infection thread initiation

The other rhizobial infection mutant studied in this thesis is *Knocks but can't enter* (*kce*). The *kce* mutant was shown to block rhizobial infection in the root hair curl. There are occasional infection threads initiated, but the infection threads never penetrate though the root epidermis. Cortical cell divisions have been observed in *kce* mutants long after initial rhizobial inoculation, however, the divisions are not maintained or organised as in WT. The nodules that developed in *kce* mutants harbour central vascular bundles (CVB) compared with WT nodules with peripheral vascular bundles (PVB). Although inverse PCR, TAIL PCR, and deep sequencing have been applied to look for the correct *Tnt1* insertion, *KCE* has yet to be cloned. Using these methods, *kce* was mapped to a 12 Mb interval. Mapping populations have been created and this work is currently being followed up.

*kce* mutants reflect the phenotype of *lin* mutants. Both of the mutants block rhizobial infection in the root hair, with no infection threads penetrating into the nodule. However, there are swollen infection threads identified in *lin* mutants which never occur in *kce* mutants. The phenotype of *kce* suggests it acts downstream of *NIN* and thus *KCE* may be on the gene list downregulated in the *nin* mutant. There are no other obvious phenotypes observed in *kce* mutants, so it is difficult to guess which processes *KCE* may coordinate.

## 3 Rhizobial infection coordinates nodule organogenesis

### 3.1 Nodule Infection is required for normal vascular development in nodules

In my thesis I have provided evidence that successful epidermal infection is required for normal nodule development during nodulation in *M. truncatula*. I found that nodules that form on the *kce* mutant have a central rather than peripheral vascular

bundle. This configuration is similar to lateral roots and actinorhizal nodules and the rhizobia-induced nodules that develop on the non-legume *Parasponia*. This outcome is independent of plant genotype as shown by the occurrence of nodules having either central or peripheral vasculature on the same plants on *vpy* and *lin* mutants in a manner that directly corresponds to the extent of infection progression. In addition, rhizobial *exoY* mutants that abort early in infection also produce nodules with a centrally-located vascular strand. The distinct structure of these growths and analysis of marker gene expression suggests that symbiotic identity is retained despite the fact that these nodules are not colonized.

Support for the idea that infection determines nodule development outcomes is provided by Hirsch et al. (Hirsch et al., 1985). They showed that *Agrobacterium tumefaciens* and Sym$^-$ *Rhizobium trifolii* transconjugants carrying nodulation sequences from *S. meliloti* were able to induce nodules with peripheral vascular bundles on *M. sativa*, but formed nodules with central vascularization when white clover roots were inoculated. When the nodules were examined it was found that despite lacking infection threads the nodules formed on *M. sativa* contained large pockets of intracellular bacteria, while the nodules on the white clover roots were not colonized. Although our experiments were limited to *M. truncatula*, the *L. japonicus aberrant localization of bacteria inside nodule 1* (*alb1*) mutant that appears to develop central vasculature in uncolonized nodules may suggest this phenomenon is widespread in legumes. However, in the case of *alb1*, additional experiments are needed to determine whether the vascular defect is related to the infection block or is due to direct involvement of *ALB1* in vascular development as proposed by the authors (Imaizumi-Anraku et al., 2000).

## 3.2 A role for auxin and cytokinin in infection-dependent nodule development

How might infection affect development in such a striking manner? There are several interesting exceptions to the link between infection and the development of peripheral vascular bundles that provide important clues to the mechanisms underlying this phenomenon. First, nodules induced by NFs alone can sometimes have normal positioning of the vascular strands (Truchet et al., 1991; Grosjean and

Huguet, 1997). Also, application of exogenous cytokinin, or the *L. japonicus snf2* mutant with constitutively active cytokinin signalling both produce nodules with peripheral vascular bundles in absence of infection (Tirichine et al., 2006; Heckmann et al., 2011). Similarly, the *snf1* mutant also produces spontaneous nodules with normal architecture (Tirichine et al., 2006). Therefore, it appears that the requirement for infection can be obviated by activation of downstream processes, in particular cytokinin signalling. Counter to this, auxin transport inhibitors like NPA induce nodules that lack vascular strands altogether (Hirsch et al., 1989; Van De Wiel et al., 1990; Takanashi et al., 2011), or form nodules with centrally proliferating vascular tissue (Wu et al., 1996; Rightmyer and Long, 2011) underscoring the central role of polar auxin transport in vascular bundle formation. NFs applied to legume roots have a dramatic effect on polar auxin transport (Mathesius et al., 1998; Boot et al., 1999). Spot application of NFs or rhizobia on white clover roots has been shown to induce a strong local repression of expression from the promoter of the auxin reporter gene *GH3* (Mathesius et al., 1998). It is not known how this effect is exerted, but cytokinin perception has been shown to be required for the rhizobia-induced changes in auxin transport that occur during nodulation (Plet et al., 2011), and flavonoids, which are essential for nodulation, also exert effects on auxin transport (Wasson et al., 2006; Subramanian et al., 2007; Zhang et al., 2009). NFs are produced by rhizobia enclosed in infection threads within the nodule (Marie et al., 1992). In addition, NF-induced nuclear calcium oscillations accompany the advance of infection through the underlying cortical cell layers demonstrating that NFs are continuously perceived as the infection thread penetrates the root (Sieberer et al., 2012). It's possible that the production of NFs within the centre of the nodule results in changes in auxin distribution that have developmental consequences. Auxin has a well-established role in vascular differentiation, and xylem formation in particular is associated with high levels of auxin stimulation in the presence of cytokinin (discussed in (Aloni et al., 2006)). This idea is consistent with the observation that expression of the auxin reporter *GH3* is initially uniform within nodules prior to infection, but as the nodule develops *GH3* expression becomes diminished at the centre of the nodule where infection occurs, and is limited to the nodule periphery and is especially high in the vascular bundles (Mathesius et al., 1998; Pacios-Bras et al., 2003; Takanashi et al., 2011). We find that marker genes associated with early cell divisions in the cortex (*CRE1*, *RR4*, and *GH3*) and with nodule vascular development (*GH3*) are reduced in

*kce* nodules suggesting that hormone regulation was altered. Expression of the meristem marker *HAP2.1* is also reduced which is consistent with the slow development of the mutant nodules. However, in order to determine whether there is a re-distribution of hormone signalling as a result of rhizobial infection a detailed spatial analysis using markers for auxin and cytokinin signalling is needed.

## 3.3 Implications for nodule evolution

The infection programme in *Parasponia* does not utilize root hairs; infection threads do not form in the epidermis and are formed only after penetration of the nodule cortex which leads to the formation of a small non-vascularised pre-nodule near where the main centrally-vascularised nodule will emerge and eventually become infected (Bender et al., 1987; Bender et al., 1987). Similarly, nodules in actinorhizal species induced by *Frankia* involve the formation of a pre-nodule, so that the initial epidermal infection and lateral organ development programmes are separate both temporally and spatially. One hypothesis for the evolution of nodulation in legumes is that these independent processes present in actinorhizal nodulation have been merged together in legumes (Gualtieri and Bisseling, 2000; Laplaze et al., 2000). Our finding that physical separation of infection from the emerging nodule leads to the development of nodules with a central vascular arrangement supports this hypothesis.

The evolution of nodulation involved a predisposition event that facilitated the emergence of nodulation in species within the Rosid 1 clade (Gualtieri and Bisseling, 2000; Doyle, 2011). It has been proposed that nodulation emerged independently in a number of different clades in the Rosid 1 and if this is indeed the case, then one would expect differential evolution of nodulation. This is supported by differences in actinorhiza plants and legume plants nodule development and the fact that several ancestors of nodulating species do not nodulate (Doyle, 2011). Thus in this scenario nodulation evolved independently in actinorhizal species and in legumes and thus the nodule is a convergent structure, with any similarities being the result of convergent evolution. Whether legume nodules evolved from actinorhizal plants as some have suggested (Gualtieri and Bisseling, 2000) or whether they occurred independently with a common predisposition event as others have suggested (Doyle,

2011), remains a point of speculation. In the actinorhiza-Frankia symbiosis, based on the current understanding, a Nod factor like molecule is not observed (personal communication, Jongho Sun). Similarly, in Parasponia, a non-legume rhizobia symbiosis, which is thought to be recently evolved, the initial invasion by rhizobia is Nod factor independent (Streng et al., 2011). Given these observations, one possibility is that the evolution of the PVB-type legume nodule structure was dependent on the appearance of rhizobium nodulation factors. The properties of Nod factors, in particular their ability to induce cytokinin signalling in the root cortex (Gonzalez-Rizzo et al., 2006) and to modify auxin transport (Boot et al., 1999; Wasson et al., 2006) may have been essential for integration of the infection and organogenesis programmes in legumes.

# 4 Conclusions

1. Nodulation signalling suppresses mycorrhization through activation of *NIN*.
2. NIN coordinates rhizobial infection through induction of a range of infection-related genes, in particular a suite a NF-Y transcription factors.
3. Two new loci have been identified that function during rhizobial infection. One of these may be associated with regulating ROS.
4. Appropriate rhizobial infection is essential for correct nodule organogenesis.

# References

**Aloni R, Aloni E, Langhans M, Ullrich CI** (2006) Role of cytokinin and auxin in shaping root architecture: regulating vascular differentiation, lateral root initiation, root apical dominance and root gravitropism. Ann Bot **97:** 883-893

**Amor BB, Shaw SL, Oldroyd GE, Maillet F, Penmetsa RV, Cook D, Long SR, Denarie J, Gough C** (2003) The NFP locus of Medicago truncatula controls an early step of Nod factor signal transduction upstream of a rapid calcium flux and root hair deformation. Plant J **34:** 495-506

**Ane J-M, Kiss GB, Riely BK, Penmetsa RV, Oldroyd GED, Ayax C, Levy J, Debelle F, Baek J-M, Kalo P, et al.** (2004) Medicago truncatula DMI1 Required for Bacterial and Fungal Symbioses in Legumes. Science **303:** 1364-1367

**Ardourel M, Demont N, Debelle F, Maillet F, de Billy F, Prome JC, Denarie J, Truchet G** (1994) Rhizobium meliloti lipooligosaccharide nodulation factors: different structural requirements for bacterial entry into target root hair cells and induction of plant symbiotic developmental responses. Plant Cell **6:** 1357-1374

**Arrighi JF, Barre A, Ben Amor B, Bersoult A, Soriano LC, Mirabella R, de Carvalho-Niebel F, Journet EP, Gherardi M, Huguet T, et al.** (2006) The Medicago truncatula lysin motif-receptor-like kinase gene family includes NFP and new nodule-expressed genes. Plant Physiol **142:** 265-279

**Arrighi JF, Godfroy O, de Billy F, Saurat O, Jauneau A, Gough C** (2008) The RPG gene of Medicago truncatula controls Rhizobium-directed polar growth during infection. Proc Natl Acad Sci U S A **105:** 9817-9822

**Aslam SN, Newman M-A, Erbs G, Morrissey KL, Chinchilla D, Boller T, Jensen TT, De Castro C, Ierano T, Molinaro A, et al.** (2008) Bacterial Polysaccharides Suppress Induced Innate Immunity by Calcium Chelation. Current Biology **18:** 1078-1083

**Bender G, Goydych W, Rolfe B, Nayudu M** (1987) The role of Rhizobium conserved and host specific nodulation genes in the infection of the non-legume Parasponia andersonii. Molecular and General Genetics MGG **210:** 299-306

**Bender GL, Nayudu M, Goydych W, Rolfe BG** (1987) Early infection events in the nodulation of the non-legume Parasponia andersonii by Bradyrhizobium. Plant Science **51:** 285-293

**Bensmihen S, de Billy F, Gough C** (2011) Contribution of NFP LysM Domains to the Recognition of Nod Factors during the *Medicago truncatula Sinorhizobium meliloti* Symbiosis. PLoS ONE **6:** e26114

**Besma Ben A, Sidney LS, Giles EDO, Fabienne M, Penmetsa RV, Douglas C, Sharon RL, Jean D, Clare G** (2003) The *NFP* locus of *Medicago truncatula* controls an early step of Nod factor signal transduction upstream of a rapid calcium flux and root hair deformation. The Plant Journal **34:** 495-506

**Boisson-Dernier A, Chabaud M, Garcia F, Becard G, Rosenberg C, Barker DG** (2001) Agrobacterium rhizogenes-transformed roots of Medicago truncatula for the study of nitrogen-fixing and endomycorrhizal symbiotic associations. Mol Plant Microbe Interact **14:** 695-700

**Boot KJM, van Brussel AaN, Tak T, Spaink HP, Kijne JW** (1999) Lipochitin Oligosaccharides from Rhizobium leguminosarum bv. viciae Reduce Auxin Transport Capacity in Vicia sativa subsp. nigra Roots. Molecular Plant-Microbe Interactions **12:** 839-844

**Borisov AY, Madsen LH, Tsyganov VE, Umehara Y, Voroshilova VA, Batagov AO, Sandal N, Mortensen A, Schauser L, Ellis N, et al.** (2003) The Sym35 Gene Required for Root Nodule Development in Pea Is an Ortholog of Nin from Lotus japonicus. Plant Physiol. **131:** 1009-1017

**Brendan KR, Géraldine L, Jean-Michel A, Douglas RC** (2007) The symbiotic ion channel homolog DMI1 is localized in the nuclear membrane of *Medicago truncatula* roots. The Plant Journal **49:** 208-216

**Broghammer A, Krusell L, Blaise M, Sauer J, Sullivan JT, Maolanon N, Vinther M, Lorentzen A, Madsen EB, Jensen KJ, et al.** (2012) Legume receptors perceive the rhizobial lipochitin

oligosaccharide signal molecules by direct binding. Proc Natl Acad Sci U S A **109:** 13859-13864

**Capoen W, Sun J, Wysham D, Otegui MS, Venkateshwaran M, Hirsch S, Miwa H, Downie JA, Morris RJ, Ane JM, et al.** (2011) Nuclear membranes control symbiotic calcium signaling of legumes. Proc Natl Acad Sci U S A **108:** 14348-14353

**Castresana J** (2000) Selection of conserved blocks from multiple alignments for their use in phylogenetic analysis. Mol Biol Evol **17:** 540-552

**Charpentier M, Bredemeier R, Wanner G, Takeda N, Schleiff E, Parniske M** (2008) Lotus japonicus CASTOR and POLLUX are ion channels essential for perinuclear calcium spiking in legume root endosymbiosis. Plant Cell **20:** 3467-3479

**Charron D, Pingret JL, Chabaud M, Journet EP, Barker DG** (2004) Pharmacological evidence that multiple phospholipid signaling pathways link Rhizobium nodulation factor perception in Medicago truncatula root hairs to intracellular responses, including Ca2+ spiking and specific ENOD gene expression. Plant Physiol **136:** 3582-3593

**Cheng HP, Walker GC** (1998) Succinoglycan is required for initiation and elongation of infection threads during nodulation of alfalfa by Rhizobium meliloti. Journal of bacteriology **180:** 5183-5191

**Combier J-P, Frugier F, de Billy F, Boualem A, El-Yahyaoui F, Moreau S, Vernié T, Ott T, Gamas P, Crespi M, et al.** (2006) MtHAP2-1 is a key transcriptional regulator of symbiotic nodule development regulated by microRNA169 in Medicago truncatula. Genes & development **20:** 3084-3088

**Combier JP, de Billy F, Gamas P, Niebel A, Rivas S** (2008) Trans-regulation of the expression of the transcription factor MtHAP2-1 by a uORF controls root nodule development. Genes & development **22:** 1549-1559

**Cooper JB, Long SR** (1994) Morphogenetic Rescue of Rhizobium meliloti Nodulation Mutants by trans-Zeatin Secretion. Plant Cell **6:** 215-225

**Crdenas L, Vidali L, Domnguez J, Prez H, Snchez F, Hepler PK, Quinto C** (1998) Rearrangement of actin microfilaments in plant root hairs responding to rhizobium etli nodulation signals. Plant Physiol **116:** 871-877

**Curaba J, Chen X** (2008) Biochemical activities of Arabidopsis RNA-dependent RNA polymerase 6. J Biol Chem **283:** 3059-3066

**D'Haeseleer K, De Keyser A, Goormachtig S, Holsters M** (2010) Transcription factor MtATB2: about nodulation, sucrose and senescence. Plant Cell Physiol **51:** 1416-1424

**Dalmay T, Hamilton A, Rudd S, Angell S, Baulcombe DC** (2000) An RNA-dependent RNA polymerase gene in Arabidopsis is required for posttranscriptional gene silencing mediated by a transgene but not by a virus. Cell **101:** 543-553

**De Smet I, Lau S, Voss U, Vanneste S, Benjamins R, Rademacher EH, Schlereth A, De Rybel B, Vassileva V, Grunewald W, et al.** (2010) Bimodular auxin response controls organogenesis in Arabidopsis. Proc Natl Acad Sci U S A **107:** 2705-2710

**De Smet I, Tetsumura T, De Rybel B, Frey NF, Laplaze L, Casimiro I, Swarup R, Naudts M, Vanneste S, Audenaert D, et al.** (2007) Auxin-dependent regulation of lateral root positioning in the basal meristem of Arabidopsis. Development **134:** 681-690

**De Smet I, Tetsumura T, De Rybel B, Frey NFd, Laplaze L, Casimiro I, Swarup R, Naudts M, Vanneste S, Audenaert D, et al.** (2007) Auxin-dependent regulation of lateral root positioning in the basal meristem of Arabidopsis. Development **134:** 681-690

**den Hartog M, Musgrave A, Munnik T** (2001) Nod factor-induced phosphatidic acid and diacylglycerol pyrophosphate formation: a role for phospholipase C and D in root hair deformation. Plant J **25:** 55-65

**Den Herder G, De Keyser A, De Rycke R, Rombauts S, Van de Velde W, Clemente MR, Verplancke C, Mergaert P, Kondorosi E, Holsters M, et al.** (2008) Seven in absentia proteins affect plant growth and nodulation in Medicago truncatula. Plant Physiol **148:** 369-382

**Den Herder G, Yoshida S, Antolin-Llovera M, Ried MK, Parniske M** (2012) Lotus japonicus E3 Ligase SEVEN IN ABSENTIA4 Destabilizes the Symbiosis Receptor-Like Kinase SYMRK and Negatively Regulates Rhizobial Infection. Plant Cell **24:** 1691-1707

**Den Herder G, Yoshida S, Antolin-Llovera M, Ried MK, Parniske M** (2012) Lotus japonicus E3 Ligase SEVEN IN ABSENTIA4 Destabilizes the Symbiosis Receptor-Like Kinase SYMRK and Negatively Regulates Rhizobial Infection. Plant Cell

**Denarie J, Debelle F, Prome JC** (1996) Rhizobium lipo-chitooligosaccharide nodulation factors: signaling molecules mediating recognition and morphogenesis. Annu Rev Biochem **65:** 503-535

**Depicker A, Montagu MV** (1997) Post-transcriptional gene silencing in plants. Curr Opin Cell Biol **9:** 373-382

**Downie JA** (2010) The roles of extracellular proteins, polysaccharides and signals in the interactions of rhizobia with legume roots. FEMS microbiology reviews **34:** 150-170

**Doyle JJ** (2011) Phylogenetic perspectives on the origins of nodulation. Mol Plant Microbe Interact **24:** 1289-1295

**Edgar RC** (2004) MUSCLE: multiple sequence alignment with high accuracy and high throughput. Nucleic Acids Res **32:** 1792-1797

**Edwards A, Heckmann AB, Yousafzai F, Duc G, Downie JA** (2007) Structural implications of mutations in the pea SYM8 symbiosis gene, the DMI1 ortholog, encoding a predicted ion channel. Mol Plant Microbe Interact **20:** 1183-1191

**Ehrhardt DW, Wais R, Long SR** (1996) Calcium Spiking in Plant Root Hairs Responding to Rhizobium Nodulation Signals. Cell **85:** 673-681

**Endre G, Kereszt A, Kevei Z, Mihacea S, Kalo P, Kiss GB** (2002) A receptor kinase gene regulating symbiotic nodule development. Nature **417:** 962-966

**Engstrom EM, Ehrhardt DW, Mitra RM, Long SR** (2002) Pharmacological analysis of nod factor-induced calcium spiking in Medicago truncatula. Evidence for the requirement of type IIA calcium pumps and phosphoinositide signaling. Plant Physiol **128:** 1390-1401

**Esseling JJ, Lhuissier FG, Emons AM** (2003) Nod factor-induced root hair curling: continuous polar growth towards the point of nod factor application. Plant Physiol **132:** 1982-1988

**Fang Y, Hirsch aM** (1998) Studying early nodulin gene ENOD40 expression and induction by nodulation factor and cytokinin in transgenic alfalfa. Plant physiology **116:** 53-68

**Ferraioli S, Tatè R, Rogato A, Chiurazzi M, Patriarca EJ** (2004) Development of ectopic roots from abortive nodule primordia. Molecular plant-microbe interactions : MPMI **17:** 1043-1050

**Fukaki H, Tameda S, Masuda H, Tasaka M** (2002) Lateral root formation is blocked by a gain-of-function mutation in the SOLITARY-ROOT/IAA14 gene of Arabidopsis. Plant J **29:** 153-168

**Gage DJ** (2004) Infection and invasion of roots by symbiotic, nitrogen-fixing rhizobia during nodulation of temperate legumes. Microbiol Mol Biol Rev **68:** 280-300

**Geurts R, Bisseling T** (2002) Rhizobium nod factor perception and signalling. Plant Cell **14 Suppl:** S239-249

**Geurts R, Heidstra R, Hadri A-E, Downie JA, Franssen H, Kammen Av, Bisseling T** (1997) Sym2 of Pea Is Involved in a Nodulation Factor-Perception Mechanism That Controls the Infection Process in the Epidermis. Plant physiology **115:** 351-359

**Gleason C, Chaudhuri S, Yang T, Munoz A, Poovaiah BW, Oldroyd GED** (2006) Nodulation independent of rhizobia induced by a calcium-activated kinase lacking autoinhibition. Nature **441:** 1149-1152

**Gobbato E, Marsh JF, Vernie T, Wang E, Maillet F, Kim J, Miller JB, Sun J, Bano SA, Ratet P, et al.** (2012) A GRAS-Type Transcription Factor with a Specific Function in Mycorrhizal Signaling. Curr Biol **22:** 2236-2241

**Godiard L, Lepage A, Moreau S, Laporte D, Verdenaud M, Timmers T, Gamas P** (2011) MtbHLH1, a bHLH transcription factor involved in Medicago truncatula nodule vascular patterning and nodule to plant metabolic exchanges. The New phytologist **191:** 391-404

**Gonzalez-Rizzo S, Crespi M, Frugier F** (2006) The Medicago truncatula CRE1 Cytokinin Receptor Regulates Lateral Root Development and Early Symbiotic Interaction with Sinorhizobium meliloti. Plant Cell **18:** 2680-2693

**Grosjean C, Huguet T** (1997) A persistent meristem is formed in nodular structures elicited by Nod factor or by a Rhizobium meliloti exopolysaccharide mutant in alfalfa plants which nodulate spontaneously. Plant Science **127:** 215-225

**Groth M, Takeda N, Perry J, Uchida H, Draxl S, Brachmann A, Sato S, Tabata S, Kawaguchi M, Wang TL, et al.** (2010) NENA, a Lotus japonicus homolog of Sec13, is required for rhizodermal infection by arbuscular mycorrhiza fungi and rhizobia but dispensable for cortical endosymbiotic development. Plant Cell **22:** 2509-2526

**Gualtieri G, Bisseling T** (2000) The evolution of nodulation. Plant molecular biology **42:** 181-194

**Guindon S, Delsuc F, Dufayard JF, Gascuel O** (2009) Estimating maximum likelihood phylogenies with PhyML. Methods Mol Biol **537:** 113-137

**Guindon S, Dufayard JF, Lefort V, Anisimova M, Hordijk W, Gascuel O** (2010) New algorithms and methods to estimate maximum-likelihood phylogenies: assessing the performance of PhyML 3.0. Syst Biol **59:** 307-321

**Guindon S, Lethiec F, Duroux P, Gascuel O** (2005) PHYML Online--a web server for fast maximum likelihood-based phylogenetic inference. Nucleic Acids Res **33:** W557-559

**Haney CH, Long SR** (2010) Plant flotillins are required for infection by nitrogen-fixing bacteria. Proceedings of the National Academy of Sciences of the United States of America **107:** 478-483

**Haney CH, Riely BK, Tricoli DM, Cook DR, Ehrhardt DW, Long SR** (2011) Symbiotic Rhizobia Bacteria Trigger a Change in Localization and Dynamics of the Medicago truncatula Receptor Kinase LYK3. the Plant Cell Online**:** 1-15

**Heckmann AB, Sandal N, Bek AS, Madsen LH, Jurkiewicz A, Nielsen MW, Tirichine L, Stougaard J** (2011) Cytokinin induction of root nodule primordia in Lotus japonicus is regulated by a mechanism operating in the root cortex. Mol Plant Microbe Interact **24:** 1385-1395

**Hirsch AM, Bhuvaneswari TV, Torrey JG, Bisseling T** (1989) Early nodulin genes are induced in alfalfa root outgrowths elicited by auxin transport inhibitors. Proc Natl Acad Sci U S A **86:** 1244-1248

**Hirsch AM, Drake D, Jacobs TW, Long SR** (1985) Nodules are induced on alfalfa roots by Agrobacterium tumefaciens and Rhizobium trifolii containing small segments of the Rhizobium meliloti nodulation region. J Bacteriol **161:** 223-230

**Hirsch S, Kim J, Munoz A, Heckmann AB, Downie JA, Oldroyd GED** (2009) GRAS Proteins Form a DNA Binding Complex to Induce Gene Expression during Nodulation Signaling in Medicago truncatula. Plant Cell **21:** 545-557

**Hirsch S, Oldroyd GE** (2009) GRAS-domain transcription factors that regulate plant development. Plant Signal Behav **4:** 698-700

**Horváth B, Yeun LH, Domonkos Á, Halász G, Gobbato E, Ayaydin F, Miró K, Hirsch S, Sun J, Tadege M, et al.** (2011) Medicago truncatula IPD3 Is a Member of the Common Symbiotic Signaling Pathway Required for Rhizobial and Mycorrhizal Symbioses. Molecular Plant-Microbe Interactions **24:** 1345-1358

**Horvath B, Yeun LH, Domonkos A, Halasz G, Gobbato E, Ayaydin F, Miro K, Hirsch S, Sun J, Tadege M, et al.** (2011) Medicago truncatula IPD3 is a member of the common symbiotic signaling pathway required for rhizobial and mycorrhizal symbioses. Mol Plant Microbe Interact **24:** 1345-1358

**Hossain MS, Liao J, James EK, Sato S, Tabata S, Jurkiewicz A, Madsen LH, Stougaard J, Ross L, Szczyglowski K** (2012) Lotus japonicus ARPC1 is required for rhizobial infection. Plant Physiol

**Imaizumi-anraku H, Kawaguchi M, Koiwa H, Akao S** (1997) Two Ineffective-Nodulating Mutants of Lotus japonicus — Different Phenotypes Caused by the Blockage of Endocytotic Bacterial Release and Nodule Maturation —. plant cell physiol. **38:** 871-881

**Imaizumi-Anraku H, Kouchi H, Syono K, Akao S, Kawaguchi M** (2000) Analysis of ENOD40 expression in alb1 , a symbiotic mutant of Lotus japonicus that forms empty nodules with incompletely developed nodule vascular bundles. Molecular and General Genetics MGG **264:** 402-410

**Imaizumi-Anraku H, Takeda N, Charpentier M, Perry J, Miwa H, Umehara Y, Kouchi H, Murakami Y, Mulder L, Vickers K, et al.** (2005) Plastid proteins crucial for symbiotic fungal and bacterial entry into plant roots. Nature **433:** 527-531

**Jamet A, Mandon K, Puppo A, Herouart D** (2007) H2O2 is required for optimal establishment of the Medicago sativa/Sinorhizobium meliloti symbiosis. J Bacteriol **189:** 8741-8745

**Jamet A, Sigaud S, Van de Sype G, Puppo A, Herouart D** (2003) Expression of the bacterial catalase genes during Sinorhizobium meliloti-Medicago sativa symbiosis and their crucial role during the infection process. Mol Plant Microbe Interact **16:** 217-225

**Jones KM, Kobayashi H, Davies BW, Taga ME, Walker GC** (2007) How rhizobial symbionts invade plants: the Sinorhizobium-Medicago model. Nature reviews. Microbiology **5:** 619-633

**Jones KM, Sharopova N, Lohar DP, Zhang JQ, VandenBosch KA, Walker GC** (2008) Differential response of the plant Medicago truncatula to its symbiont Sinorhizobium meliloti or an exopolysaccharide-deficient mutant. Proceedings of the National Academy of Sciences of the United States of America **105:** 704-709

**Journet EP, El-Gachtouli N, Vernoud V, de Billy F, Pichon M, Dedieu a, Arnould C, Morandi D, Barker DG, Gianinazzi-Pearson V** (2001) Medicago truncatula ENOD11: a novel RPRP-encoding early nodulin gene expressed during mycorrhization in arbuscule-containing cells. Molecular plant-microbe interactions : MPMI **14:** 737-748

**Kalo P, Gleason C, Edwards A, Marsh J, Mitra RM, Hirsch S, Jakab J, Sims S, Long SR, Rogers J, et al.** (2005) Nodulation Signaling in Legumes Requires NSP2, a Member of the GRAS Family of Transcriptional Regulators. Science **308:** 1786-1789

**Kanamori N, Madsen LH, Radutoiu S, Frantescu M, Quistgaard EMH, Miwa H, Downie JA, James EK, Felle HH, Haaning LL, et al.** (2006) A nucleoporin is required for induction of Ca2+ spiking in legume nodule development and essential for rhizobial and fungal symbiosis. Proceedings of the National Academy of Sciences of the United States of America **103:** 359-364

**Kerscher O, Felberbaum R, Hochstrasser M** (2006) Modification of proteins by ubiquitin and ubiquitin-like proteins. Annu Rev Cell Dev Biol **22:** 159-180

**Kiss E, Olah B, Kalo P, Morales M, Heckmann AB, Borbola A, Lozsa A, Kontar K, Middleton P, Downie JA, et al.** (2009) LIN, a novel type of U-box/WD40 protein, controls early infection by rhizobia in legumes. Plant Physiol **151:** 1239-1249

**Kiss E, Oláh B, Kaló P, Morales M, Heckmann AB, Borbola A, Lózsa A, Kontár K, Middleton P, Downie JA, et al.** (2009) LIN, a novel type of U-box/WD40 protein, controls early infection by rhizobia in legumes. Plant physiology **151:** 1239-1249

**Kosuta S, Hazledine S, Sun J, Miwa H, Morris RJ, Downie JA, Oldroyd GE** (2008) Differential and chaotic calcium signatures in the symbiosis signaling pathway of legumes. Proc Natl Acad Sci U S A **105:** 9823-9828

**Kosuta S, Held M, Hossain MS, Morieri G, Macgillivary A, Johansen C, Antolin-Llovera M, Parniske M, Oldroyd GE, Downie AJ, et al.** (2011) Lotus japonicus symRK-14 uncouples the cortical and epidermal symbiotic program. Plant J **67:** 929-940

**Kuppusamy KT, Endre G, Prabhu R, Penmetsa RV, Veereshlingam H, Cook DR, Dickstein R, VandenBosch KA** (2004) LIN, a Medicago truncatula Gene Required for Nodule Differentiation and Persistence of Rhizobial Infections. Plant Physiol. **136:** 3682-3691

**Kuppusamy KT, Endre G, Prabhu R, Penmetsa RV, Veereshlingam H, Cook DR, Dickstein R, Vandenbosch KA** (2004) LIN, a Medicago truncatula gene required for nodule differentiation and persistence of rhizobial infections. Plant Physiol **136:** 3682-3691

**Lamb C, Dixon RA** (1997) The Oxidative Burst in Plant Disease Resistance. Annu Rev Plant Physiol Plant Mol Biol **48:** 251-275

**Laplaze L, Benkova E, Casimiro I, Maes L, Vanneste S, Swarup R, Weijers D, Calvo V, Parizot B, Herrera-Rodriguez MB, et al.** (2007) Cytokinins act directly on lateral root founder cells to inhibit root initiation. Plant Cell **19:** 3889-3900

**Laplaze L, Duhoux E, Franche C, Frutz T, Svistoonoff S, Bisseling T, Bogusz D, Pawlowski K** (2000) Casuarina glauca Prenodule Cells Display the Same Differentiation as the Corresponding Nodule Cells. Molecular Plant-Microbe Interactions **13:** 107-112

**Lefebvre B, Timmers T, Mbengue M, Moreau S, Herve C, Toth K, Bittencourt-Silvestre J, Klaus D, Deslandes L, Godiard L, et al.** (2010) A remorin protein interacts with symbiotic receptors and regulates bacterial infection. Proc Natl Acad Sci U S A **107:** 2343-2348

**Leigh Ja, Signer ER, Walker GC** (1985) Exopolysaccharide-deficient mutants of Rhizobium meliloti that form ineffective nodules. Proceedings of the National Academy of Sciences of the United States of America **82:** 6231-6235

**Levy J, Bres C, Geurts R, Chalhoub B, Kulikova O, Duc G, Journet E-P, Ane J-M, Lauber E, Bisseling T, et al.** (2004) A Putative Ca2+ and Calmodulin-Dependent Protein Kinase Required for Bacterial and Fungal Symbioses. Science **303:** 1361-1364

**Lewis DR, Negi S, Sukumar P, Muday GK** (2011) Ethylene inhibits lateral root development, increases IAA transport and expression of PIN3 and PIN7 auxin efflux carriers. Development **138:** 3485-3495

**Leyser O** (2010) The power of auxin in plants. Plant Physiol **154:** 501-505

**Limpens E, Franken C, Smit P, Willemse J, Bisseling T, Geurts R** (2003) LysM Domain Receptor Kinases Regulating Rhizobial Nod Factor-Induced Infection. Science **302:** 630-633

**Liu T, Liu Z, Song C, Hu Y, Han Z, She J, Fan F, Wang J, Jin C, Chang J, et al.** (2012) Chitin-induced dimerization activates a plant immune receptor. Science **336:** 1160-1164

**Long SR** (1989) Rhizobium genetics. Annu Rev Genet **23:** 483-506

**Loren C, Antonio C, Delphine P, Virginie G, Yves T, Stéphanie B-M, Ludivine T, Jean-Pierre R, Françoise D-V, Emilio F, et al.** (2009) The nodule inception-like protein 7 modulates nitrate sensing and metabolism in Arabidopsis. The Plant Journal **57:** 426-435

**Madsen EB, Madsen LH, Radutoiu S, Olbryt M, Rakwalska M, Szczyglowski K, Sato S, Kaneko T, Tabata S, Sandal N, et al.** (2003) A receptor kinase gene of the LysM type is involved in legumeperception of rhizobial signals. Nature **425:** 637-640

**Madsen LH, Tirichine L, Jurkiewicz A, Sullivan JT, Heckmann AB, Bek AS, Ronson CW, James EK, Stougaard J** (2010) The molecular network governing nodule organogenesis and infection in the model legume Lotus japonicus. Nature Communications **1:** 1-12

**Maillet F, Poinsot V, Andre O, Puech-Pages V, Haouy A, Gueunier M, Cromer L, Giraudet D, Formey D, Niebel A, et al.** (2011) Fungal lipochitooligosaccharide symbiotic signals in arbuscular mycorrhiza. Nature **469:** 58-63

**Malamy JE, Benfey PN** (1997) Organization and cell differentiation in lateral roots of Arabidopsis thaliana. Development **124:** 33-44

**Marie C, Barny MA, Downie JA** (1992) Rhizobium leguminosarum has two glucosamine synthases, GlmS and NodM, required for nodulation and development of nitrogen-fixing nodules. Mol Microbiol **6:** 843-851

**Marsh JF, Rakocevic A, Mitra RM, Brocard L, Sun J, Eschstruth A, Long SR, Schultze M, Ratet P, Oldroyd GED** (2007) Medicago truncatula NIN Is Essential for Rhizobial-Independent Nodule Organogenesis Induced by Autoactive Calcium/Calmodulin-Dependent Protein Kinase. Plant Physiol. **144:** 324-335

**Mathesius U, Schlaman HR, Spaink HP, Of Sautter C, Rolfe BG, Djordjevic Ma** (1998) Auxin transport inhibition precedes root nodule formation in white clover roots and is regulated by flavonoids and derivatives of chitin oligosaccharides. The Plant journal : for cell and molecular biology **14:** 23-34

**Mbengue M, Camut S, de Carvalho-Niebel F, Deslandes L, Froidure S, Klaus-Heisen D, Moreau S, Rivas S, Timmers T, Herve C, et al.** (2010) The Medicago truncatula E3 ubiquitin ligase PUB1

interacts with the LYK3 symbiotic receptor and negatively regulates infection and nodulation. Plant Cell **22:** 3474-3488

**Messinese E, Mun J-H, Yeun LH, Jayaraman D, RougÃ© P, Barre A, Lougnon Gr, Schornack S, Bono J-J, Cook DR, et al.** (2007) A Novel Nuclear Protein Interacts With the Symbiotic DMI3 Calcium- and Calmodulin-Dependent Protein Kinase of Medicago truncatula. Molecular Plant-Microbe Interactions **20:** 912-921

**Messinese E, Mun JH, Yeun LH, Jayaraman D, Rouge P, Barre A, Lougnon G, Schornack S, Bono JJ, Cook DR, et al.** (2007) A novel nuclear protein interacts with the symbiotic DMI3 calcium- and calmodulin-dependent protein kinase of Medicago truncatula. Mol Plant Microbe Interact **20:** 912-921

**Middleton PH, Jakab J, Penmetsa RV, Starker CG, Doll J, Kalo P, Prabhu R, Marsh JF, Mitra RM, Kereszt A, et al.** (2007) An ERF Transcription Factor in Medicago truncatula That Is Essential for Nod Factor Signal Transduction. Plant Cell **19:** 1221-1234

**Mitra RM, Gleason CA, Edwards A, Hadfield J, Downie JA, Oldroyd GE, Long SR** (2004) A Ca2+/calmodulin-dependent protein kinase required for symbiotic nodule development: Gene identification by transcript-based cloning. Proc Natl Acad Sci U S A **101:** 4701-4705

**Miwa H, Sun J, Oldroyd GE, Downie JA** (2006) Analysis of Nod-factor-induced calcium signaling in root hairs of symbiotically defective mutants of Lotus japonicus. Mol Plant Microbe Interact **19:** 914-923

**Miyahara A, Richens J, Starker C, Morieri G, Smith L, Long S, Downie JA, Oldroyd GE** (2010) Conservation in function of a SCAR/WAVE component during infection thread and root hair growth in Medicago truncatula. Mol Plant Microbe Interact **23:** 1553-1562

**Moreno-Risueno Ma, Van Norman JM, Moreno a, Zhang J, Ahnert SE, Benfey PN** (2010) Oscillating Gene Expression Determines Competence for Periodic Arabidopsis Root Branching. Science **329:** 1306-1311

**Mourrain P, Beclin C, Elmayan T, Feuerbach F, Godon C, Morel JB, Jouette D, Lacombe AM, Nikic S, Picault N, et al.** (2000) Arabidopsis SGS2 and SGS3 genes are required for posttranscriptional gene silencing and natural virus resistance. Cell **101:** 533-542

**Murray JD** (2011) Invasion by invitation: rhizobial infection in legumes. Mol Plant Microbe Interact **24:** 631-639

**Murray JD, Karas BJ, Sato S, Tabata S, Amyot L, Szczyglowski K** (2007) A cytokinin perception mutant colonized by Rhizobium in the absence of nodule organogenesis. Science **315:** 101-104

**Murray JD, Muni RRD, Torres-Jerez I, Tang Y, Allen S, Andriankaja M, Li G, Laxmi A, Cheng X, Wen J, et al.** (2011) Vapyrin, a gene essential for intracellular progression of arbuscular mycorrhizal symbiosis, is also essential for infection by rhizobia in the nodule symbiosis of Medicago truncatula. The Plant journal : for cell and molecular biology **65:** 244-252

**Nagpal P, Khanuja SPS, Stanfield SW** (1992) Suppression of the ndv mutant phenotype of Rhizobium meliloti by cloned exo genes. Molecular Microbiology **6:** 479-488

**Negi S, Ivanchenko MG, Muday GK** (2008) Ethylene regulates lateral root formation and auxin transport in Arabidopsis thaliana. Plant J **55:** 175-187

**Okushima Y, Fukaki H, Onoda M, Theologis A, Tasaka M** (2007) ARF7 and ARF19 regulate lateral root formation via direct activation of LBD/ASL genes in Arabidopsis. Plant Cell **19:** 118-130

**Oldroyd GE, Engstrom EM, Long SR** (2001) Ethylene inhibits the Nod factor signal transduction pathway of Medicago truncatula. Plant Cell **13:** 1835-1849

**Oldroyd GE, Mitra RM, Wais RJ, Long SR** (2001) Evidence for structurally specific negative feedback in the Nod factor signal transduction pathway. Plant J **28:** 191-199

**Oldroyd GED, Murray JD, Poole PS, Downie JA** (2011) The Rules of Engagement in the Legume-Rhizobial Symbiosis. Annual review of genetics **45:** 119-144

**Op den Camp R, De Mita S, Lillo A, Cao Q, Limpens E, Bisseling T, Geurts R** (2011) A phylogenetic strategy based on a legume-specific whole genome duplication yields symbiotic cytokinin type-A Response Regulators. Plant physiology **157:** 2013-2022

**Op den Camp R, Streng A, De Mita S, Cao Q, Polone E, Liu W, Ammiraju JSS, Kudrna D, Wing R, Untergasser A, et al.** (2010) LysM-Type Mycorrhizal Receptor Recruited for Rhizobium Symbiosis in Nonlegume Parasponia. Science (New York, N.Y.)

**Ovchinnikova E, Journet EP, Chabaud M, Cosson V, Ratet P, Duc G, Fedorova E, Liu W, den Camp RO, Zhukov V, et al.** (2011) IPD3 controls the formation of nitrogen-fixing symbiosomes in pea and Medicago Spp. Mol Plant Microbe Interact **24:** 1333-1344

**Pacios-Bras C, Schlaman HR, Boot K, Admiraal P, Langerak JM, Stougaard J, Spaink HP** (2003) Auxin distribution in Lotus japonicus during root nodule development. Plant Mol Biol **52:** 1169-1180

**Parniske M** (2008) Arbuscular mycorrhiza: the mother of plant root endosymbioses. Nat Rev Micro **6:** 763-775

**Peck MC, Fisher RF, Long SR** (2006) Diverse flavonoids stimulate NodD1 binding to nod gene promoters in Sinorhizobium meliloti. J Bacteriol **188:** 5417-5427

**Pellock BJ, Cheng H-P, Walker GC** (2000) Alfalfa Root Nodule Invasion Efficiency Is Dependent on Sinorhizobium melilotiPolysaccharides. Journal of bacteriology **182:** 4310-4318

**Penmetsa RV, Cook DR** (1997) A Legume Ethylene-Insensitive Mutant Hyperinfected by Its Rhizobial Symbiont. Science **275:** 527-530

**Penmetsa RV, Frugoli JA, Smith LS, Long SR, Cook DR** (2003) Dual genetic pathways controlling nodule number in Medicago truncatula. Plant Physiol **131:** 998-1008

**Péret B, De Rybel B, Casimiro I, Benková E, Swarup R, Laplaze L, Beeckman T, Bennett MJ** (2009) Arabidopsis lateral root development: an emerging story. Trends in plant science **14:** 399-408

**Peret B, Swarup R, Jansen L, Devos G, Auguy F, Collin M, Santi C, Hocher V, Franche C, Bogusz D, et al.** (2007) Auxin influx activity is associated with Frankia infection during actinorhizal nodule formation in Casuarina glauca. Plant Physiol **144:** 1852-1862

**Perilli S, Moubayidin L, Sabatini S** (2010) The molecular basis of cytokinin function. Curr Opin Plant Biol **13:** 21-26

**Petutschnig EK, Jones AM, Serazetdinova L, Lipka U, Lipka V** (2010) The lysin motif receptor-like kinase (LysM-RLK) CERK1 is a major chitin-binding protein in Arabidopsis thaliana and subject to chitin-induced phosphorylation. J Biol Chem **285:** 28902-28911

**Pike LJ** (2009) The challenge of lipid rafts. J Lipid Res **50 Suppl:** S323-328

**Pislariu CI, Murray J, Wen J, Cosson V, Duvvuru Muni RR, Wang M, Benedito V, Andriankaja A, Cheng X, Torres Jerez I, et al.** (2012) A Medicago truncatula tobacco-retrotransposon (Tnt1)-insertion mutant collection with defects in nodule development and symbiotic nitrogen fixation. Plant Physiol

**Plet J, Wasson A, Ariel F, Le Signor C, Baker D, Mathesius U, Crespi M, Frugier F** (2011) MtCRE1-dependent cytokinin signaling integrates bacterial and plant cues to coordinate symbiotic nodule organogenesis in Medicago truncatula. The Plant Journal **65:** 622-633

**Poli A, Di Donato P, Abbamondi GR, Nicolaus B** (2011) Synthesis, production, and biotechnological applications of exopolysaccharides and polyhydroxyalkanoates by archaea. Archaea **2011:** 693253

**Ponting CP, Ito T, Moscat J, Diaz-Meco MT, Inagaki F, Sumimoto H** (2002) OPR, PC and AID: all in the PB1 family. Trends Biochem Sci **27:** 10

**Radutoiu S, Madsen LH, Madsen EB, Felle HH, Umehara Y, Gronlund M, Sato S, Nakamura Y, Tabata S, Sandal N, et al.** (2003) Plant recognition of symbiotic bacteria requires two LysM receptor-like kinases. Nature **425:** 585-592

**Radutoiu S, Madsen LH, Madsen EB, Jurkiewicz A, Fukai E, Quistgaard EM, Albrektsen AS, James EK, Thirup S, Stougaard J** (2007) LysM domains mediate lipochitin-oligosaccharide recognition and Nfr genes extend the symbiotic host range. EMBO J **26:** 3923-3935

**Radutoiu S, Madsen LH, Madsen EB, Jurkiewicz A, Fukai E, Quistgaard EMH, Albrektsen AS, James EK, Thirup S, Stougaard J** (2007) LysM domains mediate lipochitin-oligosaccharide recognition and Nfr genes extend the symbiotic host range. The EMBO journal **26:** 3923-3935

**Rakocevic A, Mondy S, Tirichine L, Cosson V, Brocard L, Iantcheva A, Cayrel A, Devier B, Abu El-Heba GA, Ratet P** (2009) MERE1, a low-copy-number copia-type retroelement in Medicago truncatula active during tissue culture. Plant Physiol **151:** 1250-1263

**Ramu SK, Peng HM, Cook DR** (2002) Nod factor induction of reactive oxygen species production is correlated with expression of the early nodulin gene rip1 in Medicago truncatula. Mol Plant Microbe Interact **15:** 522-528

**Remy W, Taylor TN, Hass H, Kerp H** (1994) Four hundred-million-year-old vesicular arbuscular mycorrhizae. Proc Natl Acad Sci U S A **91:** 11841-11843

**Rightmyer AP, Long SR** (2011) Pseudonodule Formation by Wild-Type and Symbiotic Mutant Medicago truncatula in Response to Auxin Transport Inhibitors. Molecular Plant-Microbe Interactions **24:** 1372-1384

**Rival P, de Billy F, Bono JJ, Gough C, Rosenberg C, Bensmihen S** (2012) Epidermal and cortical roles of NFP and DMI3 in coordinating early steps of nodulation in Medicago truncatula. Development

**Robledo M, Jiménez-Zurdo JI, Velázquez E, Trujillo ME, Zurdo-Piñeiro JL, Ramírez-Bahena MH, Ramos B, Díaz-Mínguez JM, Dazzo F, Martínez-Molina E, et al.** (2008) Rhizobium cellulase CelC2 is essential for primary symbiotic infection of legume host roots. Proceedings of the National Academy of Sciences **105:** 7064-7069

**Roponen I** (1970) The Effect of Darkness on the Leghemoglobin Content and Amino Acid Levels in the Root Nodules of Pea Plants. Physiologia Plantarum **23:** 452-460

**Saito K, Yoshikawa M, Yano K, Miwa H, Uchida H, Asamizu E, Sato S, Tabata S, Imaizumi-Anraku H, Umehara Y, et al.** (2007) NUCLEOPORIN85 is required for calcium spiking, fungal and bacterial symbioses, and seed production in Lotus japonicus. Plant Cell **19:** 610-624

**Sakakibara H** (2006) Cytokinins: activity, biosynthesis, and translocation. Annu Rev Plant Biol **57:** 431-449

**Santos R, Herouart D, Puppo A, Touati D** (2000) Critical protective role of bacterial superoxide dismutase in rhizobium-legume symbiosis. Mol Microbiol **38:** 750-759

**Santos R, Herouart D, Sigaud S, Touati D, Puppo A** (2001) Oxidative burst in alfalfa-Sinorhizobium meliloti symbiotic interaction. Mol Plant Microbe Interact **14:** 86-89

**Schauser L, Roussis A, Stiller J, Stougaard J** (1999) A plant regulator controlling development of symbiotic root nodules. Nature **402:** 191-195

**Schauser L, Wieloch W, Stougaard J** (2005) Evolution of NIN-Like Proteins in Arabidopsis, Rice, and Lotus japonicus. Journal of Molecular Evolution **60:** 229-237

**Shaw SL, Long SR** (2003) Nod factor inhibition of reactive oxygen efflux in a host legume. Plant Physiol **132:** 2196-2204

**Shimoda Y, Han L, Yamazaki T, Suzuki R, Hayashi M, Imaizumi-Anraku H** (2012) Rhizobial and fungal symbioses show different requirements for calmodulin binding to calcium calmodulin-dependent protein kinase in Lotus japonicus. Plant Cell **24:** 304-321

**Sieberer BJ, Chabaud M, Fournier J, Timmers AC, Barker DG** (2012) A switch in Ca2+ spiking signature is concomitant with endosymbiotic microbe entry into cortical root cells of Medicago truncatula. Plant J **69:** 822-830

**Simsek S, Ojanen-Reuhs T, Stephens SB, Reuhs BL** (2007) Strain-ecotype specificity in Sinorhizobium meliloti-Medicago truncatula symbiosis is correlated to succinoglycan oligosaccharide structure. J Bacteriol **189:** 7733-7740

**Singer WD, Brown HA, Jiang X, Sternweis PC** (1996) Regulation of phospholipase D by protein kinase C is synergistic with ADP-ribosylation factor and independent of protein kinase activity. J Biol Chem **271:** 4504-4510

**Smit P, Limpens E, Geurts R, Fedorova E, Dolgikh E, Gough C, Bisseling T** (2007) Medicago LYK3, an entry receptor in rhizobial nodulation factor signaling. Plant physiology **145:** 183-191

**Smit P, Raedts J, Portyanko V, Debelle F, Gough C, Bisseling T, Geurts R** (2005) NSP1 of the GRAS protein family is essential for rhizobial Nod factor-induced transcription. Science **308:** 1789-1791

**Smith DL, Starrett DA, Gross KC** (1998) A gene coding for tomato fruit beta-galactosidase II is expressed during fruit ripening. Cloning, characterization, and expression pattern. Plant Physiol **117:** 417-423

**Smith LG, Oppenheimer DG** (2005) Spatial control of cell expansion by the plant cytoskeleton. Annu Rev Cell Dev Biol **21:** 271-295

**Smith TF, Gaitatzes C, Saxena K, Neer EJ** (1999) The WD repeat: a common architecture for diverse functions. Trends Biochem Sci **24:** 181-185

**Stracke S, Kistner C, Yoshida S, Mulder L, Sato S, Kaneko T, Tabata S, Sandal N, Stougaard J, Szczyglowski K, et al.** (2002) A plant receptor-like kinase required for both bacterial and fungal symbiosis. Nature **417:** 959-962

**Streng A, op den Camp R, Bisseling T, Geurts R** (2011) Evolutionary origin of rhizobium Nod factor signaling. Plant Signal Behav **6:** 1510-1514

**Subramanian S, Stacey G, Yu O** (2007) Distinct, crucial roles of flavonoids during legume nodulation. Trends Plant Sci **12:** 282-285

**Sun J, Miwa H, Downie JA, Oldroyd GE** (2007) Mastoparan activates calcium spiking analogous to Nod factor-induced responses in Medicago truncatula root hair cells. Plant Physiol **144:** 695-702

**Swarup K, Benkova E, Swarup R, Casimiro I, Peret B, Yang Y, Parry G, Nielsen E, De Smet I, Vanneste S, et al.** (2008) The auxin influx carrier LAX3 promotes lateral root emergence. Nat Cell Biol **10:** 946-954

**Tadege M, Wen J, He J, Tu H, Kwak Y, Eschstruth A, Cayrel A, Endre G, Zhao PX, Chabaud M, et al.** (2008) Large-scale insertional mutagenesis using the Tnt1 retrotransposon in the model legume Medicago truncatula. The Plant Journal **54:** 335-347

**Takanashi K, Sugiyama A, Sato S, Tabata S, Yazaki K** (2012) LjABCB1, an ATP-binding cassette protein specifically induced in uninfected cells of Lotus japonicus nodules. J Plant Physiol **169:** 322-326

**Takanashi K, Sugiyama A, Yazaki K** (2011) Involvement of auxin distribution in root nodule development of Lotus japonicus. Planta **234:** 73-81

**Takanashi K, Sugiyama A, Yazaki K** (2011) Involvement of auxin distribution in root nodule development of Lotus japonicus. Planta

**Takeda N, Haage K, Sato S, Tabata S, Parniske M** (2011) Activation of a Lotus japonicus subtilase gene during arbuscular mycorrhiza is dependent on the common symbiosis genes and two cis-active promoter regions. Mol Plant Microbe Interact **24:** 662-670

**Takeda N, Maekawa T, Hayashi M** (2012) Nuclear-localized and deregulated calcium- and calmodulin-dependent protein kinase activates rhizobial and mycorrhizal responses in Lotus japonicus. Plant Cell **24:** 810-822

**Tansengco ML, Hayashi M, Kawaguchi M, Imaizumi-Anraku H, Murooka Y** (2003) crinkle, a novel symbiotic mutant that affects the infection thread growth and alters the root hair, trichome, and seed development in Lotus japonicus. Plant Physiol **131:** 1054-1063

**Taylor LP, Grotewold E** (2005) Flavonoids as developmental regulators. Curr Opin Plant Biol **8:** 317-323

**Timmers aC, Auriac MC, Truchet G** (1999) Refined analysis of early symbiotic steps of the Rhizobium-Medicago interaction in relationship with microtubular cytoskeleton rearrangements. Development (Cambridge, England) **126:** 3617-3628

**Tirichine L, Imaizumi-Anraku H, Yoshida S, Murakami Y, Madsen LH, Miwa H, Nakagawa T, Sandal N, Albrektsen AS, Kawaguchi M, et al.** (2006) Deregulation of a Ca2+/calmodulin-dependent kinase leads to spontaneous nodule development. Nature **441:** 1153-1156

**Tirichine L, James EK, Sandal N, Stougaard J** (2006) Spontaneous root-nodule formation in the model legume Lotus japonicus: a novel class of mutants nodulates in the absence of rhizobia. Mol Plant Microbe Interact **19:** 373-382

**Tirichine L, Sandal N, Madsen LH, Radutoiu S, Albrektsen AS, Sato S, Asamizu E, Tabata S, Stougaard J** (2007) A Gain-of-Function Mutation in a Cytokinin Receptor Triggers Spontaneous Root Nodule Organogenesis. Science **315:** 104-107

**Tirichine L, Sandal N, Madsen LH, Radutoiu S, Albrektsen AS, Sato S, Asamizu E, Tabata S, Stougaard J** (2007) A gain-of-function mutation in a cytokinin receptor triggers spontaneous root nodule organogenesis. Science **315:** 104-107

**Truchet G, Roche P, Lerouge P, Vasse J, Camut S, de Billy F, Prome J-C, Denarie J** (1991) Sulphated lipo-oligosaccharide signals of Rhizobium meliloti elicit root nodule organogenesis in alfalfa. Nature **351:** 670-673

**Tsyganova AV, Tsyganov VE, Findli KK, Borisov A, Tikhonovich NA, Brevin NG** (2009) [Distribution of legume arabinogalactanprotein-extensin (AGPE) glycoproteins in symbiotically defective pea mutants with abnormal infection threads]. Tsitologiia **51:** 53-62

**Van de Velde W, Zehirov G, Szatmari A, Debreczeny M, Ishihara H, Kevei Z, Farkas A, Mikulass K, Nagy A, Tiricz H, et al.** (2010) Plant peptides govern terminal differentiation of bacteria in symbiosis. Science **327:** 1122-1126

**Van De Wiel C, Norris JH, Bochenek B, Dickstein R, Bisseling T, Hirsch AM** (1990) Nodulin Gene Expression and ENOD2 Localization in Effective, Nitrogen-Fixing and Ineffective, Bacteria-Free Nodules of Alfalfa. Plant Cell **2:** 1009-1017

**Varma Penmetsa R, Uribe P, Anderson J, Lichtenzveig J, Gish J-C, Nam YW, Engstrom E, Xu K, Sckisel G, Pereira M, et al.** (2008) The Medicago truncatula ortholog of Arabidopsis EIN2, sickle, is a negative regulator of symbiotic and pathogenic microbial associations. The Plant Journal **55:** 580-595

**Vernoud V, Journet E-P, Barker DG** (1999) MtENOD20, a Nod Factor-Inducible Molecular Marker for Root Cortical Cell Activation. Molecular Plant-Microbe Interactions **12:** 604-614

**Voroshilova Va, Demchenko KN, Brewin NJ, Borisov AY, Tikhonovich Ia** (2009) Initiation of a legume nodule with an indeterminate meristem involves proliferating host cells that harbour infection threads. The New phytologist **181:** 913-923

**Walker L, Estelle M** (1998) Molecular mechanisms of auxin action. Curr Opin Plant Biol **1:** 434-439

**Wang D, Griffitts J, Starker C, Fedorova E, Limpens E, Ivanov S, Bisseling T, Long S** (2010) A nodule-specific protein secretory pathway required for nitrogen-fixing symbiosis. Science (New York, N.Y.) **327:** 1126-1129

**Wasson AP, Pellerone FI, Mathesius U** (2006) Silencing the Flavonoid Pathway in Medicago truncatula Inhibits Root Nodule Formation and Prevents Auxin Transport Regulation by Rhizobia. The Plant cell **18:** 1617-1629

**Wei M, Yokoyama T, Minamisawa K, Mitsui H, Itakura M, Kaneko T, Tabata S, Saeki K, Omori H, Tajima S, et al.** (2008) Soybean seed extracts preferentially express genomic loci of Bradyrhizobium japonicum in the initial interaction with soybean, Glycine max (L.) Merr. DNA Res **15:** 201-214

**Wu C, Dickstein R, Cary AJ, Norris JH** (1996) The Auxin Transport Inhibitor N-(1-Naphthyl)phthalamic Acid Elicits Pseudonodules on Nonnodulating Mutants of White Sweetclover. Plant Physiol **110:** 501-510

**Xie F, Murray JD, Kim J, Heckmann AB, Edwards A, Oldroyd GED, Downie JA** (2011) Legume pectate lyase required for root infection by rhizobia. Proceedings of the National Academy of Sciences

**Yang C, Signer ER, Hirsch aM** (1992) Nodules Initiated by Rhizobium meliloti Exopolysaccharide Mutants Lack a Discrete, Persistent Nodule Meristem. Plant physiology **98:** 143-151

**Yang WC, Katinakis P, Hendriks P, Smolders A, de Vries F, Spee J, van Kammen A, Bisseling T, Franssen H** (1993) Characterization of GmENOD40, a gene showing novel patterns of cell-specific expression during soybean nodule development. Plant J **3:** 573-585

**Yano K, Shibata S, Chen W-L, Sato S, Kaneko T, Jurkiewicz A, Sandal N, Banba M, Imaizumi-Anraku H, Kojima T, et al.** (2009) CERBERUS, a novel U-box protein containing WD-40 repeats, is required for formation of the infection thread and nodule development in the legume–Rhizobium symbiosis. The Plant Journal **60:** 168-180

**Yano K, Tansengco ML, Hio T, Higashi K, Murooka Y, Imaizumi-Anraku H, Kawaguchi M, Hayashi M** (2006) New nodulation mutants responsible for infection thread development in Lotus japonicus. Molecular plant-microbe interactions : MPMI **19:** 801-810

**Yano K, Yoshida S, MÃller J, Singh S, Banba M, Vickers K, Markmann K, White C, Schuller B, Sato S, et al.** (2008) CYCLOPS, a mediator of symbiotic intracellular accommodation. Proceedings of the National Academy of Sciences **105:** 20540-20545

**Yao S-Y, Luo L, Har KJ, Becker A, Rüberg S, Yu G-Q, Zhu J-B, Cheng H-P** (2004) Sinorhizobium meliloti ExoR and ExoS Proteins Regulate both Succinoglycan and Flagellum Production. Journal of bacteriology **186:** 6042-6049

**Yokota K, Fukai E, Madsen LH, Jurkiewicz A, Rueda P, Radutoiu S, Held M, Hossain MS, Szczyglowski K, Morieri G, et al.** (2009) Rearrangement of actin cytoskeleton mediates invasion of Lotus japonicus roots by Mesorhizobium loti. Plant Cell **21:** 267-284

**Yokota K, Soyano T, Kouchi H, Hayashi M** (2010) Function of GRAS proteins in root nodule symbiosis is retained in homologs of a non-legume, rice. Plant & cell physiology **51:** 1436-1442

**Yoo KS, Ok SH, Jeong BC, Jung KW, Cui MH, Hyoung S, Lee MR, Song HK, Shin JS** (2011) Single cystathionine beta-synthase domain-containing proteins modulate development by regulating the thioredoxin system in Arabidopsis. Plant Cell **23:** 3577-3594

**Young ND, Debelle F, Oldroyd GED, Geurts R, Cannon SB, Udvardi MK, Benedito VA, Mayer KFX, Gouzy J, Schoof H, et al.** (2011) The Medicago genome provides insight into the evolution of rhizobial symbioses. Nature **advance online publication**

**Zhang J, Subramanian S, Stacey G, Yu O** (2009) Flavones and flavonols play distinct critical roles during nodulation of Medicago truncatula by Sinorhizobium meliloti. Plant J **57:** 171-183

# Publications

1. **Dian Guan**, Nicola Stacey, Chengwu Liu, Jiangqi Wen, Kirankumar Mysore, Ivone Torres-Jerez, Million Tadege, Michael Udvardi, Giles E. D. Oldroyd, and Jeremy D. Murray. Rhizobial infection is associated with peripheral vasculature development in nodules of *Medicago truncatula*. Plant Physiology. Under review.

2. Co-author in Jiyoung Kim et al paper (in preparation)
3. Co-author in Senjuti Sinharoy et al paper (in preparation)
4. NIN suppression of mycorrhization in nodulation work followed by Dr. Chengwu Liu, publication in the future

# Appendix

Table 1. rhizobial infection mutants screen plants phenotype

Table 2. *kce Tnt1* insertions

Table 3. *kce* mutant *MERE1* transponsons identified in deep sequencing

Table 4. probe sets and gene annotations induced in WT 5dpi and under NIN positive control

5. *kce* and R108 *LIN* sequence

6. Medium recipes